INVESTIGATION OF MOLECULAR MECHANISMS OF LIPID DROPLETS CATABOLIC PATHWAYS AND THEIR INTERACTIONS IN ICHTHYOSIS DISEASE

by
HALE KESİM

Submitted to the Graduate School of Engineering and Natural Sciences
in partial fulfillment of
the requirements for the degree of Master of Science

Sabancı University
December 2021

INVESTIGATION OF MOLECULAR MECHANISMS OF LIPID DROPLETS CATABOLIC PATHWAYS AND THEIR INTERACTIONS IN ICHTHYOSİS DISEASE

APPROVED BY:

ABSTRACT

INVESTIGATION OF MOLECULAR MECHANISMS OF LIPID DROPLETS CATABOLIC PATHWAYS AND THEIR INTERACTIONS IN ICHTHYOSIS DISEASE

Hale Kesim

Molecular Biology, Genetics, and Bioengineering, Master of Science, 2021

Thesis Supervisor: Assoc. Prof. Özlem Kutlu

Keywords: Lipid droplets, Ichthyosis, Lipolysis, Chaperone-mediated Autophagy, Lipophagy

In cells, excessive lipids are stored as neutral lipids in an organelle called lipid droplets (LDs) to prevent lipotoxicity. In recent years, the importance of these droplets in lipid metabolism, cell signaling, and membrane trafficking was proven with the identification of over 150 proteins on LD surfaces. Additionally, LDs can be catabolized and used as an energy source in the need of energy by three mechanisms, namely lipolysis, chaperone-mediated autophagy (CMA), and lipophagy. Autosomal recessive congenital ichthyosis (ARCI) is a non-syndromic form of ichthyosis, resulting in scaly skin, dehydration, and electrolytic imbalance. Many genes, causing ARCI disease, have been proven to be involved in abnormal lipid metabolism and associated with LD accumulation. Patatin-like phospholipase domain containing-1 (PNPLA1) is a protein that involves in phospholipid metabolism and a mutation in this gene causes the development of ARCI pathology. For a better understanding of the effect of PNPLA1 gene mutations on LD metabolism, LD catabolic pathways and their interactions were investigated in this master thesis. Therefore, lipolysis, CMA, and lipophagy mechanisms of fibroblast cells derived from ARCI patients that have p.D172N mutation were analyzed. Localization of LDs with lipolysis-, lipophagy- and CMA-related proteins in fibroblast cells compared to healthy fibroblasts were checked under confocal microscopy by labeling protein of interest with different fluorophores. In addition, the amount of protein expression was analyzed by immunoblotting, and the change in the gene regulation was determined by RT-qPCR. As a result, it was found that PNPLA1 gene mutation in ARCI patient cells shows aberrant LD accumulation and sizes due to the defective lipolysis and lipophagy mechanism, demonstrating the crucial role of PNPLA1 protein in catabolic regulation of LDs.

ÖZET

İKTİYOZ HASTALIĞINDA YAĞ DAMLACIKLARI YIKIM MEKANİZMALARININ BİRBİRLERİ İLE ETKİLEŞİMLERİNİN MOLEKÜLER DÜZEYDE ARAŞTIRILMASI

Hale Kesim

Moleküler Biyoloji, Genetik ve Biyomühendislik, Yüksek Lisans Tezi, 2021

Tez Danışmanı: Doç. Dr. Özlem Kutlu

Anahtar kelimeler: Lipid Damlacıkları, İktiyoz, Lipoliz, Şaperon aracılı otofaji, Lipofaji

Hücreler tarafından fazla miktarda alınan lipitler, lipotoksisiteyi önlemek amacı ile lipit damlacıkları (LD'ler) adı verilen bir organelde nötr lipidler olarak depolanırlar. Son yıllarda, bu damlacıkların lipid metabolizmasında, hücre sinyal mekanizmasında ve membran trafiğindeki önemi, LD yüzeyinde tanımlanan 150'den fazla protein ile kanıtlanmıştır. Hücrelerde bir enerji ihtiyacı meydana geldiğinde bu damlacıklar enerji kaynağı olarak kullanabilmektedir. Bu sebeple LD'lerin yıkımı lipoliz, şaperon aracılı otofaji (CMA) ve lipofaji olmak üzere üç temel mekanizma ile gerçekleştirilir. Otozomal resesif konjenital iktiyoz (ORKİ), pullu deri, dehidrasyon ve elektrolitik dengesizlik ile sonuçlanan sendromik olmayan bir iktiyoz şeklidir. ORKİ hastalığına neden olan birçok genin anormal lipid metabolizmasına dahil olduğu ve LD birikimi ile ilişkili olduğu kanıtlanmıştır. Patatin benzeri fosfolipaz alanı içeren-1 (PNPLA-1), fosfolipid metabolizmasında yer alan bir proteindir ve bu gende meydana gelen bir mutasyon ORKİ patolojisinin gelişmesine neden olmaktadır. Bu yüksek lisans tezinde PNPLA1 gen mutasyonlarının LD metabolizması üzerindeki etkisinin daha iyi anlaşılması için LD katabolik yolakları ve bunların etkileşimleri araştırılmıştır. Bu nedenle, p.D172N mutasyonuna sahip ORKİ hastalarından elde edilen fibroblast hücrelerinin lipoliz, CMA ve lipofaji mekanizmaları analiz edilmiştir. Sağlıklı fibroblast hücreleri ile kıyaslayarak ORKİ hastalarının fibroblast hücrelerinde lipoliz, lipofaji ve CMA ile ilişkili proteinlerle LD'lerin lokalizasyonu incelenmiştir. İlgili proteinler farklı floroforlar ile işaretlenerek konfokal mikroskopi altında analiz edilmiştir. Ek olarak, protein ekspresyonlarını belirlemek için immunoblot yöntemi kullanılırken gen düzenlemesindeki değişiklikleri belirlemek amacı ile RT-qPCR analizleri yapılmıştır. Sonuç olarak, ORKİ hasta hücrelerinde PNPLA1 gen mutasyonunun, kusurlu lipoliz ve lipofaji mekanizması nedeniyle anormal LD birikimi ve boyutları gösterdiği bulunmuştur. Bu sonuçlar, LD'lerin yıkım mekanizmalarının regülasyonunda PNPLA1 proteininin önemli bir rolü olduğunu ortaya koymaktadır.

ACKNOWLEDGEMENTS

I would like to express my deepest gratitude to my supervisor Assoc. Prof. Özlem Kutlu for her endless support, understanding, and patience. She was always there for me whenever I needed or had a problem and provided me with a wide variety of opportunities during my master. I am also grateful for her guidance and encouragement. It was a pleasure working under her supervision.

I would like to thank my thesis committee members, Assist. Prof. Sibel Çetinel and Assoc. Prof. Emrah Şefik Abamor for being my committee member, evaluating my thesis, and giving valuable feedbacks about my work and my thesis. I am also thankful to Sibel Çetinel since, during my master, she always helped me whenever I needed any chemical or any technical support.

Furthermore, this thesis was supported by TUBITAK-1001 with project number 118Z134. Therefore, I would like to thank TUBITAK (The Scientific and Technological Research Council of Turkey) for financially supporting me and my master project.

For their support and friendship, I would like to thank to my labmates; Hümeyra Nur Kaleli, Gizem Çelebi, Abuzer Alp Yetişgin, Veysel Oğulcan Kaya, Hande Eda Şutova, Atike Seyitoğlu, Sevilay Burcu Şahin, Saliha Durak and Ebru Demir. I would like to give grateful thanks to Hümeyra Kaleli for her patient, friendship, and endless support. She was a great friend and great teacher for me, and I learned cell culture basics from her. I would like to express my special thanks to Gizem Çelebi for their support, friendship, help, and also for being my quarantine friend. We worked hard but we also had a lot of fun and crazy memories together.

Moreover, I am also thankful to have great friends in Sabanci University; Esra Şengül, Asuman İnan, Sezgin Mengi, Begüm Büyüksavaş, Barış Batuhan Topal, Beril Üstünkaya, Ayhan Parlar. I especially thank to Esra Şengül, Asuman İnan and Sezgin Mengi for their endless help and great friendship. Quarantine was sufferable and more fun with you. I will miss our tea and coffee meetings. I would like to thank my friends Can Egil, Bükre Kıran Üner, Paula Sanchez, Ezgi Berfin Çeper, İdil İlkcan Kayı, Meryem Bakır, Ayşenur Arslan and Ogün Aygün who have always been and continue to be by my side. I am very lucky to have amazing friends like you.

Lastly, I would like to express my appreciation and many thanks to my mother Leman Kesim, my father Hasan Kesim, and my sister Hande Kesim for their endless support, trust, and love. They have always been by my side, and I am sure that they will always be by my side no matter what happens. I am so grateful to have a great family like you.

TABLE OF CONTENTS

LIST OF FIGURES

LIST OF TABLES

LIST OF SYMBOLS AND ABBREVIATIONS

α	Alpha
β	Beta
µ	Micro
µl	Microliter
µM	Micromolar
ω	Omega
ABCA12	Atp Binding Cassette Subfamily A Member 12
ACAT	Cholesterol Acyltransferase Enzymes
ACSL	Long-Chain Fatty Acid Coa Ligases
AGPAT	1-Acylglycerol-3-Phosphate-O-Acyltransferase
ALOX12B	Arachidonate 12-Lipoxygenase
ALOXE3	Arachidonate Lipoxygenase 3
AMPK	AMP-Activated Protein Kinase
ARCI	Autosomal Recessive Congenital Ichthyosis
ATG	Autophagy-Related Protein
ATGL	Adipose Triglyceride Lipase
AUP1	Ancient Ubiquitous Protein 1
BAG-1	Bcl-Associated Athonogene 1
Bif-1	Blood-Inducing Factor 1
BSA	Bovine Serum Albumine
C.*elegans*	*Caenorhabditis Elegans*
CASP14	Caspase 14
CCCP	Carbonyl Cyanide M-Chlorophenyl Hydrazone

CERS3	Ceramide Synthase 3
CGI-58	Comparative Gene Identification-58
CMA	Chaperone-Mediated Autophagy
CQ	Chloroquine
CYP4F22	Cytochrome P450 Family 4 Subfamily F Member 22
DAG	Diacylglycerol
DGAT	Diglyceride Acyltransferase
DMEM	Dulbecco's Modified Eagle Medium
EDTA	Ethylenediaminetetraacetic Acid
EF1α	Elongation Factor 1 Alpha
ER	Endoplasmic Reticulum
FIT	Fat Storage-Inducing Transmembrane Proteins
GFAP	Glial Fibrillary Acidic Protein
GFP	Green Fluorescent Protein
GPAT	Glycerol-3-Phosphate Acyltransferase
HIP	Hsc70-Interacting Protein
HOP	Hsc70-Hsp90 Organizing Protein
Hsc70	Heat Shock Cognate 70 Kda Protein
HSL	Hormone-Sensitive Lipase
Hsp90	Heat Shock Protein 90
LAMP2	Lysosome-Associated Membrane Protein 2
LC3	Microtubule-Associated Proteins 1A/1B Light Chain 3B
LD	Lipid Droplet
LIPN	Lipase Family Member N

LIR	LC3-Interacting Region
MAG	Monoacylglycerol
MAGL	Monoacylglycerol Lipases
MAPK	Mitogen-Activated Protein Kinase
MEM	Minimal Essential Medium
mTOR	Mammalian Target Of Rapamycin
NaCl	Sodium Chloride
NaOH	Sodium Hydroxide
NIPAL4	NIPA Like Domain Containing 4
OA	Oleic Acid
PAP	Phosphatidate Phosphatase
PBS	Phosphate-Buffered Saline
PC	Phosphatidylcholine
PE	Phosphatidylethanolamine
Pex30	Peroxisomal Membrane Protein 30
PFA	Paraformaldehyde
PHLPP1	Ph Domain And Leucine Rich Repeat Protein Phosphatase 1
PI	Phosphatidylinositol
PI3K	Phosphoinositide 3-Kinase
PI3P	Phosphatidylinositol 3-Phosphate
PKA	Protein Kinase A
PKC	Protein Kinase C
PLIN	Perilipin
PMSF	Phenylmethylsulfonyl Fluoride

PNPLA	Patatin-Like Phospholipase Domain Protein
PS	Phosphatidylserine
Rab7	Ras-Related Protein Rab7
RARα	Retinoic Acid Receptor Alpha
RFP	Red Fluorescent Protein
RT	Room Temperature
SDR9C7	Short Chain Dehydrogenase/Reductase Family 9C Member 7
SDS	Sodium Dodecyl Sulfate
SE	Sterol Ester
SIRT1	Sirtuin 1
SLC27A4	Solute Carrier Family 27 Member 4
SM	Sphingomyeline
SNARE	Soluble N-Ethylmaleimide-Sensitive Factor Attachment Protein Receptor
TAG	Triacylglycerol
TFEB	Transcription Factor EB
TGM1	Transglutaminase 1
ULK1	Unc-51 Like Autophagy Activating Kinase 1
VPS34	Phosphatidylinositol 3-Kinase Catalytic Subunit Type 3
WIPI1-4	Wd Repeat Domain Phosphoinositide-Interacting Protein 1-4

1. INTRODUCTION

1.1. Lipid Droplets

Lipids are one of the fundamental components of cells for various organisms. However, when there is an excessive amount of lipids, these lipids cause a lipotoxic effect in the cells. Therefore, they are converted to neutral lipids and stored in a specific organelle called lipid droplets (LDs). The existence of LDs has been identified with the early years of light microscopy (Jarc & Petan, 2019; Walther & Farese, 2012; Xu, Zhang, & Liu, 2018). In the beginning, they were known as inert depots, which can be used in the absence of an energy source for producing energy and surviving. Surprisingly, proteomic analysis of LDs revealed that apart from being inert depots, they also have important roles in the cells such as maintaining energy homeostasis, protein degradation and storage, membrane trafficking, and cell signaling (Cohen, 2018; Meyers, Weiskittel, & Dalhaimer, 2017; Ohsaki, Suzuki, & Fujimoto, 2014; Xu et al., 2018). Moreover, it was known that LDs can be a platform for viral replication, and the required energy for this process can be supplied from them (Renne, Klug, & Carvalho, 2020; Welte, 2015).

LDs are unique and dynamic organelles derived from the endoplasmic reticulum (ER) and conserved for many years among various organisms (Hugenroth & Bohnert, 2020; Renne et al., 2020). They consist of a hydrophobic core that is surrounded by a phospholipid monolayer with a vast number of proteins **(Fig.1-1).** Their cores contain neutral lipids, predominantly triacylglycerol (TAG) and sterol esters (SE). Dependent on the cell type, the ingredient and the ratio of the core components might differ. Furthermore, LDs can store other endogenous neutral lipids such as retinyl esters, ether

lipids, waxes, and free cholesterols (Gao, Huang, Song, & Yang, 2019; Gizem Onal, Kutlu, Gozuacik, & Dokmeci Emre, 2017; Walther, Chung, & Farese, 2017).

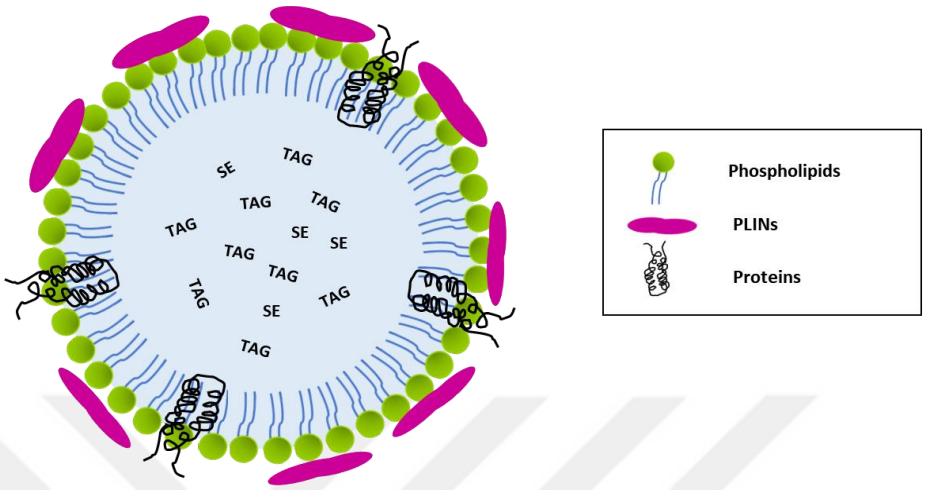

Figure 1-1: Structure of Lipid Droplets. LDs are an organelle which, consists of a hydrophobic core storing neutral lipids such as TAG and SE surrounded by a phospholipid monolayer. Additionally, PLIN proteins are located on these droplet surfaces and they protect LDs from degradation. Other types of proteins involved in lipid metabolism, membrane trafficking, and signaling can be found on LD surfaces.

In LDs, the composition of their membranes is also crucial and has an effect on their synthesis, maturation, and catabolism through the lipophagy pathway. It was reported that the changes in the ratio between these components affect the regulation of the droplets (Gizem Onal et al., 2017). Unlike other cell membranes, the surface of LDs possesses a monolayer membrane structure that comprises amphiphilic lipids, which are generally phospholipids. In mammalian cells, their membranes are mainly constituted from phosphatidylcholine (PC) and that's followed by phosphatidylethanolamine (PE), phosphatidylinositol (PI), phosphatidylserine (PS), sphingomyelin (SM), lyso-PC, and lyso-PE. They can also have free cholesterol and phosphatidic acid in little amounts (Olzmann & Carvalho, 2019; Gizem Onal et al., 2017; Walther et al., 2017). In the structure, the acyl group of these phospholipids interacts with the hydrophobic core lipids of LDs, while their polar groups interact with the cytosol. Thus, the hydrophilic surface of the droplets enables the movement of the core components throughout the cytoplasm. Moreover, these membrane phospholipids act as surfactants with decreasing the surface

tension of LDs therefore, increasing the stability of the droplet in aqueous environments (Meyers et al., 2017; Olzmann & Carvalho, 2019).

LD surfaces are decorated with a wide variety of proteins and proteomic analysis conducted using different species showed that over 150 proteins reside on these droplets. According to their functions, the proteins can be classified into subgroups (Gizem Onal et al., 2017). In mammalian cells, LD surfaces are mostly composed of LD structural proteins that regulate their functions and help to preserve their morphology. These proteins mostly consist of PAT family members PLIN, or perilipin, that have 5 members in mammals (PLIN1-5). PLINs are the key proteins protecting the LDs from lipolysis by inhibiting the access of lipases into the LDs core (Nettebrock & Bohnert, 2020; Gizem Onal et al., 2017). In contrast to PLIN2 and PLIN3 that are expressed in all the tissue types, the expression of other PLINs can be limited with some tissues. Additionally, PLINs can be either cytosolic or localized (PLIN1 and PLIN2) on the LD surfaces (Sztalryd & Brasaemle, 2017; Xu et al., 2018).

Another type of proteins found on LDs are lipid metabolism-related proteins such as long-chain fatty acid CoA ligases (ACSL), diacylglycerol transferase enzymes (DGATs), and acyl-CoA: cholesterol acyltransferase enzymes (ACATs), which are functioning in LD biogenesis, patatin-like phospholipase domain protein 2 (PNPLA2), hormone-sensitive lipases and monoacylglycerol lipases (MAGLs) that are functioning in LD breakdown (Gizem Onal et al., 2017; Xu et al., 2018). LDs also have proteins regulating membrane trafficking such as Rab proteins and SNARE (soluble N-ethylmaleimide-sensitive factor attachment protein receptor) that assists the LD fusion. Moreover, signaling proteins (such as MAPKs, PKC, and PI3K) and proteins mediate protein degradation. For example, ancient ubiquitous protein 1 (AUP1) has been shown to localize on LDs (Gizem Onal et al., 2017; Spandl, Lohmann, Kuerschner, Moessinger, & Thiele, 2011; Xu et al., 2018). In addition to these protein subgroups, there are ribosomes proteins, histones, and cytoskeletal proteins that have been shown to find on LDs (Jones, 2012; Gizem Onal et al., 2017; Xu et al., 2018; Zehmer et al., 2009).

The formation of LDs can be taken place via fission of preformed LDs or de novo in ER. The process can be induced when there are excess free fatty acids inside the cells. LD biogenesis is initiated by the synthesis of neutral lipids and requires the activation of free

fatty acids by coenzyme A synthetase (esterification of free fatty acids to acyl-CoA)(Cohen, 2018; Gizem Onal et al., 2017; Schuldiner & Bohnert, 2017). In mammals, TAG synthesis is a multistep enzymatic process and requires the enzymes glycerol-3-phosphate acyltransferase (GPAT), 1-acylglycerol-3-phosphate-O-acyltransferase (AGPAT), phosphatidate phosphatase (PAP), diglyceride acyltransferase (DGAT). In the end, activated free fatty acids, acyl-CoAs, are turned into TAGs with the help of DGAT1 and DGAT2 enzymes. On the other hand, SE synthesis is taken place through acetyl-CoA cholesterol acetyltransferases ACAT1 and ACAT2 (Gao et al., 2019; Ohsaki et al., 2014; Gizem Onal et al., 2017; Wilfling, Haas, Walther, & Farese, 2014).

The synthesis of TAG or SE is enough to start the formation of LDs. Due to their hydrophobic nature, these synthesized neutral lipids disperse into the leaflets of ER, however, when their concentrations exceed a critical point, they start to coalesce and form oil lens-like structures at the distinct sites of ER due to demixing (Henne, Reese, & Goodman, 2019; Hugenroth & Bohnert, 2020; Olzmann & Carvalho, 2019; Renne et al., 2020). These lenses might fuse since the surface-to-volume ratio is decreased when they fuse into larger lenses. Hence, the cytosolic leaflets of ER initiate budding through the cytosol named as directional budding. In this process, ER membrane lipid content, surface tension, line tension, and monolayer curvature are crucial mediators (Gao et al., 2019; Renne et al., 2020). Additionally, fat storage-inducing transmembrane proteins (FIT), seipin, Pex30, and PLIN1 have been shown to indicate the site of biogenesis and assist the budding. It was shown that mutated proteins have an impact on LD formation efficiency and their morphologies (Barneda & Christian, 2017; Nettebrock & Bohnert, 2020; Olzmann & Carvalho, 2019). Moreover, it was revealed that during budding, FIT2 can directly bind to DAG and TAG, supporting the idea that FITs can be an inducer for the budding of LDs through direct interactions with DAG and TAG. However, how these proteins affect LD formation is still not clear (Gross, Zhan, & Silver, 2011; Olzmann & Carvalho, 2019).

After the budding, LDs continue expanding via continuous neutral lipid synthesis in ER, the enzymes found on the droplet surfaces or fusion with the previously formed LDs. Additionally, expansion of LDs requires extra phospholipids necessary for their membranes and that is supplied from ER membranes. During the expansion, LD-specific proteins start to localize on the droplet surfaces. In the last step, newly formed LDs can

stay in contact with ER or can be released into the cytosol (Olzmann & Carvalho, 2019; Gizem Onal et al., 2017; Renne et al., 2020).

1.2. Catabolic pathways of LDs

1.1.1. Lipolysis

Cells can use lipids as an energy source when they have metabolic needs. However, TAGs cannot pass into the cells without their hydrolysis to free fatty acids, therefore, they undergo a process called lipolysis (Kong et al., 2020; R. Zechner et al., 2012). Lipolysis is a catabolic process, in which TAGs are degraded to glycerol and three fatty acids by cytoplasmic lipases. Additionally, TAGs, stored inside the LDs, can be hydrolyzed via neutral lipolysis at pH~7 (Rudolf Zechner, Madeo, & Kratky, 2017; Zembroski & Buhman, 2020). There are three lipases important for this process, which are adipose triglyceride lipase (ATGL/PNPLA2), hormone-sensitive lipase (HSL), and monoacylglycerol lipase (MAGL), respectively. They result in the sequential hydrolysis of TAGs to their constituents. ATGL has a strong activity to hydrolyze TAG and weak activity on retinyl esters, whereas, HSL has high activity on DAG (diacylglycerol) and cholesterol esters and less activity on TAG, MAG (monoacylglycerol), and retinyl esters (Jarc & Petan, 2019; Sztalryd & Brasaemle, 2017; C.-W. Wang, 2016; T. Wang et al., 2020).

During basal or fed conditions, ATGL and HSL are predominantly found in the cytoplasm, however, MAGL, perilipin 1, and ATGL co-activator CGI-58 (comparative gene identification-58) bind to LD surface (Meyers et al., 2017). Perilipin 1 stimulates the storage of TAGs and protects their lipolysis through the binding to CGI-58 (Dalhaimer, 2019; Sztalryd & Brasaemle, 2017; Walther & Farese, 2012). Under starvation conditions, the nutrient-sensing signaling pathways trigger the activation of protein kinase A (PKA) via its phosphorylation, and this results in the phosphorylation of perilipin 1 at two serine residues (S492 and S517), leading to the release of CGI-58 into the cytoplasm (Meyers et al., 2017; Thiam, Farese Jr, & Walther, 2013; Yu & Li, 2017). Subsequently, ATGL localizes to LD surfaces during the stimulation of lipolysis and

CGI-58 binds to the N-terminus of ATGL to active the lipases for the hydrolysis of TAG (Meyers et al., 2017; Thiam et al., 2013). As a result, activated ATGL hydrolyzes the TAGs to diacylglycerols (DAGs) and a fatty acid. On the other hand, activated PKA also phosphorylates HSL at the residues S855 and S951, therefore, leading to its activation. HSL is the rate-limiting factor in the hydrolysis of DAG, and with the phosphorylation of perilipin 1, activated HSL is recruited to the LD surfaces, resulting in the hydrolysis of DAGs to monoacylglycerols (MAGs) and a fatty acid(Meyers et al., 2017; Gizem Onal et al., 2017; Zembroski & Buhman, 2020). In the final step, glycerol and free fatty acid are produced from MAG and this process is catalyzed by monoacylglycerol lipases (MAGL). Since MAGs are released to the cytoplasm, their hydrolysis is taken place in the cytoplasm, therefore MAGLs are not bound to the LD surfaces and act in the cytosol during lipolysis (Gizem Onal et al., 2017; Thiam et al., 2013; Walther & Farese, 2012). **(Fig. 1-2)**. In adipose tissues, lipolysis products can be released to the bloodstream and used as a substrate for β-oxidation to produce energy. However, in the other tissues, these can be directly consumed inside the cells with β-oxidation through mitochondria or peroxisomes (D'Andrea, 2016; Gizem Onal et al., 2017).

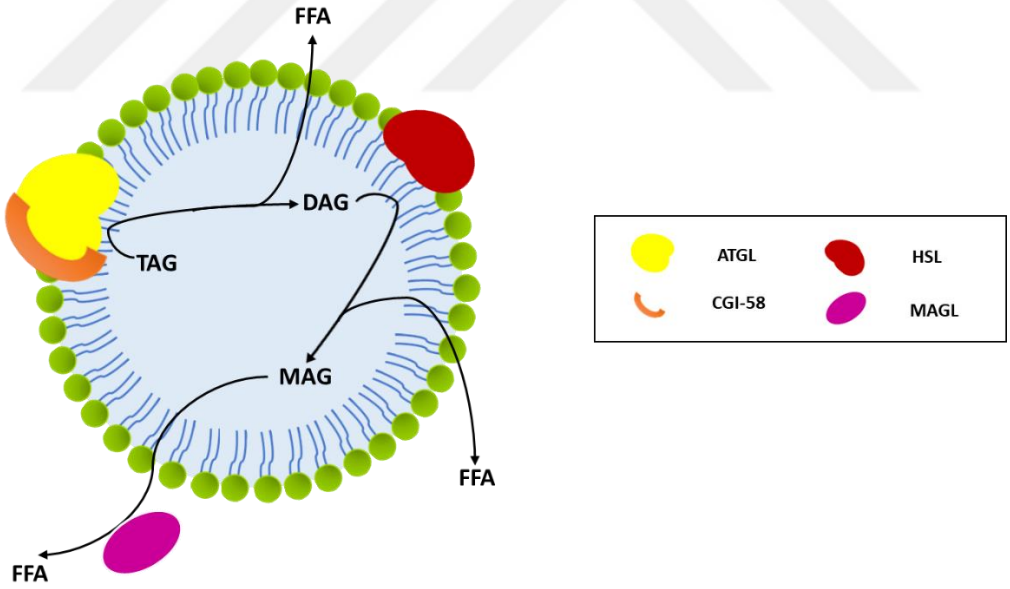

Figure 1-2: Lipolysis of Lipid Droplets. When ATGL is activated with the help of its coactivator CGI-58, it localizes on LD surface and turns TAG into DAG and free fatty acid (FFA). Subsequently, DAG is hydrolyzed to MAG and FFA via HSL. Lastly, MAG is released to the cytoplasm and degraded to FFA by MAGL.

1.2.1. Autophagy

Autophagy is a well-known catabolic process that contributes to maintaining cell homeostasis via the removal of dysfunctional organelles and macromolecules from the cell. The major goal of the process is recycling essential nutrients into cells for reuse in critical cellular processes under stress conditions such as nutrient deprivation, oxidative stress, and growth factor deficiency. For this reason, cytoplasmic materials are degraded by lysosomes. There are 3 main autophagic pathways; namely, macroautophagy, microautophagy, and chaperon-mediated autophagy (CMA) (Dikic & Elazar, 2018; Kocaturk et al., 2019).

In microautophagy, a portion of the cytoplasm is engulfed by lysosomal membranes, and these components are degraded via lysosomal enzymes. In the second autophagic pathway CMA, proteins that have KFERQ motifs are selectively targeted to lysosomes via chaperon proteins, eventually leading to selective degradation of these proteins (Y. Yang & Klionsky, 2020).

Macroautophagy is one of the major catabolic pathways and in this pathway, double-membrane vesicles, which are called autophagosomes form and engulf the targeted substrate. Macroautophagy can be either selective or bulk. A part of the cytoplasm is targeted non-selectively for degradation in the bulk autophagic pathway. In contrast, selective autophagy targets specific cellular components such as mitochondria, ER, and ribosomes for their specific degradation via autophagic machinery (Kocaturk et al., 2019; Y. Yang & Klionsky, 2020). Macroautophagy takes place in 5 steps: initiation, nucleation of the membrane, phagophore formation and expansion, autophagosome-lysosome fusion, and degradation of cargo inside autolysosome **(Fig 1-3)** (Hansen, Rubinsztein, & Walker, 2018; Kocaturk et al., 2019).

Autophagy is regulated via cellular sensors important in maintaining the energy homeostasis of cells, which are AMP-activated kinase (AMPK) and the mechanistic target of rapamycin (mTOR). Under stress conditions, the mTOR complex is inhibited whereas, AMPK is activated due to the change in ATP/ADP ratio, which subsequently leads to activation of Unc-51-like kinase 1 (ULK1) initiation complex through

phosphorylation. Thus, the class III phosphatidylinositol 3-kinase (PI3K) complex becomes activated via the ULK1 initiation complex and this complex stimulates membrane nucleation. VPS34, which is a component of PI3K complex, mediates the production of phosphatidylinositol 3-phosphate (PI3P) that is critical in the recruitment of phosphatidylinositol 3-phosphate (PI3P)-binding domain-containing autophagic proteins such as WIPI1–4 and DFCP1, during phagophore formation. Recruitment of PI3P-binding domain-containing proteins results in the binding of other types of autophagy-related proteins (ATGs) that are responsible for membrane expansion and autophagosome formation (Dikic & Elazar, 2018; Hansen et al., 2018; Kocaturk et al., 2019).

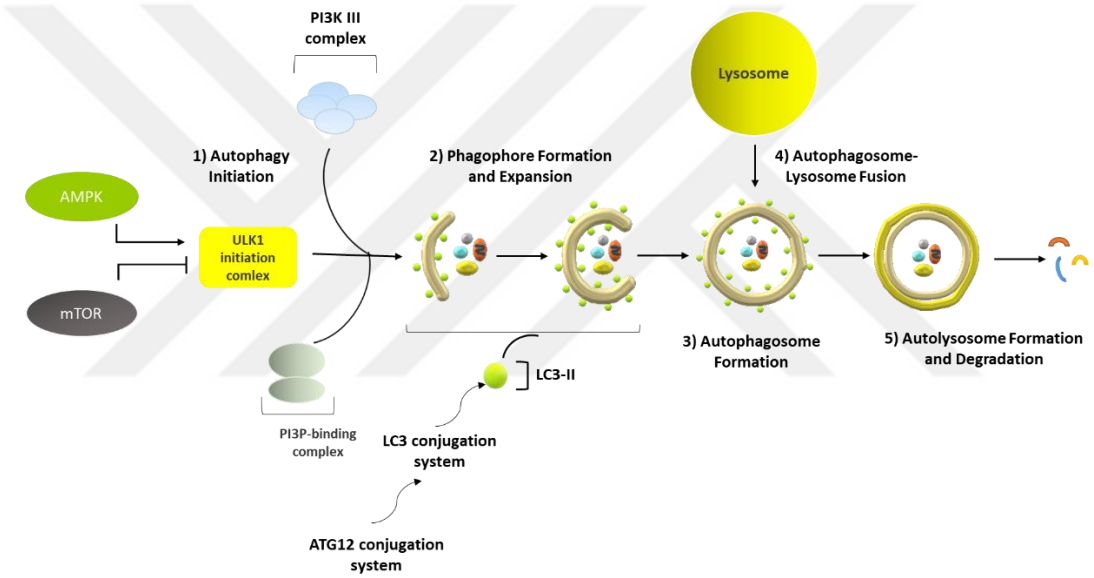

Figure 1-3: Mechanism of Macroautophagy. Under stress or starvation conditions, with the help of AMPK activation and mTOR inhibition, autophagy is initiated. Subsequently, membrane nucleation is taken place and phagophore is formed around the substrate to be degraded. When phagophore is extended and form autophagosome, this autophagosome fuses with lysosome, forming autolysosomes. In the last step, the substrate is degraded inside the autolysosomes via lysosomal enzymes.

In phagophore expansion, two ubiquitin-like conjugation systems are important. In the first system, ATG7 and ATG10 act as E1 and E2 conjugating enzymes. These enzymes catalyze the generation of the ATG12 conjugation system that acts as an E3-like enzyme for the LC3 conjugation system. In the LC3 conjugation system, LC3 is cleaved via ATG4

to form LC3-I and this stimulates the conjugation of phosphatidylethanolamine (PE) to the protein, resulting in LC3-II formation. Subsequently, the lipidated form of LC3 is integrated into autophagosomal membranes and this leads to autophagosome formation. After autophagosome formation, it fuses with lysosomes, and formed autolysosomes. In autolysosomes, targeted molecules are degraded via lysosomal enzymes and essential components are recycled into cells (Hansen et al., 2018; Kocaturk et al., 2019).

1.2.1.1. Lipophagy

Recent studies proved the relation between autophagy and lipid droplets catabolism, and lipophagy was described as a type of selective macroautophagic pathway that recognizes and degrades LDs inside the cells (Kloska, Węsierska, Malinowska, Gabig-Cimińska, & Jakóbkiewicz-Banecka, 2020; G. Onal et al., 2019; Schott et al., 2019). This pathway is firstly identified in mouse hepatocytes under starvation conditions. LD accumulation and a reduction in the β-oxidation of TGs were detected, when lipophagy was inhibited chemically (with 3-methyladenine) or genetically (via knocking down of *ATG7* and *ATG5*) in these cells. In the same study, knocking down of *ATG5* in mouse embryonic fibroblast cells was increased the TG content of the cells, confirming that autophagy blockage effects and inhibits LD breakdown. Additionally, electron microscopy analysis was proved the lipophagic degradation of LDs via LC3 immunogold staining (Gizem Onal et al., 2017; Singh et al., 2009). The role of lipophagy in LDs breakdown was confirmed using different species and cell types such as yeasts, *C. elegans*, macrophages, neurons, T cells, fibroblast, and prostate carcinoma cells showing that lipophagy is a ubiquitous and conserved mechanism among a variety of species (M. B. Khawar, Gao, & Li, 2019; Martinez-Lopez & Singh, 2015; Ward et al., 2016).

The exact mechanism of how LDs are recognized in lipophagy is not completely understood. However, huntingtin might be a candidate receptor for this recognition, since it has a role in the association of p62 with LC3-II and inducing the lipophagy activation through the release of ULK1 from the mTOR-ULK1 complex under stress conditions (Kounakis, Chaniotakis, Markaki, & Tavernarakis, 2019; Rui et al., 2015). Additionally, Rab protein family members, especially Rab7 (Ras-related Protein Rab-7), have been shown to play important roles in lipophagy. Rab7 is a key regulator for late endocytic

membrane fusion and autophagosome maturation via assisting the association of many SNARE proteins and the members of the HOPS tethering complex (Kloska et al., 2020; Schulze, Sathyanarayan, & Mashek, 2017). A study with hepatocytes was revealed that Rab7 and LD association is increased when the lipophagy is induced during nutrient deficiency. A mutant version of Rab7, which has a GTP-binding deficiency, is led to LD accumulation in the same cells, suggesting that Rab7 might be a critical LD-localized protein regulating hepatocellular lipophagy (Schroeder et al., 2015; Schulze et al., 2017). Additionally, it was shown that Rab7 does not directly interact with PLIN1 in adipocytes, however, PLIN1 suppresses lipophagy by inhibiting the binding of Rab7 to the LD surfaces (Lizaso, Tan, & Lee, 2013). Later, it was found that lipophagy stimulation induces degradation of PLIN1 in Bif-1 (blood-inducing factor 1)-dependent manner, and TG breakdown is decreased in Bif-1 defective cells, suggesting Bif-1 might be another candidate affecting lipophagy regulation (Muhammad Babar Khawar et al., 2021; Y. Liu et al., 2016; Gizem Onal et al., 2017).

Lipophagy and lipolysis are not completely independent pathways, and research has proven an association between lipophagy, HSL, and ATGL in LD breakdown. It was shown that ATGL has an LC3-interacting region (LIR) and LC3 can interact with this protein at the LD surfaces through binding to the residues in the LIR. Under serum deficiency, ATGL lacking the LIR is failed to translocate to the surface of LDs, confirming that LC3 plays an important role in the ATGL translocation and hence the degradation of TAGs (Cui et al., 2021; Martinez-Lopez et al., 2016; Sathyanarayan, Mashek, & Mashek, 2017; Schulze et al., 2017). Additionally, it was revealed that lysosome and LC3 association with LDs are enhanced via ATGL in hepatocytes and this lipase can stimulate lipopagy by inducing the activity of SIRT1, which is an important autophagy regulator (Sathyanarayan et al., 2017). Knocking down of ATGL in macrophages resulted in a reduction in the lipophagy activity, showing that ATGL mediates the regulation of LD degradation through lipophagy. Furthermore, PNPLA5 has been shown to induce lipophagy in different types of cells through generating DAG for the synthesis of the autophagosome membranes (M. B. Khawar et al., 2019; Schulze et al., 2017).

1.2.1.2. Chaperone-Mediated Autophagy

Cellular proteins are continuously in a cycle of synthesis and degradation to maintain protein homeostasis for the important cellular events. For this reason, recycling their constitutive amino acids is also crucial and can be achieved by several mechanisms through proteasomes or lysosomes (Cuervo & Wong, 2014; Kaushik & Cuervo, 2012; W. Li et al., 2019). They can be degraded in lysosomes via different autophagic pathways such as macroautophagy, microautophagy, and chaperone-mediated autophagy (CMA). However, CMA has a characteristic mechanism separated from other autophagic pathways, since substrate proteins are directly targeted to the lysosomes without any vesicle formation (Tasset & Cuervo, 2016; Q. Yang, Wang, & Zhu, 2019). Additionally, proteins are the only substrates and these substrates are targeted one by one for the degradation with high selectivity (Kaushik & Cuervo, 2015; Kaushik & Cuervo, 2018).

CMA takes place in several steps, which are substrate identification and targeting lysosomes, translocation to the lysosomal lumen, and degradation by lysosomal proteases. Previous studies proved that not all proteins can be a substrate for this pathway and the proteins that have a special motif, called KFERQ-like motif, can be targeted (Cuervo & Wong, 2014; Lescat et al., 2020). This motif is flanked by a glutamine (Q) and consists of one or two positively charged amino acids like lysine (K) or arginine (R), one or two of the hydrophobic amino acids like leucine (L), isoleucine (I), valine (V), or phenylalanine (F), and one of the negatively charged amino acids like glutamic acid (E) or aspartic acid (D) (Tekirdag & Cuervo, 2018; Q. Yang et al., 2019). Interestingly, proteins can complete their motifs later by undergoing phosphorylation, which contributes negatively charged residue, or acetylation of K, which acts as Q (Cuervo & Wong, 2014; Kaushik & Cuervo, 2018; Q. Yang et al., 2019). Furthermore, KFERQ-motif can be located in the N-terminal, C-terminal, or center of the proteins, however, for CMA activation, this motif should be easily recognizable by Hsc70 chaperones (Kaushik & Cuervo, 2012). The motif is recognized and targeted to the lysosomal surface via heat shock cognate 70 kDa protein (Hsc70), a cytosolic chaperone, with the help of cochaperones such as Hsp90, Hsp40, carboxyl terminus of Hsc70-interacting protein (HIP), Hsc70-Hsp90 organizing protein (HOP), and Bcl-associated athonogene 1 protein (BAG-1) (Juste & Cuervo, 2019; Kaushik & Cuervo, 2018; Q. Yang et al., 2019).

After targeting, the cytosolic part of the lysosome-associated membrane protein 2A (LAMP2A) interacts with the substrate. During binding, the protein is found in its monomeric form, however, multimerization of LAMP2A is necessary for the substrate translocation. Moreover, the Hsp90 protein interacts with this newly formed multimeric complex and helps to stabilize it. The unfolding of targeted protein is required for its translocation to the lysosomal lumen, even though it is not necessary for LAMP2A binding (Cuervo & Wong, 2014; Kaushik & Cuervo, 2018; Tekirdag & Cuervo, 2018). To complete the translocation, a form of Hsc70 that resides in the lysosomal lumen is also crucial and mediates the process. After substrate reaches the lysosomal lumen, it is immediately degraded into their amino acids by lysosomal lumen proteases called cathepsin, and multimeric complex disassembles (Juste & Cuervo, 2019; Tekirdag & Cuervo, 2018).

The activity of CMA is dynamically changed according to the conditions and increased during the stress conditions such as nutrient starvation, oxidative stress, and hypoxia (Kaushik & Cuervo, 2018). Therefore, the pathway is under the control of different signaling pathways and molecules. Glial fibrillary acidic protein (GFAP) and elongation factor 1 alpha (EF1α) modulate the process coordinatively in a GTP-dependent manner. GFAP associates with the multimeric complex and stabilizes it. Additionally, a phosphorylated form of GFAP (pGFAP) binds to EF1α, which is located at the lysosomal membrane. When GTP is present, EF1α is released. Since the affinity of GFAP to pGFAP is higher than to the multimeric complex, it leaves from the translocation complex and forms a dimer with pGFAP, leading to disassembly of the translocation complex (Cuervo & Wong, 2014; Juste & Cuervo, 2019; Kaushik & Cuervo, 2012; Tekirdag & Cuervo, 2018).

CMA is also regulated through mTORC2/AKT1/PHLPP1 signaling pathway. In this pathway, Akt1 leads to the phosphorylation of GFAP at the lysosomal membrane, resulting in the inhibition of CMA. Moreover, Akt1 activity is associated with mTORC2 and PHLPP1 activity. Akt1 phosphorylated by mTORC2 causes the phosphorylation of GFAP, whereas, PHLPP1 leads to dephosphorylation of AKT1 and further dephosphorylation of GFAP, increasing CMA activity (Kaushik & Cuervo, 2018; Tekirdag & Cuervo, 2018; Q. Yang et al., 2019). In addition to this, it was shown that retinoic acid receptor alpha (RARα) signaling adversely regulates CMA, and inhibition

of this receptor family with chemical compounds like all-trans-retinoic acids or genetically has resulted in an enhanced CMA activity (Anguiano et al., 2013; Kaushik & Cuervo, 2018; W. Li et al., 2019).

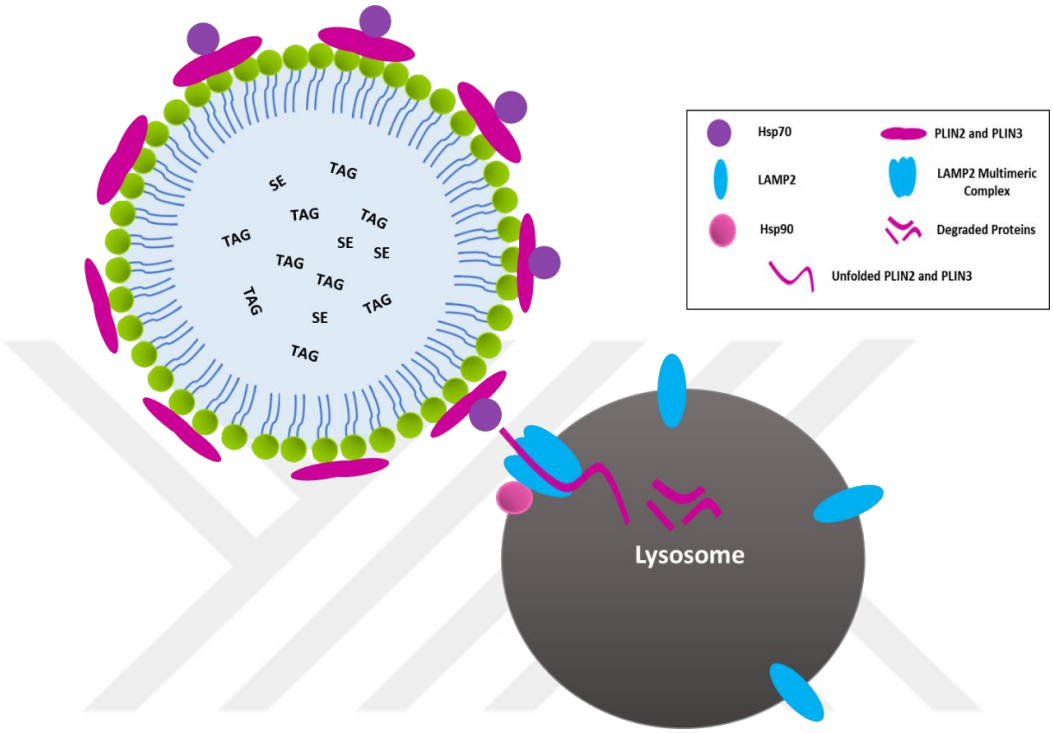

Figure 1-4: Chaperone-mediated autophagic degradation of PLIN2 and PLIN3. PLIN2 and PLIN3 that have KFERQ-like motifs are recognized by Hsc70 proteins and targeted to lysosomes for their degradation. When these proteins are delivered to the lysosomes, they are recognized by LAMP2 proteins, and subsequently, LAMP2 multimerization complex is formed for translocation of the substrate proteins. For the translocation, the proteins need to be unfolded. After unfolding, these proteins are translocated into lysosomes via the multimeric complex that is stabilized by hsc90 proteins and is degraded with the help of lysosomal enzymes.

In recent years, the importance of CMA on LDs catabolism has been proved. The findings showed that LD coat proteins PLIN2 and PLIN3 have the KFERQ-like motifs (LDRLQ and SLKVQ respectively) in their sequences and can be removed via CMA (Roberts & Olzmann, 2020; Martina Schweiger & Zechner, 2015). Interestingly, blocking of CMA has resulted in attenuated interaction of ATGL and lipophagy proteins with LDs, causing the accumulation of these droplets inside the cells. Additionally, under nutrient

deficiency, the degradation of PLIN2 and PLIN3 are increased, leading to the enhanced association of ATGL and lipophagy proteins with LDs. It was reported that the levels of PLIN2 and PLIN3 on the LD surface are regulated via CMA and inhibition of this pathway is resulted in an increase in the amount of PLIN2 and PLIN3, which are located on the surface of the droplets (Kaushik & Cuervo, 2015; Kaushik & Cuervo, 2016; Gizem Onal et al., 2017; Martina Schweiger & Zechner, 2015). As a result, when lipolysis is induced, PLIN2 and PLIN3 are recognized by hsc70 and removed from the particular locations on the LD membrane via CMA, leading to the recruitment of ATGL and lipophagy-related proteins for the degradation of LDs. Thus, CMA is critical and acts as an upstream regulator for the degradation of LDs via facilitating the recruitment of lipases and lipophagy proteins (**Fig. 1-4**) (Catarino, Pereira, & Girão, 2017; Roberts & Olzmann, 2020; Ward et al., 2016).

1.3. Autosomal Recessive Congenital Ichthyosis (ARCI) and PNPLA1 Gene

Ichthyosis is a heterogeneous group of Mendelian disorders of cornification disease that causes a defect in the stratum corneum layer of the epidermis and is mostly characterized by dry, scaly skin and hyperkeratosis (Schmuth et al., 2013; Takeichi & Akiyama, 2016; Traupe, Fischer, & Oji, 2014; L. Youssefian et al., 2019). The stratum corneum layer of the skin mainly consists of corneocytes and intercellular lipids that are derived from keratinocytes and these compartments are linked by corneodesmesomes. For the formation of this layer, keratinocytes need to undergo a complex differentiation process, resulting in the cornification of keratinocytes and the formation of lamellar bodies that contain a high amount of intercellular lipids (Feingold & Jiang, 2011; Vahlquist, Fischer, & Törmä, 2018).

In the stratum spinosum layer, lipids and proteins are necessary for maintaining the function of stratum corneum. These lipids are transported to the stratum corneum layer. For this reason, lamellar bodies are formed through the packaging of free fatty acids, cholesterols, and glycosylceramides, as well as several enzymes and antimicrobial peptides. The release of these lamellar bodies to the intercellular spaces occurs in the stratum granulosum layer via the fusion of lamellar bodies with the plasma membrane.

Additionally, cholesterol sulfate found in the cytoplasm can freely diffuse into this intercellular space. Simultaneous with the generation of lamellar bodies, cornified envelope that acts as a scaffold for these bodies is also formed. In this process, loricrin and involucrin are crosslinked together with other structural proteins by transglutaminases, completing the stratum corneum layer formation. Since ARCI cause impairment in stratum corneum, mutations in the many genes that involve in the synthesis and metabolism of epidermal lipids, keratinization differentiation, and stratum corneum maintenance can be associated with ARCI formation (Akiyama, 2017; Feingold & Jiang, 2011; Grall et al., 2012; Murase et al., 2020; Sugiura & Akiyama, 2015; Uitto, Youssefian, Saeidian, & Vahidnezhad, 2020; Vahlquist et al., 2018).

Ichthyosis has two distinct forms; syndromic ichthyosis and non-syndromic ichthyosis. Non-syndromic ichthyosis consists of common ichthyoses and has many subgroups such as autosomal recessive congenital ichthyosis (ARCI) and keranitopathic ichthyosis (Rodríguez-Pazos, Ginarte, Vega, & Toribio, 2013; Takeichi & Akiyama, 2016; Traupe et al., 2014; L. Youssefian et al., 2019). ARCI has 3 major phenotypes: lamellar ichthyosis, congenital ichthyosiform erythroderma, and harlequin ichthyosis, which is the most severe type of ARCI. In all types of ARCI, the disorders are encountered only in the skin, however, some cases can be lethal for the patients. Common symptoms of ARCI types can be listed as scaly skin, dehydration, thermal instability, sepsis, and electrolytic imbalance (Akiyama, 2010; Kien et al., 2018; Wendy Li, Oberlin, Wilson, & Haggstrom, 2020; G. Onal et al., 2019; Vahlquist et al., 2018). Additionally, collodion baby phenotype (that is a shiny, tight outer membrane surrounding the whole body and disappears later) is generally encountered in the disease. The prevalence of the disease is 1:200.000 in the US (Richard, 1993). Many genes that are crucial for lipid metabolism and the formation of the epidermal barrier were identified as ARCI-associated genes. These genes can be listed as ABCA12, ALOX12B, ALOXE3, CASP14, CERS3, CYP4F22, LIPN, NIPAL4, PNPLA1, SDR9C7, SLC27A4, and TGM1 (Fachal et al., 2014; Freedman et al., 2021; Uitto et al., 2020; Leila Youssefian et al., 2017). Mutations in ALOXE3 and ALOX, which are lipoxygenases, and TGM1, which is a transglutaminase and crosslinks the proteins in the cornified envelope are the most frequently encountered mutations in ARCI patients (Pinkova, Buckova, Borska, & Fajkusova, 2020).

Many of the genes that are involved in ARCI formation are related to acyl ceramide synthesis and metabolisms such as CERS3, CYP4F22, and PNPLA1 (Hirabayashi, Murakami, & Kihara, 2019). PNPLA1 is a member of the patatin-like phospholipase domain-containing protein family which consists of 9 members (PNPLA1-9) in mammals. The domain has a unique structure that is α/β/α and Ser-Asp catalytic dyad (Hirabayashi et al., 2019; Kienesberger, Oberer, Lass, & Zechner, 2009). All proteins in this family include a conserved catalytic patatin domain, which has a consensus lipase motif Gly-X-Ser-X-Gly in their N-terminals and shows lipid hydrolase or transacylase activity on phospholipids, neutral lipids sphingolipids, and retinol esters (Hirabayashi et al., 2019; Kienesberger et al., 2009; G. Onal et al., 2019) (**Fig. 1-5**). These enzymes participate in pathways related to lipid metabolism and are found in a variety of species such as mammals, yeasts, and plants (Hirabayashi et al., 2019).

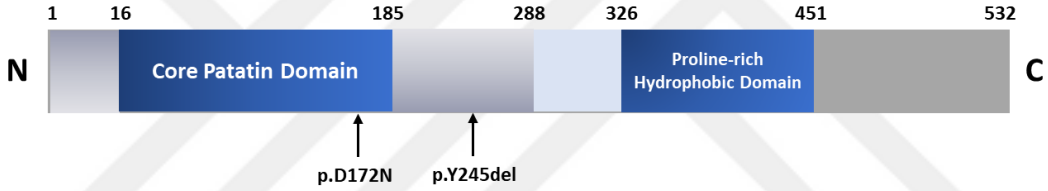

Figure 1-5: Schematic representation of PNPLA1 gene.

The gene encoding PNPLA1 protein is located on the 6p21.31 chromosome. PNPLA1 protein consists of 533 amino acids, including a patatin domain in the residues 16-185 and a proline-rich hydrophobic region in the residues 326-451 (**Fig. 1-5**) (Chang et al., 2013; Hirabayashi et al., 2019). PNLPA1 is able to localize on the LD surfaces. Additionally, the catalytic region contains Ser53 and Asp172 (Chang et al., 2013; Hirabayashi et al., 2019; G. Onal et al., 2019). Even though the gene has patatin domain similar to other PNPLA family members, it does not show any lipase activity; instead, PNPLA1 participates in the synthesis and regulation of phospholipids (Grall et al., 2012). In recent years, it was shown that PNPLA1 has a crucial role in the synthesis of a sphingolipid called ω-O-acyl ceramide. The enzyme catalyzes the reaction between ω-hydroxyceramide and linoleate to synthesize acyl ceramide using TAGs of linoleate as a donor (Akiyama, 2017; Deevska & Nikolova-Karakashian, 2017; Kien et al., 2018). It was revealed that a mutation in the PNPLA1 encoding gene can cause ARCI and the colloidal baby phenotype was seen in all newborn ARCI patients that have PNPLA1

mutation (Sugiura & Akiyama, 2015). Additionally, it was shown that in the outermost layer of epidermis, PNPLA1 was overexpressed and caused abnormal lipid accumulation in keratinocytes, resulting in ARCI pathology (Grall et al., 2012).

Ichthyosis, mostly caused by mutations in the ABHD5/CGI58 genes. These types of ichthyosis were found to be associated with neutral lipid storage disorder, and intracellular LD accumulation was characterized in these patient cells. It was found that sphingolipids affect the formation and growth of LDs. In the light of these findings, a mutation in PNPLA1 gene responsible for producing ω-O-acyl ceramide may affect LD homeostasis in ARCI patients, similar to the neutral lipid storage disorder with ichthyosis (Deevska & Nikolova-Karakashian, 2017; Missaglia, Coleman, Mordente, & Tavian, 2019; M. Schweiger, Lass, Zimmermann, Eichmann, & Zechner, 2009).

To clarify this question, we have previously studied using fibroblast cells derived from ARCI patients. The results revealed aberrant accumulation of LDs in the blood smear samples of ARCI patients that have p.Y245del and p.D172N mutation in PNPLA1 gene. Additionally, downregulation of PNPLA1 protein via PNPLA1 siRNA transfection in primary fibroblast cells of ARCI patients led to aberrant LD accumulation, whereas it did not affect the PNPLA1 localization or expression in these primary fibroblasts. Lipophagy analysis in these cells showed that the number of autophagosome formation was higher in healthy primary fibroblasts than ARCI patient cells and LC3 expression of the patient cells was significantly less when compares with the healthy control cells. Furthermore, it was observed that there was a significant difference between the ARCI patient cells and the healthy control cells in terms of the LDs colocalization with autophagosomes and the colocalizations were higher in the healthy controls cells than the patient cells. It was concluded as PNPLA1 protein might have a crucial role in the degradation of LDs via lipophagy pathway (G. Onal et al., 2019).

2. AIM OF THE STUDY

The aim of the thesis is to investigate the molecular mechanisms of lipid droplets' catabolic pathways in ARCI patients and to determine the importance of these mechanisms for disease pathology. For this reason, the thesis is focused on the PNPLA1 gene and the effect of PNPLA1 mutation on the LD catabolic pathways.

3. MATERIALS AND METHODS

3.1. Materials

Table 3-1: Cell Culture Mediums and Reagents

Mediums and Reagents	Catalog Number
Dulbecco's Modified Eagle's Medium	PAN Biotech P04-03500
1x MEM Non-Essential Amino acid	Pan Biotech P08-32100
Dulbecco’s Phosphate - Buffered Saline	PAN Biotech P04-36500
Fetal Bovine Serum (FBS) Standard Forte	PAN Biotech P30-3304
L-Glutamine	PAN Biotech P04-80100
Lipofectamine 3000	Invitrogen L3000001
Opti-MEM	Gibco 31985-047
Penicillin/Streptomycin (100X)	PAN Biotech P06-07100
Trypsin-EDTA	PAN Biotech P10-019100

Table 3-2: List of Plasmids and Primers

Plasmids and Primers	Supplier and Properties
Cathepsin B Forward Primer	Oligomer 5’ TTCTTGCGACTCTTGGGACTTC 3’
Cathepsin B Reverse Primer	Oligomer 5’ TGACGAGGATGACAGGGAACTA 3’
Control siRNA	Santa Cruz sc-37007
LAMP2 Forward Primer	Oligomer 5’ GGTTAATGGCTCCGTTTTCA 3’
LAMP2 Reverse Primer	Oligomer 5’ ATGGGCACAAGGAAGTTGTC 3’
LAMP2 siRNA	Santa Cruz sc-29390
pMRX-IP-GFP-LC3-RFP	Addgene Plasmid 84573

Table 3-3: List of Antibodies

Antibody	Catalog Number
Actin	Sigma A5441
SQSTM1	Abnova H00008878-M01
LC3	Sigma L7543
Cathepsin B	Cell Singaling 3373S
Cathepsin D	Cell Singaling 2284S
Rab 7	Cell Signaling D95F2
Bif-1	Novus NBP2-24733
LAMP2	Abcam ab25631
SNARE	Sigma HPA001204
Hsp70	Merck MAB3516
PNPLA2 (ATGL)	Cell Signaling 2138S
Alexa Flour 568 (anti-mouse)	Invitrogen A-11004
Alexa Flour 568 (anti-rabbit)	Invitrogen A-11011
Secondary anti-mouse	ImmunoResearch Lab 115035003
Secondary anti-rabbit	ImmunoResearch Lab 111035144

Table 3-4: List of Kits

Kits	Catalog Number
Extracellular Oxgen Consumption Assay	Abcam ab197243
Fatty Acid Oxidation Assay Kit	Abcam ab217602
Light Cycler 480 Syber Green I Master	Roche 4887352001
SuperScript III First-Strand Synthesis System	Invitrogen 18080-051
Triglyceride Colorimetric Assay Kit	Cayman Chemical Company 10010303

Table 3-5: List of Chemicals and Reagents

Chemicals and Reagents	Catalog Number
2-Mercaptoethanol	Neofroxx 1414
2-Propanol	Neofroxx 1496
Acrylamide Xtra Solution 30%-Mix 37.5:1 for electrophoresis	Neofroxx 1102
Albumin Fraction V (Bovine Serum Albumin, BSA)	Sigma A3059
Albumin Bovine Serum (Fatty Acid Free)	Sigma A8806
Ammonium persulfate (APS)	Neofroxx 1610
BODIPY 493/503	Invitrogen D3922
Bradford Reagent	Sigma B6916
Bromophenol blue	PanReac Applichem A3640
Calcium chloride-dihydrate	Merck A1229282
CCCP	Sigma C2759
Chloroform	Sigma C2432
Chloroquine	Sigma, C6628
DMSO	Sigma D2650
Ethanol	InterLAB 920.027.2501
GENEzol RNA Isolation Reagent	Geneaid GZR100
Glycerol	Neofroxx 1280LT001

Glycine	Neofroxx 1154
HCl	Sigma 7102
HEPES	Sigma H6147
Hoechst 33342	Invitrogen H3570
KCl	Neofroxx 1197
Lumi-Light Western Blotting Substrate	Roche 12015200001
Methanol	Sigma 32213
Milk powder	Neofroxx 1172
MitoTracker Red CMXRos	Invitrogen M7512
Nonidet P40	Applichem A1694
Nitrocellulose Membrane	Milipore IPVH00010
Nuclease free water	Roche 03315843001
PageRuler Prestained Protein Ladder	ThermoFisher 26616
Paraformaldehyde	Sigma 158127
PMSF	Sigma P7626
Protease Inhibitors Cocktail Tablets	Roche 04 693 132 001
Oleic Acid	Sigma O1383
Retinoic Acid	Sigma R2625
Saponin	Sigma 84510
SDS	Neofroxx 3250
Sodium Azide	Riedel de Haen 13412
Sodium chloride	Neofroxx 1236
Sodium Hydroxide	Merck 1.06498.1000
Tetramethylethylenediamine (TEMED)	Sigma T7024
Tris (tris-hydroxymethyl-aminomethane)	Sigma T1503
Tween 20	Neofroxx 8506
Torin 1	TOCRIS 4247
X-Ray films	Fujifilm

Table 3-6: List of Websites for Primer Design

Websites	Purpose
http://www.ensembl.org/index.html	Genome sequence analysis
https://www.uniprot.org/	Genome sequence analysis
https://primer3plus.com/	Primer design program

3.2. Methods

3.2.1. Cell Culture Primary fibroblast cells obtained via the skin biopsy of two ARCI patients that have two different mutations that are p.Y245del and p.D172N in their PNPLA1 genes were used in the experiments. Primary fibroblast K2 cells were used as a control. The cells having passage number 1-14 were used in all experiments and were cultured in Dulbecco's modified Eagle's medium (DMEM) supplemented with 10% (v/v) heat-inactivated fetal bovine serum, 1% penicillin/streptomycin, and 2mM L-glutamine. 1x MEM non-essential amino acid solution (1%) was added to the medium. Cells were incubated at 37°C/5% CO_2.

For the passage, the cells that reached 90-100% confluency were treated with trypsin/EDTA at 37°C for 5 mins for their detachment and centrifuged at 300x g for 5mins at room temperature. For the stimulation of LD formation, cells were treated with fatty acid-supplemented media including 400 µM oleic acid (OA) for 12h. Cells were treated with 10 µM retinoic acid for 12h to stimulate CMA, 250nM TORIN1 for 4h to stimulate the lipophagy, 10 µM chloroquine (CQ) for 40 mins to block CMA.

3.2.2. Fatty Acid-Supplemented Medium Preparation

3.2.2.1. 20 mM Sodium Oleate Preparation

200 µl of 1M NaOH was added into 15.7 ml dH_2O and heated up to 70˚C. Subsequently, 100 µl oleic acid was added to heated solution drop by drop and incubated for 30 mins at 70˚C. The solution was mixed several times during incubation. After the incubation, 50 µl 1M NaOH was added to the solution and incubated for 5 mins at 70˚C. The last step was repeated 4-5 times until the micelles were disappeared.

3.2.2.2. Preparation of Fatty acid-Albumin Complex and Fatty Acid-Supplemented Medium

3,5 ml of 20mM sodium oleate was added into a 5% BSA solution (BSA should be fatty acid-free) and heated up to 37 ˚C. Subsequently, the final solution was added drop by drop into a 160 ml cell culture medium, and the medium was filtered by 0.22 µm sterile filter under the laminar flow cabinet. The newly prepared medium can be stored for 1 week at 4˚C.

3.2.3. Sample Preparation for Microscopy Experiments

3.2.3.1. BODIPY® 493/503 Staining

To visualize the LDs in the cells, An apolar and hydrophobic dye BODIPY® 493/503 that specifically stains the neutral lipids inside the cells was used for the staining. Primary fibroblast cells were seeded onto coverslips in 12 well plates at a density of 40.000 cells/each well and incubated for 2 days to obtain the 70-80% confluency. After the incubation, cells were washed using 1xPBS and fixed with 4% paraformaldehyde (PFA) solution on ice for 30 mins. After the incubation, cells were washed 3 times with 1xPBS.

BODIPY working solution (1 µg/ml) was prepared via adding 0,8 µl of BODIPY stock solution (2,5 mg/ml in ethanol) into 2 ml of 150 mM NaCl solution. The solution was vortexed well and immediately added onto the fixed cells (500 µl/each well). Cells were incubated for 10 mins at RT in the dark and washed 3 times with 1xPBS. To visualize the nucleus, cells were stained with Hoechst (1:10.000 diluted) for 5 mins and washed 3 times with 1xPBS. Coverslips were mounted and observed under the confocal microscope.

3.2.3.2. Immunofluorescence Staining (Indirect Staining)

Primary fibroblast cells were seeded onto coverslips in 12 well plates at a density of 40.000 cells/each well and growth for 2 days to obtain the 70-80% confluency. On the third day, cells were washed using 1xPBS and fixed with 4% paraformaldehyde (PFA) solution on ice for 30 mins. After the incubation, cells were washed 3 times with 1xPBS and permeabilized with 3%BSA/0.1% Saponin solution on the ice at 30 mins. The solution was then removed and 100 µl of primary antibodies (1:100 or 1:200 diluted in 1xPBS) were added onto each coverslip. The cells were incubated with the primary antibodies for 1h at room temperature and washed 3 times with 1x PBS. 100 µl of 1:500 diluted secondary antibodies were added onto the coverslips and incubated for additional 1h at room temperature. After the incubation, cells were washed 3 times with 1xPBS and stained with BODIPY and Hoechst as described previously. After these stainings coverslips were mounted and observed under the confocal microscope.

3.2.4. Cell Lysate Preparation and Immunoblotting

RIPA buffer containing 1% complete protease inhibitors and 1 mM PMSF was used to lyse the cells. After the addition of RIPA, cells were incubated for 20 mins on ice and vortex every 5 mins. Subsequently, the samples were centrifuged at 1500x rpm for 15 mins and the supernatant was transferred into a new eppendorf. The concentration of the isolated proteins was determined by using Bradford Assay. 30 µg protein was used for western blotting. 3X protein loading dye mixed with the proteins and the samples were boiled for 10 minutes at 95˚C for denaturation. After the denaturation, the samples were

loaded to 10% SDS-Polyacrylamide (PAGE) gels and separated based on their molecular weight. Separated proteins were transferred to the nitrocellulose membrane at 250 mA for 1h. Blocking was carried out with 5% non-fat milk in PBS-T for 1h at room temperature. After blocking, cells were washed for 15 mins with PBS-T. Membranes were incubated overnight with primary antibodies at 4˚C. After the incubation, membranes were washed for 15 mins with PBS-T. Secondary antibodies were prepared in 5% non-fat milk solution with 1:10000 dilution for 1h at room temperature and washed with PBS-T three times for 15 mins. Membranes were placed on the cassettes and chemiluminescence reagent was added onto the membrane. At dark, films were placed onto the membranes and incubated for 40 mins. To develop and fix the X-ray films, developer and fixer solutions were used until the bands appear**.**

3.2.5. Confocal Microscopy and ImageJ Analysis

Fluorescence imaging of the cells was performed using Carl Zeiss 710 LSM confocal microscope. The size and particle accumulation of LDs were analyzed using the particle analysis tool of Image J software. ImageJ software was also used in the normalization of western blot results using the gel analysis tool.

3.2.6. Lipofectamine 3000 Transfection

Primary fibroblast cells were seeded onto coverslips in 12 well plates at a density of 40.000 cells/each well and growth for 2 days to obtain the 70-80% confluency. After the incubation, cells were transfected with 2 µg plasmid DNA using Lipofectamine 3000 as a transfection reagent. For this reason, in an eppendorf tube (A) 3,5 µl Lipofectamine 3000 reagent were mixed with 50 µl Optimem. In a different eppendorf tube (B) 2 µg plasmids and 2.5 µl P3000 reagent were added onto the 50 µL Optimem, respectively. Subsequently, Tube B was added onto tube A and vortexed thoroughly. The tube was incubated for 15 mins at room temperature. During incubation, cells were washed with 1xPBS and 1 ml Optimem was added to each well. After incubation, the mixture was

added on the top of the cells drop by drop, and the cells are incubated for 4h. After 4h, the medium was changed with complete medium. For siRNA transfection, primary fibroblast cells were seeded onto 6 well-plates at a density of 100.000 cells/each well and growth for 2 days to obtain the 80-90 % confluency. After the incubation, cells were transfected with 75pmol siRNA using Lipofectamine 3000 as a transfection reagent. For this reason, in an eppendorf tube (A) 7,5 µl Lipofectamine 3000 reagent were mixed with 125 µl optimem. In a different eppendorf tube (B) 75pmol siRNA was added onto the 50 µL optimem. Subsequently, Tube B was added onto tube A and vortexed thoroughly. The tube was incubated for 15 mins at room temperature. During incubation, cells were washed with 1xPBS and 1 ml optimem was added to each well. After incubation, the mixture was added on the top of the cells drop by drop, and the cells are incubated for 4h. After 4h, the medium was changed with complete medium.

3.2.7. RNA Isolation

RNA isolation was performed to determine the LAMP2 and cathepsin B via RT-qPCR in ARCI patient cells compared with control cells. Thus, cells were seeded in 6 wells plate at a density of 100.000 cells/each well for LAMP2 and in 10 cm tissue culture dishes at a density of 500.000 cells for cathepsin B. After the cells reach their confluency, they were transfected with siRNA for LAMP2 experiment and treated with oleic acid, chloroquine, and oleic acid-chloroquine together for cathepsin B experiment. Subsequently, the cells were washed 2 times with 1xPBS, and Genezol reagent (500 µl for 6 wells plate and 1 ml for 10 cm tissue culture plate) is added onto cells and incubated at room temperature for 5 mins. The cell lysates were then transferred into eppendorf tubes and chloroform (100 µl for 6 wells plate and 200µl for 10 cm tissue culture plate) was added. The tubes were inverted for 15 seconds and the mixtures were incubated for 15 mins at room temperature. Then, they were centrifuged at 12000x g for 10 mins at room temperature and the colorless upper phase was collected into new eppendorf tubes. 2-isopropanol (250 µl for 6 wells plate and 500 µl for 10 cm tissue culture plate) was added onto the upper phase and incubated for 15 mins at 4˚C. Followed by the incubation, centrifugation was performed at 12000 × g for 10 minutes at 4˚C and the supernatant was discarded. 75% ethanol (500 µl for 6 wells plate and 1 ml for 10 cm tissue culture plate)

was added to the pellets and the tubes were centrifuged at 12000 × g for 10 minutes at 4˚C. The tubes were incubated at room temperature for 30 mins to remove ethanol after the supernatants were discarded. The pellets dissolved with Rnase free water and RNA concentrations were measured with Thermo Fisher 2000 NanoDrop Spectrophotometer.

3.2.8. Quantitative Reverse Transcription PCR (RT-qPCR)

To determine the relative mRNA expression of LAMP2 and Cathepsin B, isolated RNAs were used to produce cDNA samples and RT-qPCR was performed. cDNAs were synthesized from 1000ng RNA samples using SuperScript III First-Strand Synthesis System by following the kit protocol. After cDNA synthesis, reaction mix was prepared with 0,5 µl 10 µM forward primer (**Table 3-2**), 0.5 µl 10 µM reverse primer (**Table 3-2**), 2 µl water, and 5 µl 2x Syber Green mix on ice at dark and 2 µl cDNA were used as a template for RT-qPCR. β-glyceraldehyde 3-phosphate dehydrogenase (GAPDH) was used as a housekeeping gene for the experiment control. Subsequently, the samples were added to 96 wells plate (Light Cycler480 multiwell plate) and the plate was sealed. After the centrifugation of the plate at 1500 × g for 2 minutes at 4°C. For the experiment, LightCycler 480 instrument (Roche) was used. RT-qPCR program was as follows; pre-incubation was 1 cycle at 95 °C for 5 minutes, amplification was 50 cycles at 95 °C for 15 secs, 58 °C for cathepsin B / 60°C for LAMP2 for 30 secs and 72°C for 5 seconds and melting curve was 1 cycle at 95 °C for 5 seconds, 65 °C for 1 minute and 95 °C continuous and cooling was 1 cycle at 40 °C for 30 seconds. The quantification was performed using ΔΔCT method.

4. RESULTS AND DISCUSSION

4.1. Preliminary studies-Lipolysis Analysis

4.1.1. Determination of the intracellular triglyceride levels in ARCI patients

Cells store the excessive lipids as neutral lipids such as TG, SE, and cholesterols inside the LDs. But in the need of energy, these lipids are degraded via lipolysis mechanism to their building blocks glycerol and free fatty acids. Therefore, measuring the TG levels of cells are important for interpreting the lipolysis mechanism(R. Zechner et al., 2012).

To compare the TG levels of control and patient cells, Triglyceride Colorimetric Assay kit (Cayman Chemical Company #10010303) was used as described in the kit protocol. This kit is based upon multiple enzymatic reactions and the final product gives a purple color that can be detected with a spectrophotometer at 540 nm. The enzymatic steps of the kit are described below;

$$\text{Triglycerides} \xrightarrow{\text{Lipoprotein Lipase}} \text{Glycerol and Fatty Acids}$$

$$\text{Glycerol + ATP} \xrightarrow{\text{Glycerol Kinase}} \text{Glycerol-3-Phosphate+ADP}$$

$$\text{Glycerol-3-Phosphate + } O_2 \xrightarrow{\text{Glycerol Phosphate Oxidase}} \text{Dihydroxyacetone Phosphate + } H_2O_2$$

$$2H_2O_2\text{+4-AAP+ESPA} \xrightarrow{\text{Peroxidase}} \text{Quinoneimine dye+}4H_2O$$

The analysis showed that TG levels of the cells having p.Y245del mutation were higher than the p.D172N.p1 and p.D172N.p2 cells. Additionally, TG levels of the patient cells

were significantly higher than control cells. In OA-induced conditions, there was a significant increase in control cells, whereas the change in the patient cells was not significant (**Fig. 4-1**). These results were consistent with our previous findings. We showed that ARCI patient cells with p.Y245del and p.D172N mutations on PNPLA1 gene contain abnormal amounts and sizes of LDs, compared to control cells (G. Onal et al., 2019). Additionally, the higher TG levels in ARCI patients' cells can be associated with a defect in the lipolysis mechanism. Since a mutation in the CGI-58 gene has been shown to act as a co-activator for ATGL, causing neutral lipid storage disorder with ichthyosis and TG accumulation in the tissues (M. Schweiger et al., 2009).

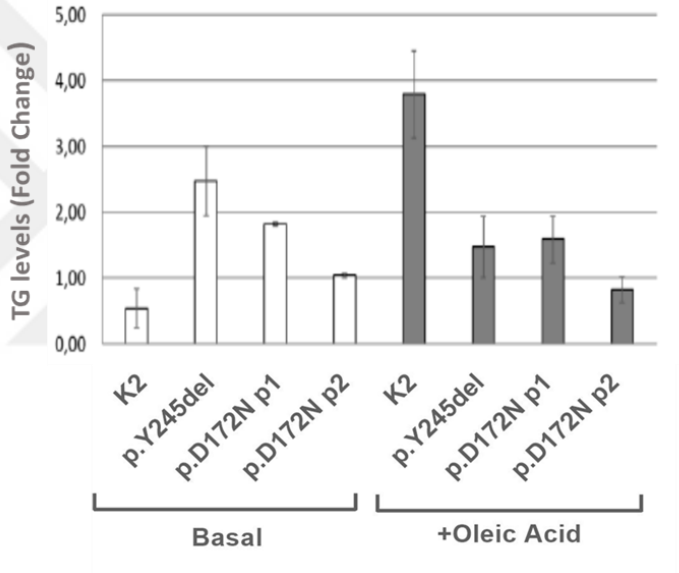

Figure 4-1: Determination of intracellular TG levels in ARCI patients. TG levels of the control and the patient cells that have p.Y245del and p.D172N mutations. were measured under basal and oleic acid-induced conditions. For oleic acid induction, cells were treated with fatty acid supplemented media for 12hrs. The measurements were obtained at 540nm wavelength. Data were represented as means of ±SEM of n = 3 independent experiments.

4.1.2. Beta Oxidation and Oxygen Consumption

Fatty acids generated by lipolysis are used as an energy source in the cells. For this reason, fatty acids are broken down via a process called beta-oxidation. Beta oxidation consists of multiple steps, which produce acetyl-CoA, FADH2, and NADH, and these molecules respectively undergo other metabolic processes, called Krebs cycle to produce ATP. For all these processes, fatty acids must be delivered to mitochondria first and then the cells must consume oxygen to produce ATP in the mitochondria (Adeva-Andany, Carneiro-Freire, Seco-Filgueira, Fernández-Fernández, & Mouriño-Bayolo, 2019; Almeida, Dhillon-LaBrooy, Carriche, Berod, & Sparwasser, 2021).

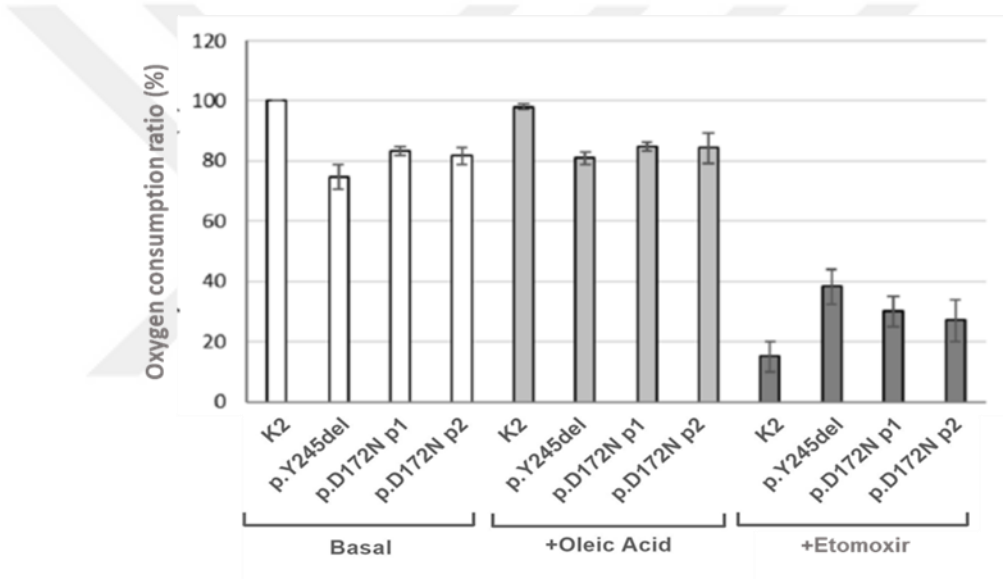

Figure 4-2: Determination of oxygen consumption ratio in ARCI patients. Oxygen consumption levels of the control, p.D172N.p1, and p.D172N.p2 cells were investigated under basal, oleic acid-induced, and etomoxir treated conditions. For oleic acid induction, cells were treated with fatty acid supplemented media for 12hrs and for the inhibition of fatty acid uptake by mitochondria. cells were treated with 10 µM Etomoxir for 3hrs. The measurements were obtained at 540nm wavelength. Data were represented as means of ±SEM of n = 3 independent experiments.

Beta oxidation and oxygen consumption of control and patient cells were measured to better understand the lipolysis and beta-oxidation mechanisms in ARCI patients. For this purpose, Fatty Acid Oxidation Assay Kit (Abcam #ab217602) and Extracellular Oxygen Consumption Assay Kit (Abcam #ab197243) were used as described in kit protocols. The

levels were evaluated under basal, oleic acid-induced, and 10µM etomoxir treated conditions (Etomoxir is an inhibitor of carnitine transporter CPT1, which prevents the fatty acid uptake by mitochondria) (O'Connor et al., 2018).

In figure **4.2,** under basal conditions, the oxygen consumption ratio of patient cells was slightly above 80%, however, not as high as the control cells. Oleic acid induction led to an increase in patient cells, but this increase was not significant. Additionally, etomoxir treatment resulted in a significant decrement of the oxygen consumption ratio of both control and patient cells and it was observed that this ratio was lower in control cells than in patient cells (**Fig.4-2**).

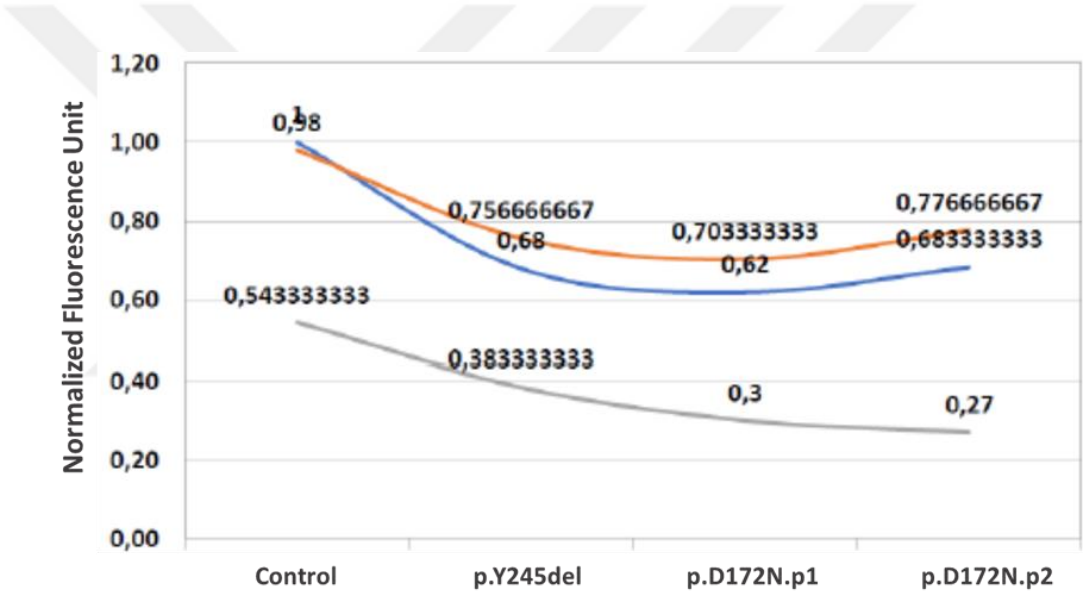

Figure 4-3: Determination of beta-oxidation in ARCI patients. Beta oxidation levels of the control and the patient cells were investigated under basal, oleic acid-induced, and etomoxir treated conditions. For oleic acid induction, cells were treated with fatty acid supplemented media for 12hrs and for the inhibition of fatty acid uptake by mitochondria. cells were treated with 10 µM Etomoxir for 3hrs. The measurements were obtained at 540nm wavelength. The blue line indicates basal conditions, the orange line indicates oleic acid-induced conditions and the grey line indicates etomoxir treated conditions. Data were represented as means of ±SEM of n = 3 independent experiments.

In Figure **4-3,** beta-oxidation of control and patient cells was analyzed. It was revealed that beta-oxidation of control cells was higher than that of patient cells and oleic acid

treatment caused a slight increase in beta-oxidation of both control and patient cells, however, etomoxir treatment caused a significant decrease in beta-oxidation ratios of all samples.

In conclusion, although ARCI patient cells can oxidize fatty acids and this oxidation increases by OA induction, the ratio was not as high as in control cells. Since beta-oxidation takes place in the mitochondria, the differences between the beta-oxidation of the cells may result from a possible mitochondrial dysfunction in our ARCI patient cells.

4.1.3. Mitochondrial Disorder and Recycling Analyses

The difference between TG levels and oxygen consumption ratios of control and patient cells brings the idea that the ARCI patients may have a mitochondrial disorder. Therefore, the membrane potential of control and patient cells were analyzed under basal conditions using 50 nM MitoTracker Red CMXRos (Invitrogen #M7512), which stains the mitochondria in live cells dependent on their mitochondrial membrane potential.

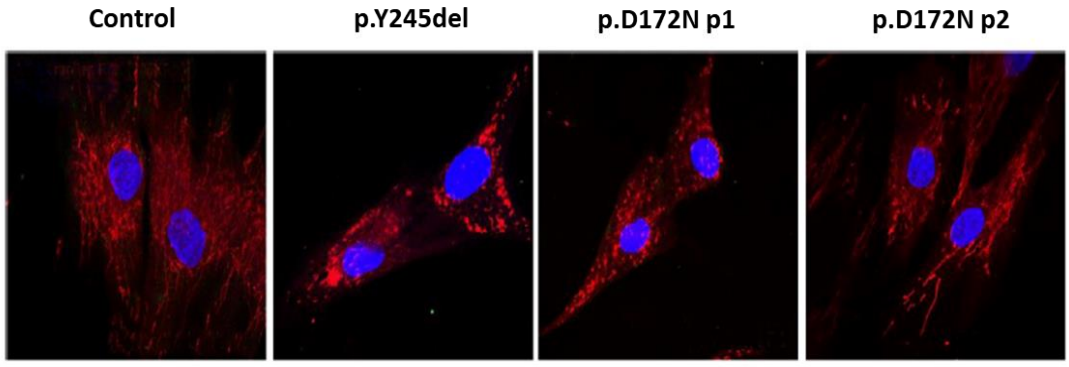

Figure 4-4: Mitochondrial disorder analysis in control and ARCI patient cells. Red signal indicates mitochondria stained with MitoTracker Red CMXRos and blue signal indicates cell nuclei stained with Hoechst 33342. Scale bar = 10 μm.

The results showed that in control cells, mitochondrial network was seen clearly, and no mitochondrial disorder was observed, whereas in patient cells the morphology was

changed, and this morphological change was higher in the patient that has p.Y245del mutation compared to control and patient cells that have p.D172N mutation (**Fig.4-4**).

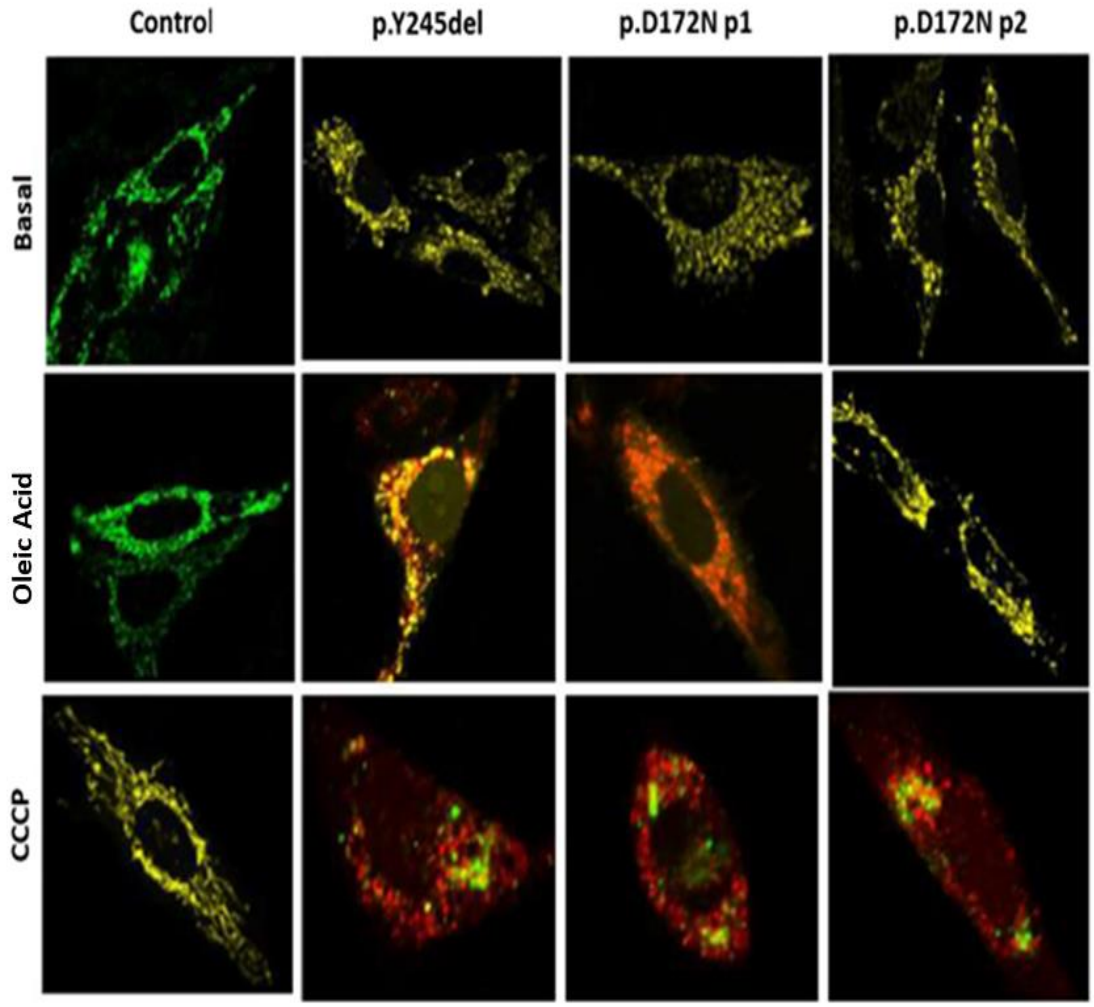

Figure 4-5: Mitophagy analysis in control and ARCI patient cells. The green signal indicates healthy mitochondria in cytoplasm and the red signal indicates mitochondria delivered to the lysosomes for their degradation via mitophagy. Scale bar = 10 μm.

Mitophagy is a selective type of autophagy mechanism that degrades the mitochondria, which has impaired membrane potential. It can be detected using MT-keima plasmid. This plasmid gives different fluorescence colors based upon the pH differences (it gives green fluorescence if the mitochondria are healthy and it gives red fluorescence if the

mitochondria are delivered to lysosomes for the degradation) (Katayama, Kogure, Mizushima, Yoshimori, & Miyawaki, 2011).

To confirm the results above mitophagy analysis was performed in control and patient cells under basal and oleic acid-induced conditions in the absence and presence of CCCP (Carbonyl cyanide m-chlorophenyl hydrazone), an inhibitor of mitochondrial oxidation. (Koncha, Ramachandran, Sepuri, & Ramaiah, 2021). The results showed that under basal conditions, green fluorescence was observed in control cells, whereas the color was changed to yellow and red in patient cells indicating that the mitochondria of patient cells were delivered to lysosomes for degradation. The color change was observed more clearly in oleic acid-induced and mitochondrial oxidation-inhibited conditions (**Fig.4-5**).

4.1.4. Intracellular Lipid Mobilization

Abnormal LD accumulation in ARCI patients may result from a defect in the mechanisms of lipolysis but may also result from defects in intracellular lipid mobilization. To investigate the intracellular lipid mobilization, control and patient cells were analyzed under basal and etomoxir-treated conditions. The results revealed that under basal conditions, LD accumulation was higher in the patient cells that have p.Y245del mutation than the other patient cells, however, average LD size was bigger in p.D172N,p2 cells. Both LD size and accumulation were lower in control cells in comparison with the patient cells. Additionally, etomoxir treatment led to a significant increase in LD accumulation and average LD sizes in control and patient cells (**Fig 4-6 (A) and (B)**).

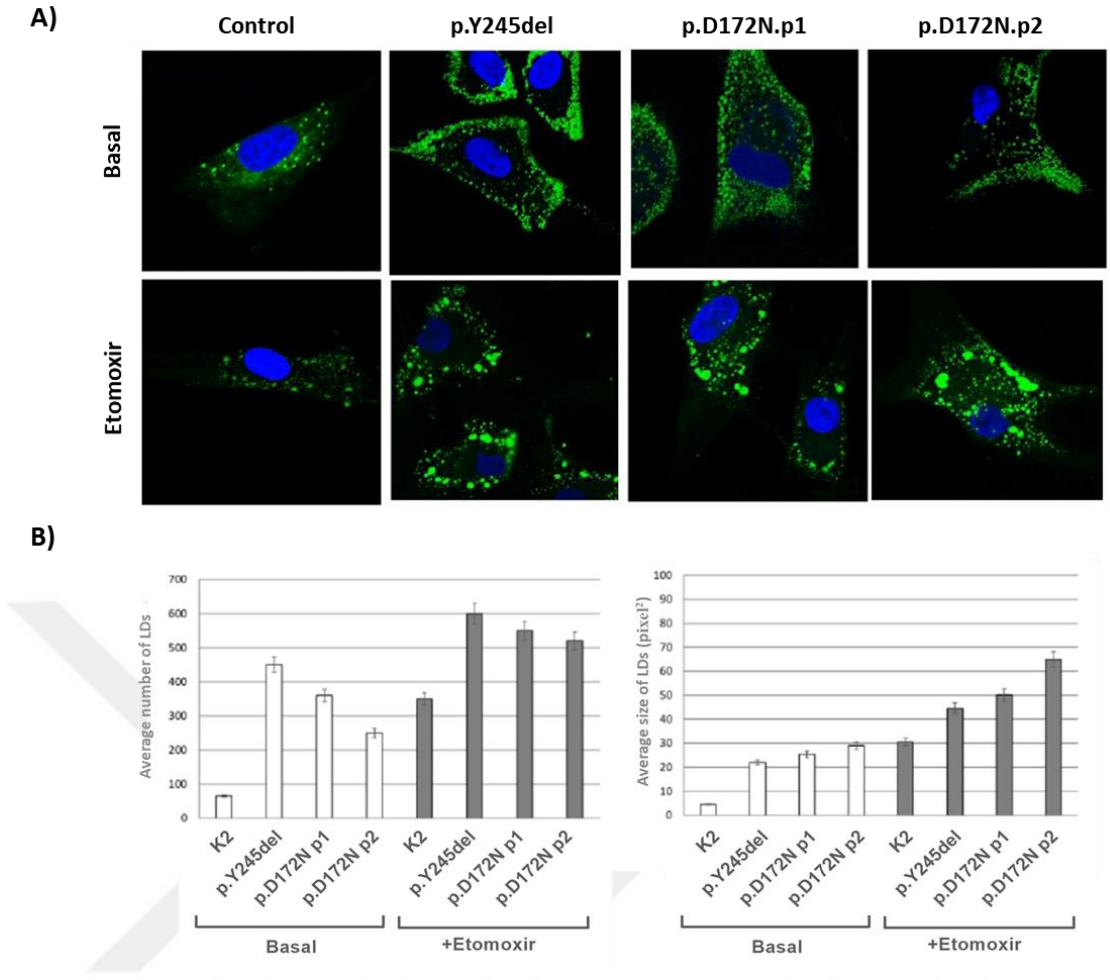

Figure 4-6: Intracellular lipid mobilization analysis in control and ARCI patient cells. The analyses were performed under basal and etomoxir treated conditions. For the inhibition of fatty acid uptake by mitochondria, cells were treated with 10 µM Etomoxir for 3hrs. (A) Microscopic imaging of BODIPY®493/503-stained oil droplets in the control and patient cells. Green signal indicates LDs stained with BODIPY®493/503 and blue signal indicates cell nuclei stained with Hoechst 33342. Scale bar = 10 µm.(B) Quantitative analyses of LDs accumulation and LDs average size. It was performed by Image J particle analysis function.

4.2. Lipid Droplets Accumulation and Size Analysis

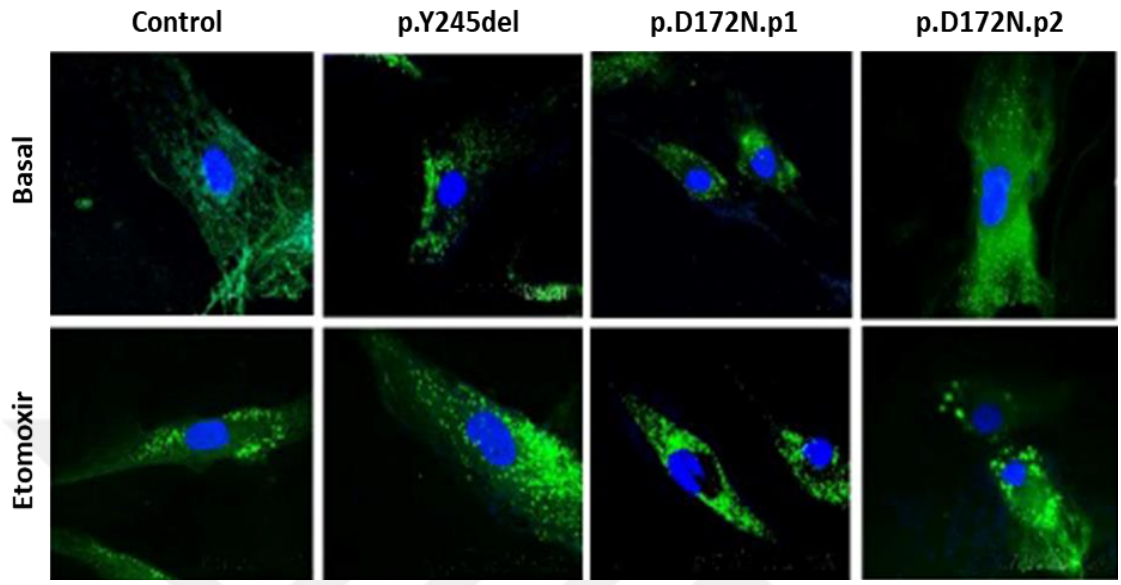

Figure 4-7: Lipid droplets size and accumulation analysis in the control and ARCI patient cells. For oleic acid induction, cells were treated with fatty acid supplemented media for 12hrs. Green signal indicates LDs stained with BODIPY®493/503 and blue signal indicates cell nuclei stained with Hoechst 33342. Scale bar = 10 µm.

PNPLA1 protein is responsible for the synthesis of ω-O-acylceramide, which is a type of sphingolipids. It has been known that sphingolipids involve the formation and growth of LDs (Deevska & Nikolova-Karakashian, 2017; Hirabayashi et al., 2019). Additionally, it was revealed that there are some types of ichthyoses related to the mutations on CGI-58 gene resulting in aberrant accumulation of cytosolic LDs in various tissues (M. Schweiger et al., 2009). However, it hasn't been analyzed whether PNPLA1 mutations had the same effect in ARCI patients. Therefore, we have previously investigated whether p.Y245del and p.D172N mutations on PNPLA1 genes have an effect on intracellular LD accumulation in ARCI patients. For the first time, we reported that these mutations caused aberrant LD accumulation in ARCI patients' primary fibroblast cells in comparison with healthy control cells (Hirabayashi et al., 2019; G. Onal et al., 2019). To confirm the previous findings, we determine the abnormalities in accumulation and size of the lipid

droplets in ARCI patient cells by comparing them with the control cells. For this reason, patient and control cells were analyzed under basal and oleic acid-induced conditions.

The results indicated that the number and size of the lipid droplets under basal conditions were higher in patient cells than in control cells, and it was observed that this situation slightly increased under the oleic acid-induced conditions (**Fig.4-7 and 4-8**). Interestingly, under both conditions, the number of LDs was higher in the patient with p.Y245del mutation whereas, the size of these droplets was larger in the patient (p2) with p.D172N mutation when compared to other cells

In conclusion, the number and size of LDs were higher in ARCI patient cells under both basal and oleic acid-induced conditions and these data were consistent with our previous findings (G. Onal et al., 2019). Since the PNPLA1 protein is known to have no lipase activity or has not yet been proven to play a role in the degradation mechanism of LDs, the LD degradation pathways need to be further analyzed to understand the abnormal LD accumulation and sizes in the ARCI patients.

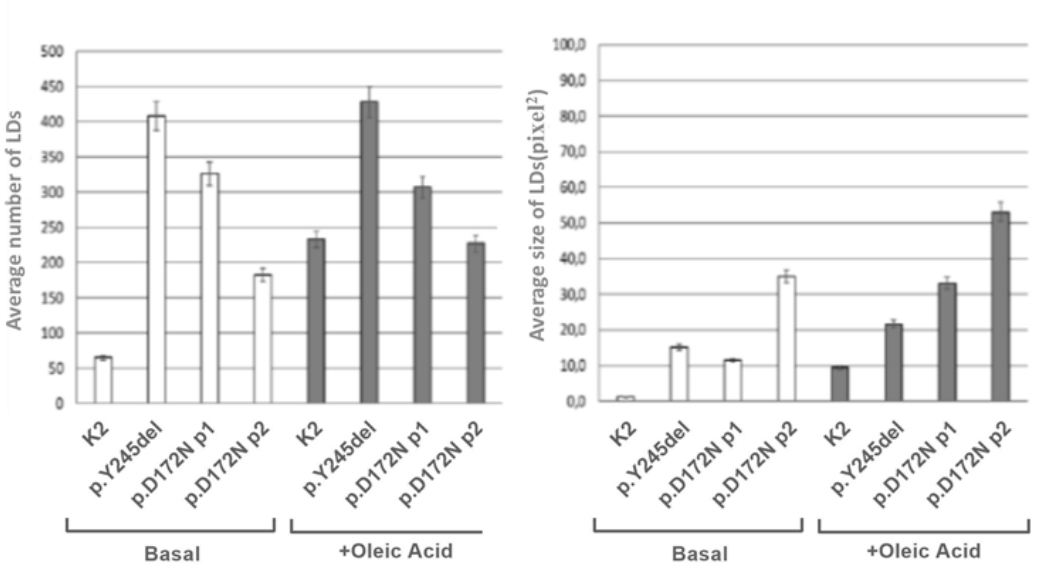

Figure 4-8: Lipid Droplets A) Number and B) Size analysis in the control and ARCI patient cells. For oleic acid induction, cells were treated with fatty acid supplemented media for 12hrs Quantitative analyses of LDs accumulation and LDs average size. It was performed by Image J particle analysis function.

4.3. Chaperon-Mediated Autophagy Analysis

4.3.1. LAMP2 and Lipid Droplets Colocalization in ARCI Patients

The importance of LAMP2 protein in LD catabolism was recently proven. The studies suggested that LAMP2 deficiency in mouse fibroblasts resulted in LD accumulation and these LDs were larger in size compared to control fibroblasts (Kaushik & Cuervo, 2015). Thus, it would be interesting to analyze whether the lipid droplet accumulation and their abnormal sizes in our ARCI patient cells were due to a defect in the LAMP2 protein or not. Therefore, LAMP2 and LDs colocalization was investigated in control and patient cells under basal, oleic acid-induced, and CMA-inhibited conditions.

Confocal microscopy analyses showed that LAMP2 and LDs colocalized in control cells under basal conditions and the colocalization increased when the cells were induced with oleic acid. However, CMA blockage decreased the colocalization of LAMP2 and LDs. Interestingly, in patient cells, LAMP2 and LDs were localized separately and neither oleic acid-induction nor CQ treatment had an effect on their localization. As a summary, CMA was activated in control cells and was even increased under oleic acid-induced conditions, however, it wasn't sufficiently active for LD degradation in patient cells under any conditions (**Fig.4-9**).

Accordingly, the colocalization of LAMP2 proteins with LDs in control cells supports the previous findings, suggesting CMA plays a role in LD breakdown (Q. Yang et al., 2019). As previously shown LAMP2 deficiency causes LD accumulation and size increase in LD droplets compared to their healthy counterparts. It also decreases the recruitment of ATGL and autophagic proteins to the substrates. Additionally, these deficiency results in the elevation of PLIN2 and PLIN3 proteins amount compared with the control mice fibroblasts (Kaushik & Cuervo, 2015). Therefore, the reason why colocalization was not observed in our ARCI patients cells in any conditions might be due to a defect in the LAMP2 protein or a defect in chaperone-mediated autophagy. Thus,

in order to understand this, a more detailed study with LAMP2 proteins and other CMA-associated proteins needs to be investigated.

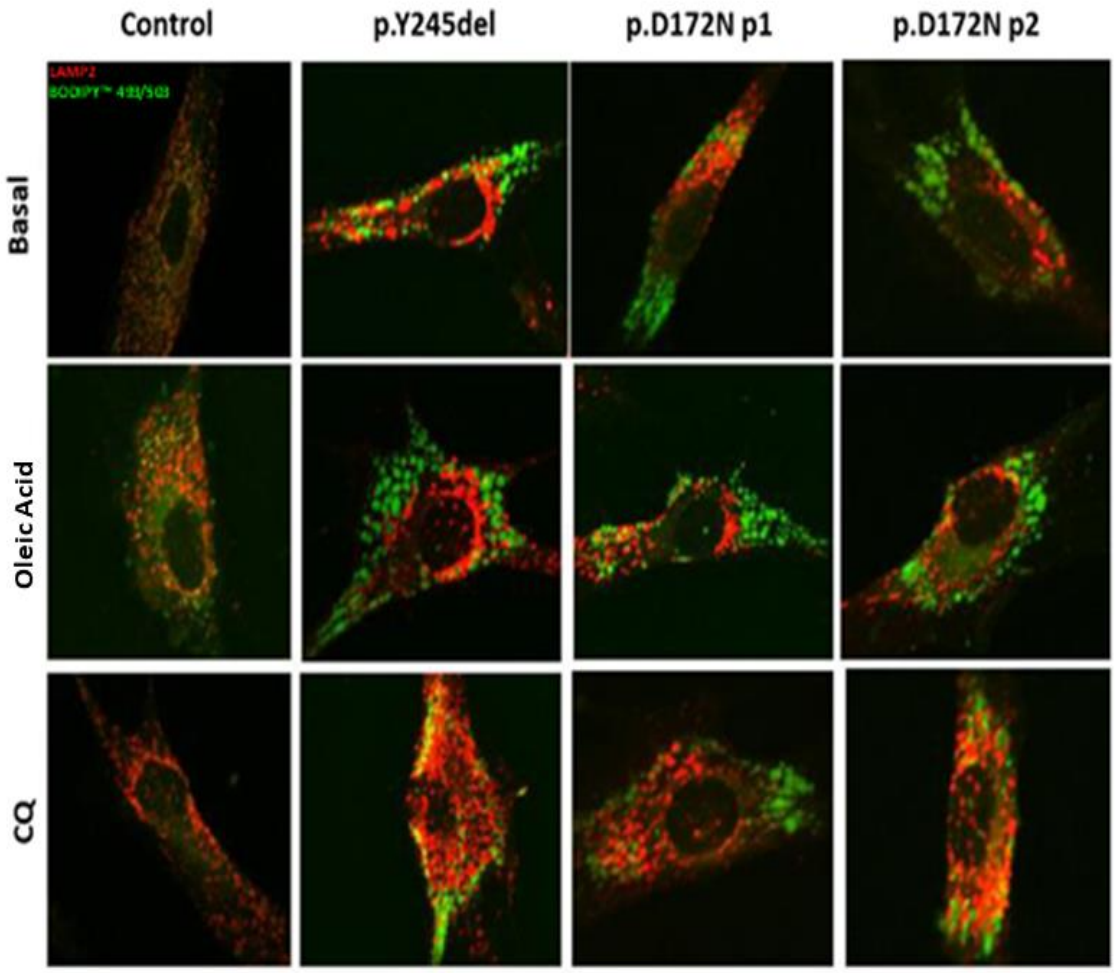

Figure 4-9: Colocalization analyzes of lipid droplets and LAMP2 proteins in control and ARCI patient cells. For oleic acid induction, cells were treated with fatty acid supplemented media for 12hrs and for CMA inhibition, cells were treated with CQ for 40 mins. Green signal indicates LDs stained with BODIPY®493/503, the red signal indicates Alexa Fluor® 568-stained LAMP2. Scale bar = 10 µm.

4.3.2. Hsc70 and Lipid Droplets Colocalization in ARCI Patients

The first step in CMA is the recognition of substrate proteins to target them to lysosomes by Hsc70 chaperones (Tekirdag & Cuervo, 2018). These proteins are heat shock proteins that target KFERQ-containing protein substrate to the lysosomes for their breakdown. It was suggested that Hsc70 binds to KFERQ motif-containing PLIN2 and PLIN3 proteins that are located on LDs surfaces and this binding mediates their transport to lysosomes (Kaushik & Cuervo, 2016, 2018; Gizem Onal et al., 2017). Therefore, Hsc70 becomes another important biomarker for CMA.

To further analyze, we checked Hsc70 expression in both control and the patient cells under basal, oleic acid-induced, and CMA-inhibited conditions. However, the patient that has p.Y245del mutation was not used for further experiments. The cells were taken from a patient with the most severe pathology compared to other patients, therefore the cell culture of these cells could not be maintained. Similar to LAMP2 and LD colocalization results, in control cells, Hsc70 and LDs were partially colocalized in basal conditions, however, the colocalization was not observed neither oleic acid-induction nor CQ treatment. In patient cells, Hsc70 and LDs were separately localized under basal conditions, and oleic acid induction or CQ treatment did not show any effect on the localization of Hsc70 and LDs (**Fig. 4-10**).

Previous studies revealed that PLIN2 and PLIN3 colocalize with Hsc70 on LDs surfaces and this colocalization is even increased with the oleic acid induction. Additionally, mutation on the KFERQ-like motif of PLIN2 protein causes LD accumulation and increased size in the mutated mice fibroblast cells. This mutation also significantly decrease the Hsc70 and PLIN2 binding (Kaushik & Cuervo, 2015; Kaushik & Cuervo, 2016). In our experiment, colocalization was seen in control cells under basal conditions, which confirms the previous data. However, under the oleic acid induction, LDs and Hsc70 proteins were localized separately. In ARCI patient cells, colocalization was not observed in any conditions. This might be resulted from the defect in Hsc70-PLINs

recognition or a possible mutation in the KFERQ-like motifs of PLIN2 and PLIN3 in ARCI patient cells.

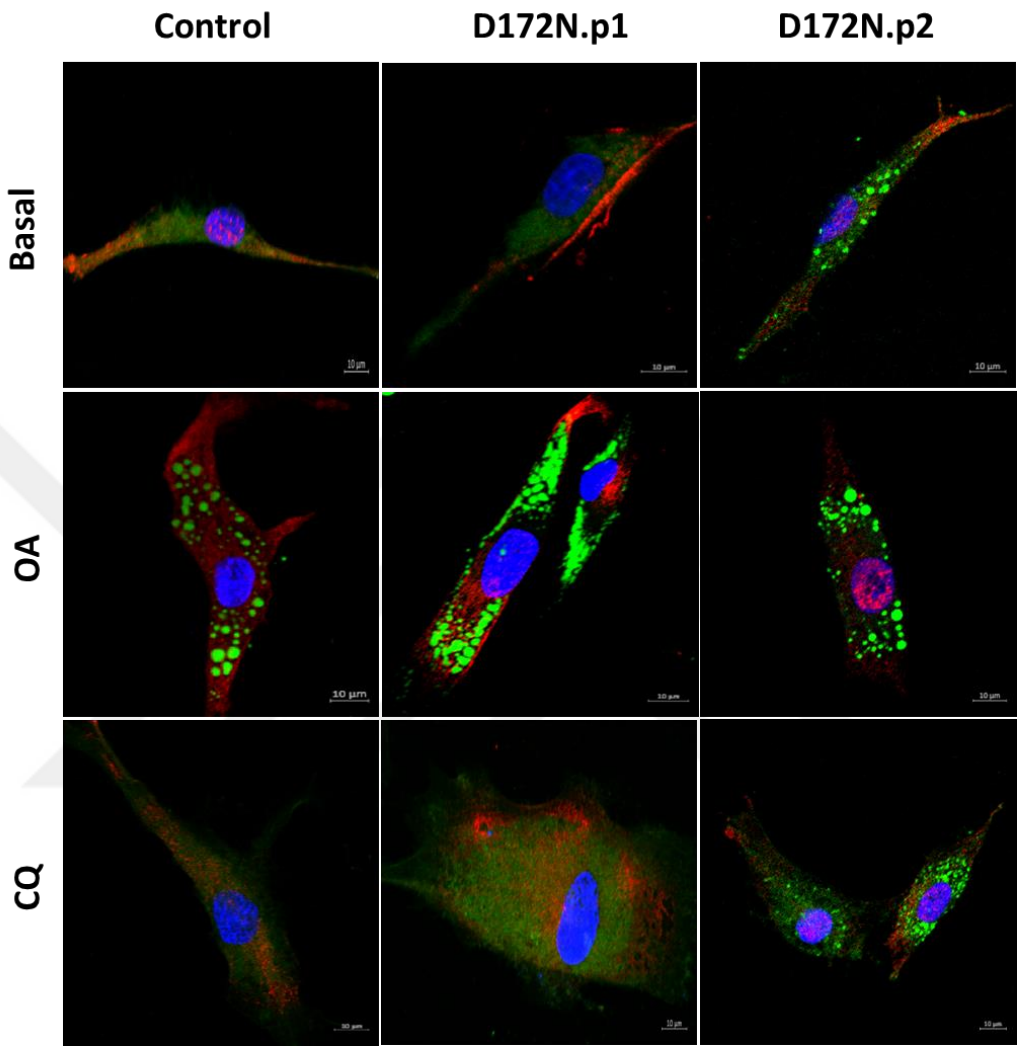

Figure 4-10: Colocalization analyzes of lipid droplets and Hsc70 proteins in control and ARCI patient cells. For oleic acid induction, cells were treated with fatty acid supplemented media for 12hrs and for CMA inhibition, cells were treated with CQ for 40 mins. Green signal indicates LDs stained with BODIPY®493/503, red signal indicates Alexa Fluor® 568-stained Hsc70 and blue signal indicates cell nuclei stained with Hoechst 33342. Scale bar = 10 µm.

4.3.3. The effects of CMA Induction and Inhibition on Lipid Droplets in ARCI Patients

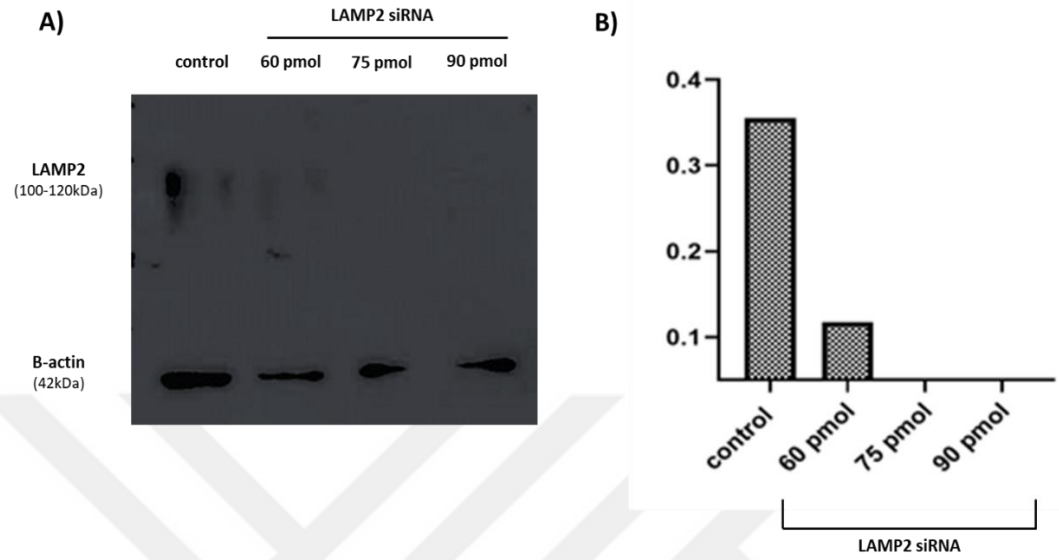

Figure 4-11: The effect of LAMP2 siRNA transfection in control cells. For determining the ideal transfection concentration of LAMP2 siRNA, control cells were transfected with 60 pmol, 75 pmol, and 90 pmol siRNAs and analyzed by immunoblotting (A) and (B).

It was shown that inhibition of CMA caused the LDs accumulation in the cells (Kaushik & Cuervo, 2015). Therefore, the effects of CMA inhibition on LDs accumulation were investigated via silencing the LAMP2 protein. To downregulate the expression of LAMP2, cells were transfected with LAMP2 siRNAs as described in the method section.

First, the optimal siRNA concentration that manage to silence LAMP2 protein was determined. Thus, control cells were transfected with 60 pmol, 75 pmol, and 90 pmol siRNAs, respectively. Western blot analyses showed that 75 pmol and 90 pmol were sufficient enough to downregulate LAMP2 protein. Therefore, 75 pmol was chosen for further experiments (**Fig 4-11**).

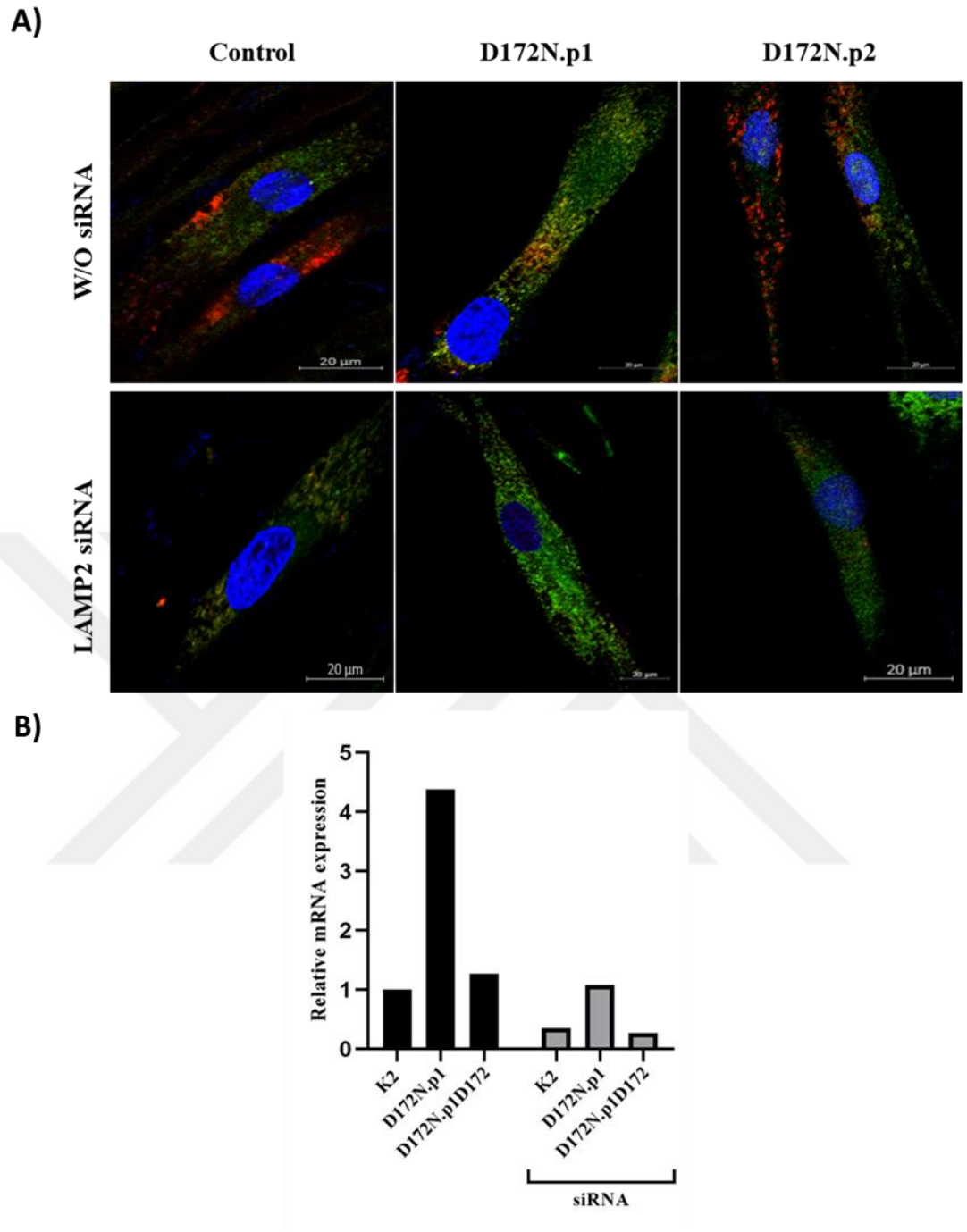

Figure 4-12: Colocalization analysis of LAMP2 and LDs (A) and RT-PCR analysis of LAMP2 mRNA expression (B) in the control and in the ARCI patient cells w/ or w/o LAMP2 siRNA transfection. A) Green signal indicates LDs stained with BODIPY®493/503, red signal indicates Alexa Fluor® 568-stained LAMP2 proteins and blue signal indicates cell nuclei stained with Hoechst 33342. Scale bar = 10 µm. B) Cells were transfected with 75 pmol LAMP2 siRNA using Lipofectamine 3000. The results were normalized to GAPDH.

After determination of the appropriate concentration of LAMP2 siRNA, control and patient cells were transfected with LAMP2 siRNA for analyzing the inhibition of CMA. Subsequently, RT-qPCR analysis was performed for confirming the downregulation of LAMP2 in control and the patient cells (**Fig.4-12(A)**). These results were also confirmed with confocal microscopy analysis (**Fig.4-12(B)**). Interestingly, the downregulation of LAMP2 in patient cells was higher than in control cells. Furthermore, in LAMP2 siRNA-transfected cells, LD average number and size analysis were conducted. The results showed that downregulation of LAMP2 did not show any significant effect on LD size and accumulation in both control and the patient cells (**Fig.4-13**).

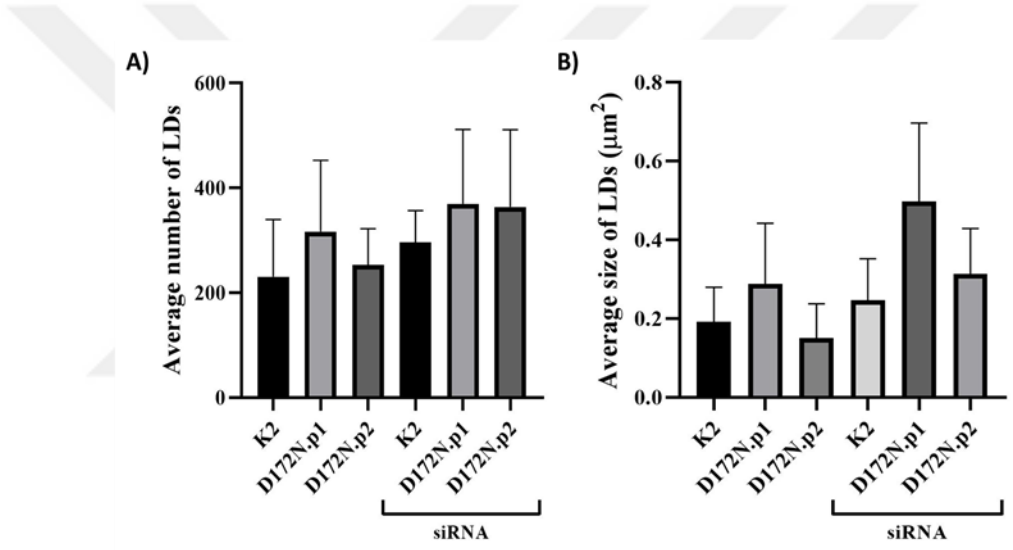

Figure 4-13: Average Number (A) and Size (B) Analysis of LAMP2 siRNA transfected ARCI patient cells. The cells were transfected with 75 pmol LAMP2 siRNA.

4.4. Lipophagy Analysis

4.4.1. LC3 Shift Assay

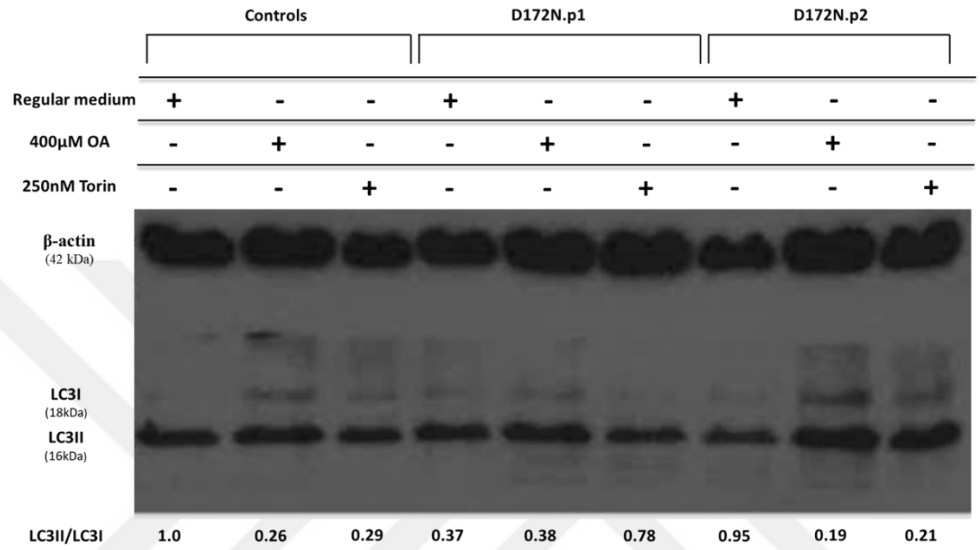

Figure 4-14: Investigation of autophagosome formation by LC3 shift assay in control and ARCI patient cells. Control and patient cells were analyzed via immunoblotting. For oleic acid induction, cells were treated with fatty acid supplemented media for 12hrs and autophagy induction, cells were treated with Torin1 for 4hrs.

LC3 is one of the crucial proteins for the lipophagy mechanism. In the cytoplasm LC3 is cleaved via Atg4 and forms LC3-I; when lipophagy is activated, PE has covalently conjugated the LC3 protein and forms LC3-II, which subsequently binds to the inner and outer membrane of the autophagosome. During the binding of PE, the molecular weight of LC3 changes, and this shift between LC3-I and LC3-II is accepted as an autophagosome marker (Hansen et al., 2018; Kaizuka et al., 2016). Thus, an LC3 shift assay was conducted in control and ARCI patient cells to investigate the autophagosome formation in the absence and presence of 250 nM Torin treatment under basal- or oleic acid-induced conditions. It was found that when autophagy was induced, the amount of LC3-I was also increasing in both control and patient cells. Therefore, no significant results were obtained in this experiment (**Fig.4-14**).

4.4.2. RFP-GFP-LC3 Dot Assay

RFP-GFP-LC3 dot assay is another method using GFP-LC3-RFP-LC3ΔG plasmid to determine the autophagic flux in the cells. In the cytosol, this plasmid cleaved by ATG4 forming GFP-LC3 and RFP-LC3ΔG. Subsequently, GFP-LC3 is lipidated and involved in the autophagosome formation, and it degraded together with the targeted substrate after the autolysosome formation. However, since RFP-LC3ΔG is mutated, it cannot involve autophagosome formation and stay in the cytosol. Therefore, GFP/RFP ratios give an idea about the autophagic flux of the cells. When this ratio is high, it indicates low autophagic flux, whereas if it is low, it indicates high autophagic flux. Additionally, red dots represent autolysosome formation, yellow dots represent both autolysosome and autophagosome formation(Kaizuka et al., 2016; Lopez, Fleming, & Rubinsztein, 2018).

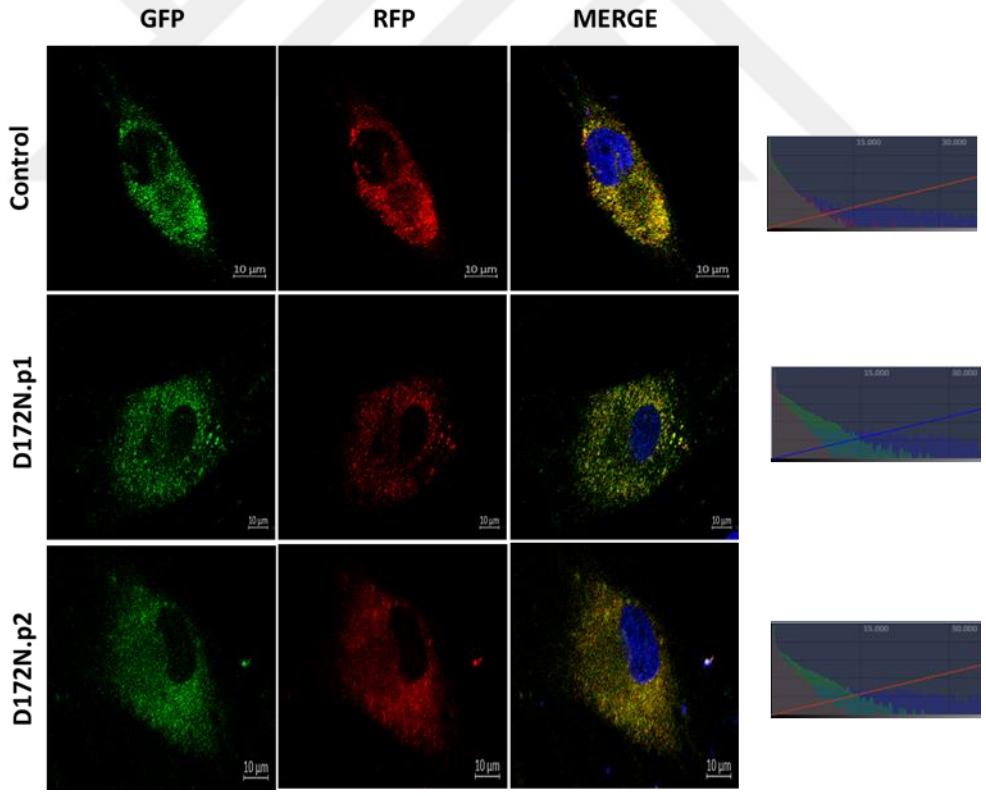

Figure 4-15: RFP-GFP-LC3 dot assay under basal conditions. Green signal indicates GFP-LC3 and red signal indicates RFP-LC3ΔG and blue signal indicates cell nuclei stained with Hoechst 33342. Scale bar = 10 µm.

The results indicated that under basal conditions, the GFP/RFP ratio was lower than the patient cells, indicating higher autophagic flux in control cells than the patient cells (**Fig.4-15**). When autophagy is induced in these cells, the intensity of the RFP signal was increased in both control and patient cells, however, the GFP/RFP ratio was lower in control cells than the patient cells, revealing higher autophagic flux in control cells (**Fig.4-16**). The higher GFP/RFP ratio of ARCI patients might be due to impaired autophagy resulting from a possible defect during autolysosome formation.

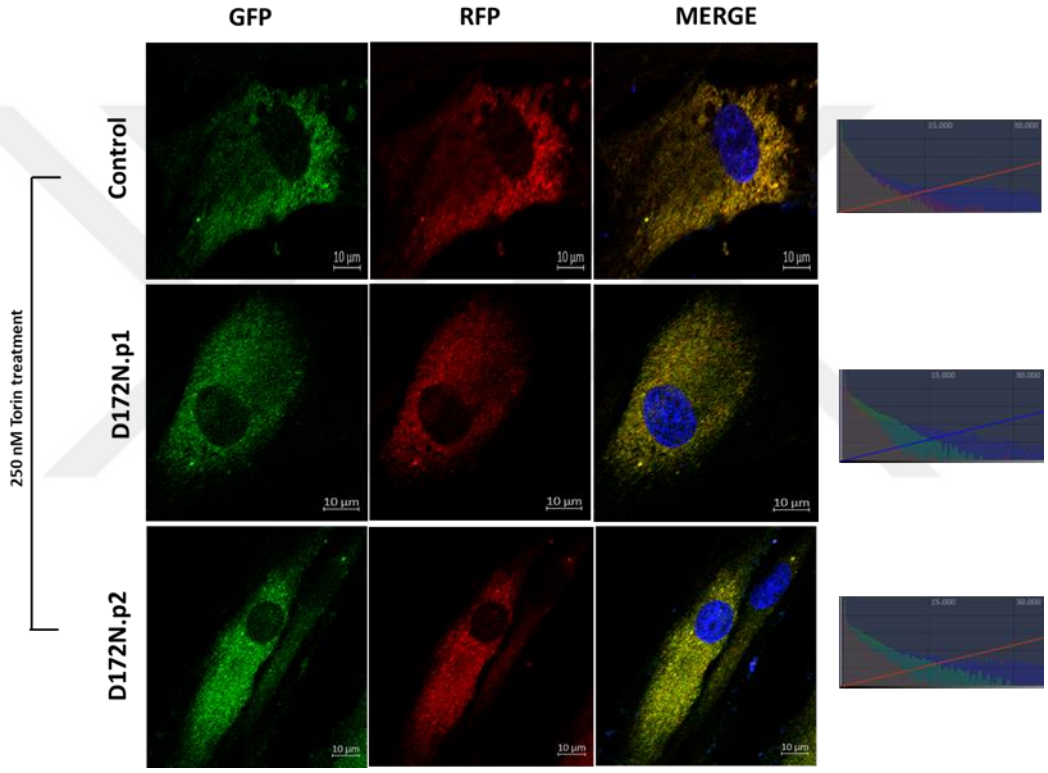

Figure 4-16: RFP-GFP-LC3 dot assay under autophagy-induced conditions. For autophagy induction, cells were treated with 250nM Torin for 4hr. Green signal indicates GFP-LC3 and red signal indicates RFP-LC3ΔG and blue signal indicates cell nuclei stained with Hoechst 33342. Scale bar = 10 µm.

4.4.3. Cathepsins and Lipid Droplets Colocalization in ARCI Patients

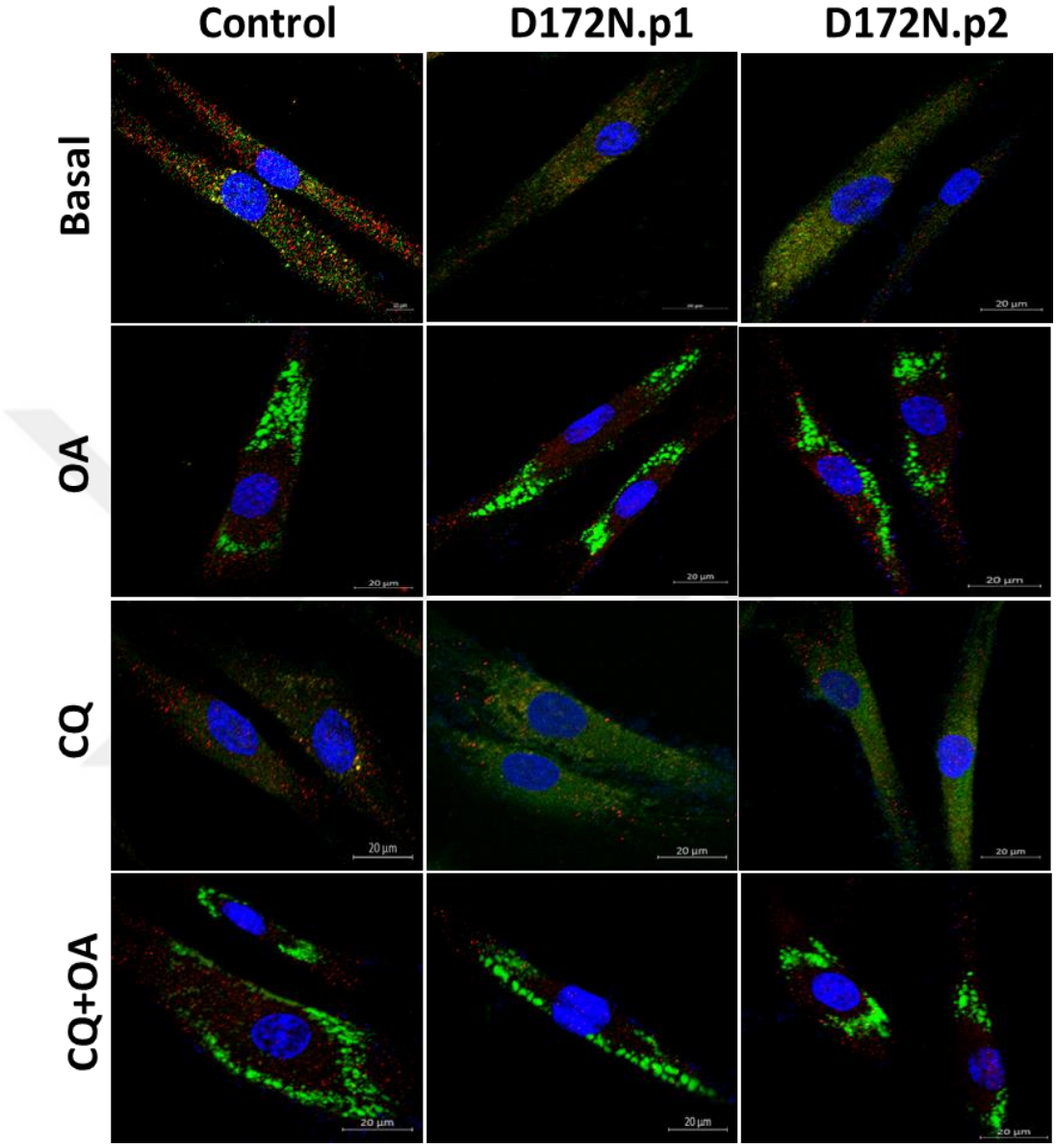

Figure 4-17: Colocalization analyzes of lipid droplets and cathepsin B proteins in control and ARCI patient cells. For oleic acid induction, cells were treated with fatty acid supplemented media for 12hrs and for CMA inhibition, cells were treated with CQ for 40 mins. Green signal indicates LDs stained with BODIPY®493/503, red signal indicates Alexa Fluor® 568-stained Cathepsin B, and blue signal indicates cell nuclei stained with Hoechst 33342. Scale bar = 10 µm.

Recently, a defect in lipophagy mechanism of ARCI patients' cells that have PNPLA1 mutation was described by our laboratory (G. Onal et al., 2019). For a better understanding of LD breakdown via lipophagy mechanism in control and patient cells, it was further investigated. Two lysosomal markers, cathepsin B and cathepsin D were selected since these proteins are ubiquitously expressed in all tissues (Steinfeld et al., 2006; Turk et al., 2012). Colocalization of the cathepsins with LDs was analyzed under basal or oleic acid-induced conditions in the presence or absence of a lysosomal inhibitor (CQ).

In control cells, cathepsin B proteins were colocalized with LDs under basal conditions and CQ treatment decreased the colocalization with LDs as well as the number of cathepsin B proteins. When these cells were treated with fatty acid supplemented media, in the absence of CQ, even though the number of cathepsin B proteins was increased by comparison with the basal conditions, cathepsin B and LDs were localized separately. Under oleic acid-induced conditions, CQ treatment had no effect on the localization of cathepsin B and LDs, however, it decreased the number of cathepsin B proteins (**Fig 4-17**). In patient cells, cathepsin B proteins were colocalized with LDs under basal conditions and CQ treatment decreased their colocalization and the number of cathepsin B proteins. When the cells were induced with oleic acid, the number of cathepsin B proteins increased while the colocalization wasn't observed (**Fig 4-17**). The mRNA expression of cathepsin B was also analyzed by RT-qPCR and the results showed that mRNA levels increased with oleic-induction whereas, it decreased under CQ treated conditions. These results were consistent with the findings in colocalization analysis (**Fig.4-18**).

Previous studies showed that cathepsin B involves in autophagy process (Gondi & Rao, 2013; Man & Kanneganti, 2016). It was reported that Cathepsin B negatively regulates the expression of lysosomal and autophagic proteins by inhibition of TFEB (transcription factor EB), thus managing the amount of lysosomes and autophagosomes (Man & Kanneganti, 2016). It was also revealed that treatment of saturated fatty acids in mature adipocytes activated the lysosomal permeabilization, subsequently, release and stimulation of cathepsin B and other lysosome-related proteases to the cytoplasm(Araujo, Cordeiro, Vasconcelos, Vitzel, & Silva, 2018; Gornicka et al., 2012). Additionally, the

study conducted with adipose tissue of obese mice revealed that, although the number of autophagosomes increased in this tissue, autophagic activity was disrupted, while the expression and the enzymatic activity of cathepsin B were significantly increased (Araujo et al., 2018; Y. Mizunoe et al., 2017). Another study conducted with 3T3L1 adipocytes proved that overexpression of cathepsin B negatively regulates the level of PLIN1 proteins in obese white adipocyte tissue, causing impairment in lipolysis mechanism (Yuhei Mizunoe et al., 2020).

The colocalization of cathepsin B and LDs may indicate the basal autophagy in control and patient cells, therefore, inhibition of this pathway with chloroquine may be the reason for the decreased colocalization of cathepsin B and LDs in control and patient cells. Additionally, oleic acid treatment to these cells might show similar effects, that were seen in adipocytes and therefore, the increased levels of cathepsin B in cytosol can be explained. Treatment can cause increased lysosomal permeability, which can increase autophagosome accumulation and upregulation of cathepsin B.

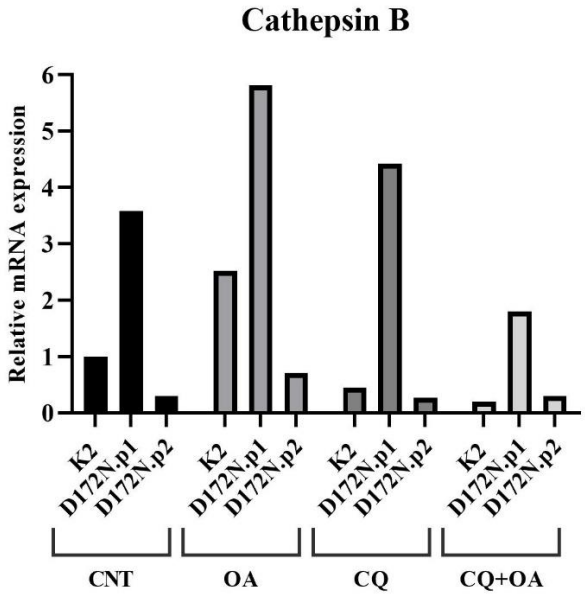

Figure 4-18: RT-PCR analysis of LAMP2 mRNA expression. Cells were treated with fatty acid supplemented media and CQ for 12h and 40 mins respectively. The results were normalized to GAPDH.

In **fig.4-19**, under basal conditions, cathepsin D proteins and LDs were colocalized both in patient cells and in control cells. Additionally, CQ treatment led to a decrease in their colocalization as well as in the amount of cathepsin D proteins, whereas oleic acid induction increased the amount of cathepsin D proteins. However, colocalization was not observed between cathepsin D proteins and LDs under these conditions.

The relationship between cathepsin D and autophagy has been investigated in previous studies. It was revealed that overexpression of cathepsin D resulted in the stimulation of autophagy increasing the LC3-II accumulation in HeLa cells (Hah et al., 2012). In another study, it was found that when cathepsin D was inhibited, autophagy levels were decreased, increasing the autophagosome accumulation and reducing the autolysosome formation in glioblastoma cells (Zheng et al., 2020). Another study showed that autophagy dysfunction resulted in impairment of the lysosomal functions leading to the decrease in the levels and enzymatic function of cathepsin D (Sarkar et al., 2014).

In our experiment, similar to the colocalization experiment of cathepsin B and LDs, colocalization of cathepsin D and LDs under basal conditions could indicate basal levels of autophagy in control and patient cells. The reduction of cathepsin D and LDs colocalization in CQ-treated control and patient cells could be demonstrated as a result of autophagy inhibition as shown in previous studies. Moreover, the separate colocalization of cathepsin D and LDs under oleic acid-induced conditions may result from increased lysosomal permeabilization leading to disruption of lipophagic degradation.

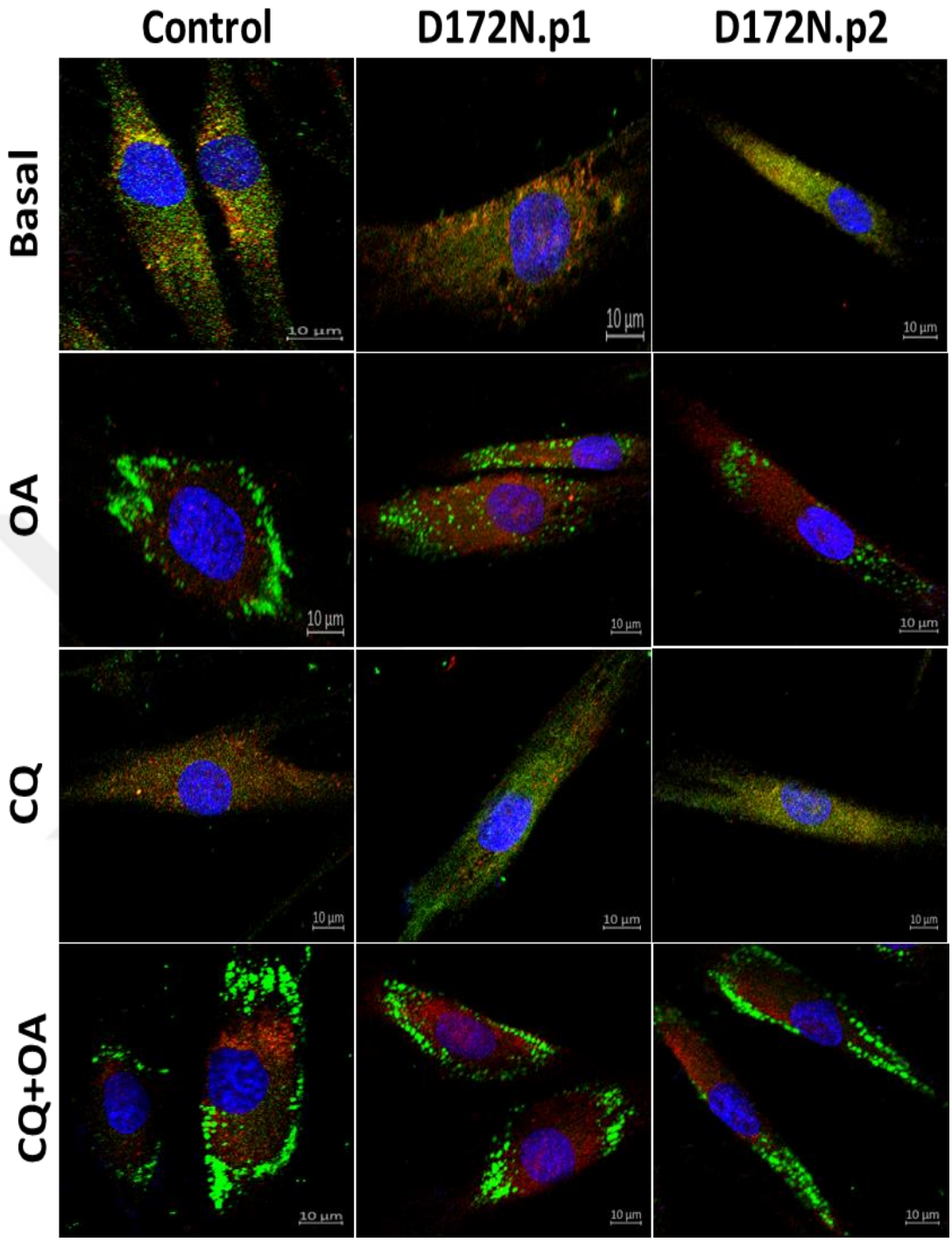

Figure 4-19: Colocalization analyzes of lipid droplets and cathepsin D proteins in control and ARCI patient cells. For oleic acid induction, cells were treated with fatty acid supplemented media for 12hrs and for CMA inhibition, cells were treated with CQ for 40 mins. Green signal indicates LDs stained with BODIPY®493/503, red signal indicates Alexa Fluor® 568-stained Cathepsin D, and blue signal indicates cell nuclei stained with Hoechst 33342. Scale bar = 10 µm.

4.4.4. Colocalization of Rab7, Bif-1, and SNARE Proteins with Lipid Droplets

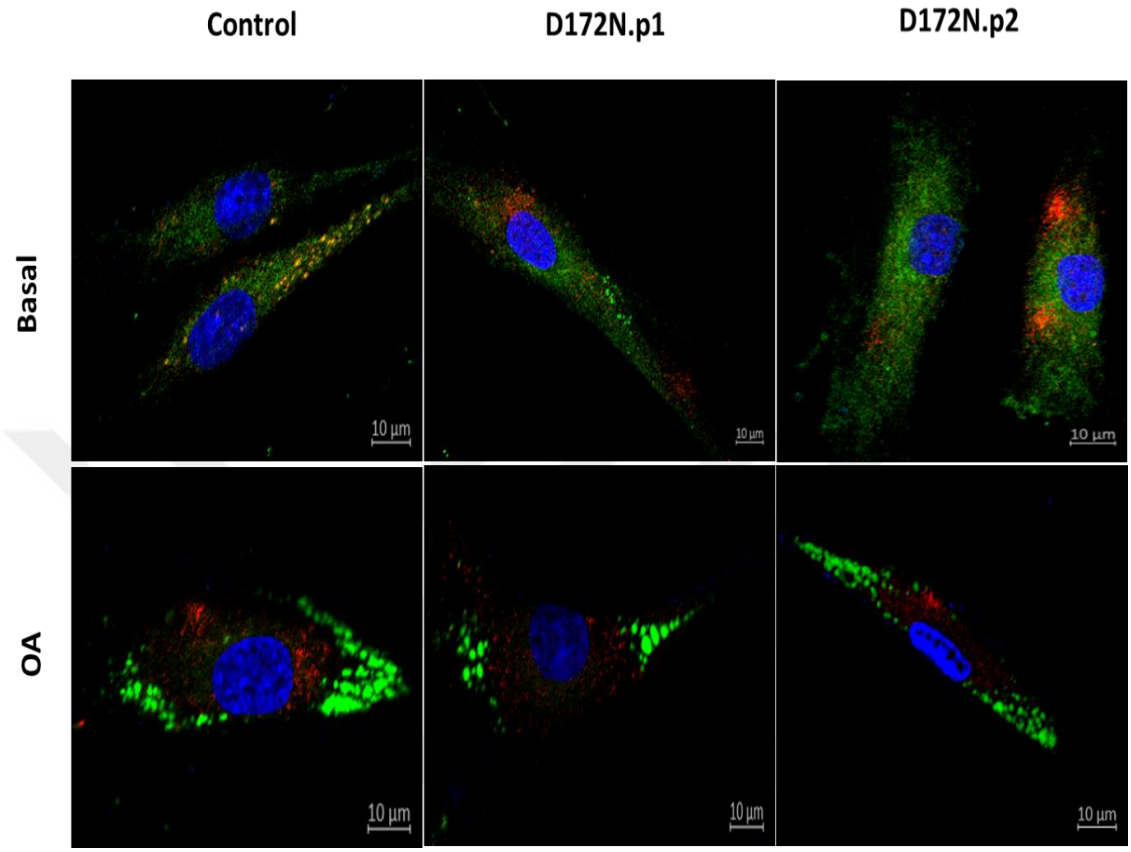

Figure 4-20: Colocalization analyzes of lipid droplets and Rab7 proteins in control and ARCI patient cells. For oleic acid induction, cells were treated with fatty acid supplemented media for 12hrs. LDs stained with BODIPY®493/503, red signal indicates Alexa Fluor® 568-stained Rab7, and blue signal indicates cell nuclei stained with Hoechst 33342. Scale bar = 10 µm.

Rab7 is a GTPase playing a crucial role in lipophagy. It was shown that this protein mediates autophagosome maturation via regulating the LDs fusion with multivesicular bodies and late endosomes (Guerra & Bucci, 2016). SNARE is another important protein playing a role in LD fusion and autophagosome biogenesis. Additionally, recent studies identified a novel lipophagy regulator, Bif-1, which mediates the degradation of PLIN proteins during lipophagy and its deficiency causes a decrease in the amount of TG hydrolysis. Therefore, colocalizations of LDs with Rab7, Bif-1, and SNARE proteins

were investigated, respectively in control and patient cells to analyze the effect of lipophagy-related proteins on LDs accumulation in ARCI disease. The experiments were conducted under basal- and oleic acid-induced conditions.

The importance of Rab7 for lipophagy has been shown in several studies. A study conducted with hepatocytes revealed that Rab7 was required for the degradation of LDs by lipophagy pathway under nutrient deficiency conditions. The stimulation of Rab7 mediates the migration of multivesicular bodies and lysosomes to the LDs for their breakdown. Blockage of Rab7 caused the reduction in lipophagic activity (Schroeder et al., 2015). In addition, it was found that Rab7 deficiency under nutrient deprivation or mTORC1 suppression conditions caused the inhibition of autophagosome-late endosome and lysosomes fusion, blocking the enzymatic activity of cathepsin B (Zhou et al., 2013). Therefore, Rab7 is crucial for lipophagy pathway by regulating the fusion of LDs with late endosomes and lysosomes (Guerra & Bucci, 2016). Considering these previous findings, we first investigated the colocalization between Rab7 and LDs in the ARCI patient cells.

The results showed that under basal conditions, Rab7 and LDs were partially colocalized in control cells, however, the colocalization was not observed in patient cells. The colocalization in control cells may indicate the fusion of LDs with late endocytic compartment, thus, indicating the basal autophagy levels and the absence of colocalization in patient cells under basal conditions may be due to a defect in the lipophagy mechanism or a defect in autophagosome fusion with late endocytic compartments. Additionally, Rab7 and LDs were localized separately in both control and the patient cells, when these cells were induced with oleic acid (**Fig. 4-20**). The separate localization of LDs and Rab7 can be resulted due to defective lipophagy mechanisms of ARCI patient cells as shown previously by our laboratory (G. Onal et al., 2019). Even though the levels of Rab7 increased with oleic acid induction, it was not sufficient enough for the degradation of LDs.

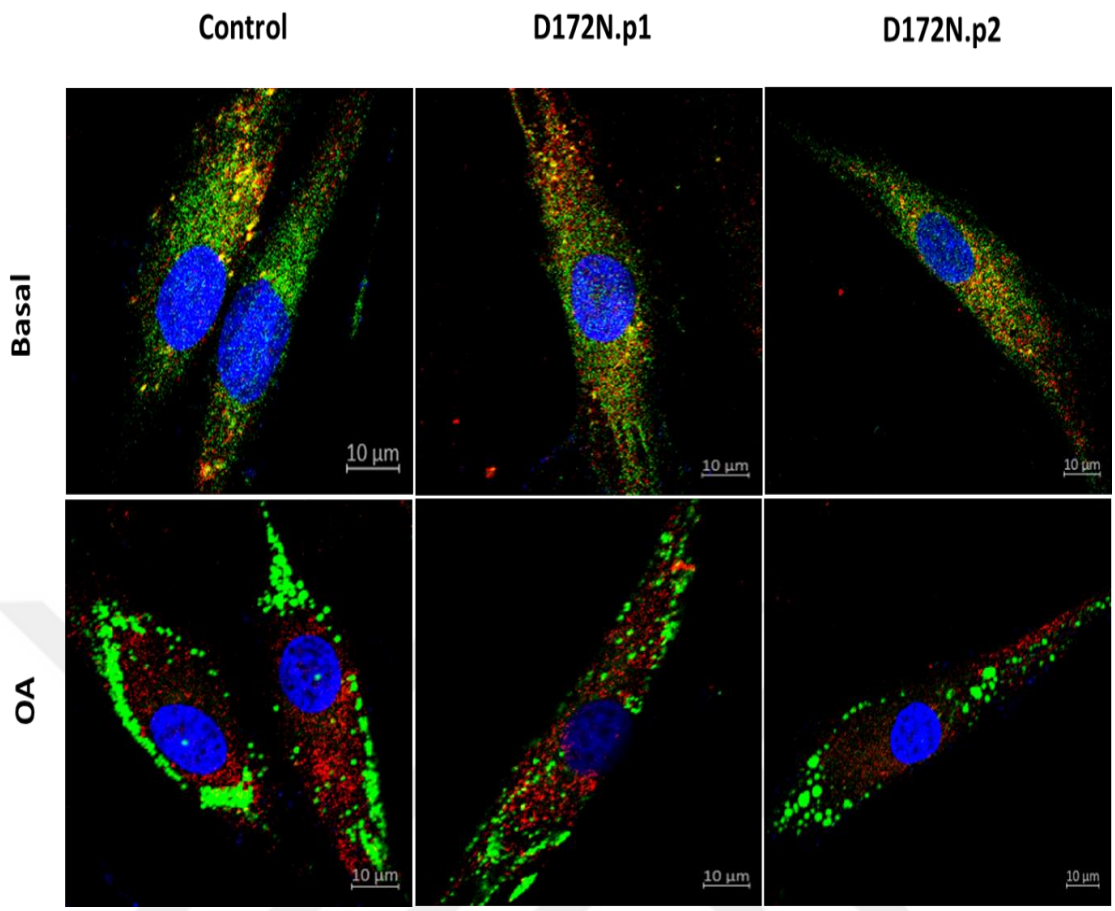

Figure 4-21: Colocalization analyzes of lipid droplets and Bif-1 proteins in control and ARCI patient cells. For oleic acid induction, cells were treated with fatty acid supplemented media for 12hrs. LDs stained with BODIPY®493/503, red signal indicates Alexa Fluor® 568-stained Bif1, and blue signal indicates cell nuclei stained with Hoechst 33342. Scale bar = 10 µm.

Previous studies revealed that Bif-1 interacts with PI3K via UVRAG and controls the trafficking of Atg9 proteins, thus, mediating the formation of autophagosome (He et al., 2013; Takahashi et al., 2007; Takahashi et al., 2011). In another study, involvement of Bif-1 in LDs breakdown was reported. In this study, Bif-1 knockdown leads to a decrease in basal level of lipolysis and downregulation of autophagy and lysosomal-related proteins such as Atg9 and LAMP1. Additionally, stimulation of lipophagy resulted in the degradation of PLIN1 in Bif-1-dependent manner (Y. Liu et al., 2016).

In **Fig. 4-21,** the colocalizations of LDs with Bif-1 proteins were observed in patient and control cells under basal conditions, which might be indicating the basal autophagy levels and autophagosome formation in both control and ARCI patient cells. When the cells were treated with fatty acid-supplemented media, the colocalization was disappeared in both control and patient cells. When cells are exposed to fatty acid supplemented media and forced to produce intracellular LDs, it could cause dysfunction of lipophagy and lysosomal pathways or the lipophagy was not sufficient enough to degrade the LDs under this condition. These may explain why the colocalization was disappeared when the cells induced with oleic acid.

SNARE, called syntaxin-17, is crucial in the fusion of autophagosome with lysosomes via complex formation with Atg14 and SNAP-29 and interacting with VAMP8, which is a lysosomal SNARE (E. Itakura & N. Mizushima, 2013; Ward et al., 2016). It has been shown that syntaxin-17 deficiency leads to the accumulation of autophagosomes while preventing their degradation (Itakura, Kishi-Itakura, & Mizushima, 2012; Eisuke Itakura & Noboru Mizushima, 2013). Additionally, it was found that syntaxin-17 is phosphorylated by TBK1 (TANK Binding Kinase 1) in response to autophagy stimulation, which is important for the ULK1 complex formation, thus affecting the initiation of autophagic mechanism (Kumar et al., 2019).

In **Fig. 4-22,** under basal conditions, the colocalization of SNARE proteins with LDs was observed in control cells whereas, colocalization could not be observed in patient cells. This could indicate the basal autophagy in control cells, however, a dysfunction in autophagy machinery could inhibit the colocalization of SNARE and LDs in ARCI patient cells. Moreover, oleic acid induction did not show any effect on patient cells, while the colocalization was disappeared in control cells. Similar to the Rab7 and Bif-1 colocalization experiments, oleic acid induction may lead to a disruption in the mechanism of lipophagy or lysosomal functions, blocking the autophagic degradation of LDs.

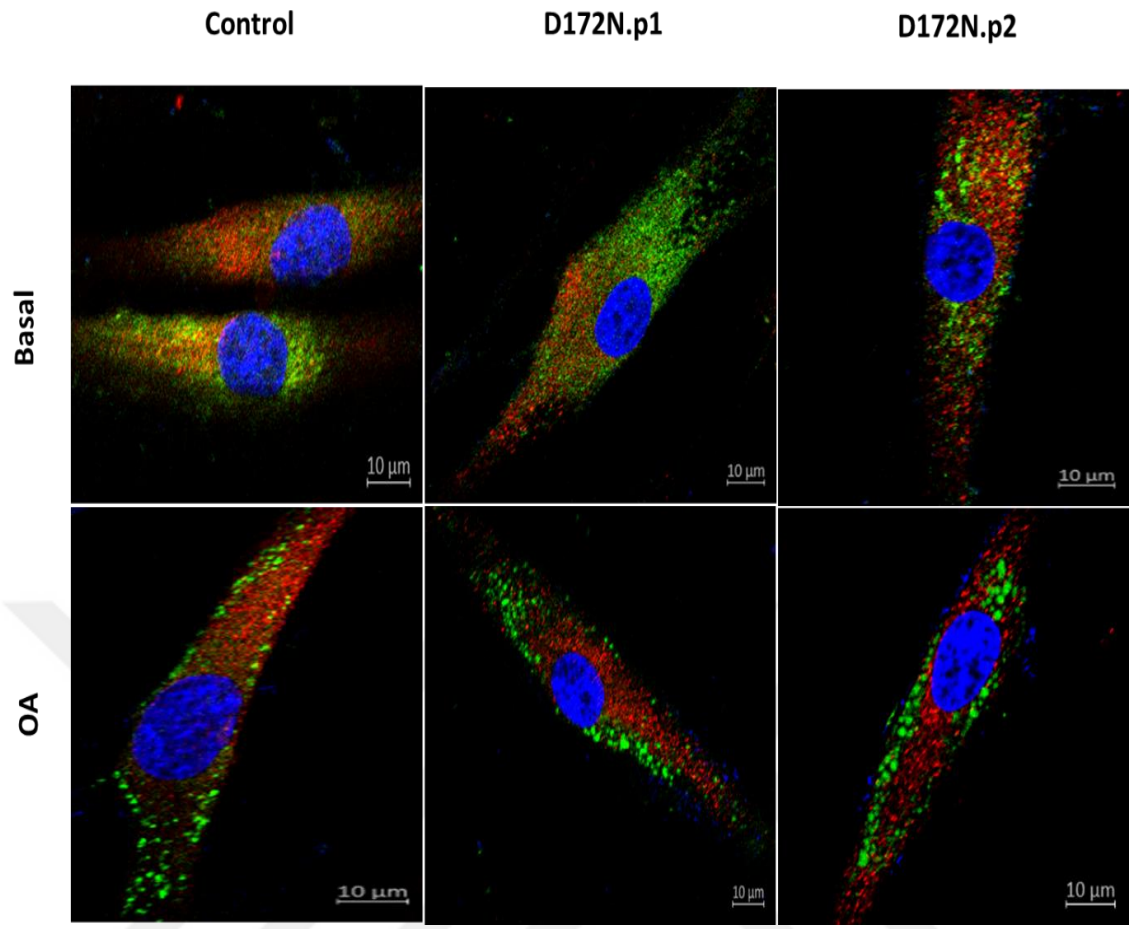

Figure 4-22: Colocalization analyzes of lipid droplets and SNARE proteins in control and ARCI patient cells. For oleic acid induction, cells were treated with fatty acid supplemented media for 12hrs. LDs stained with BODIPY®493/503, red signal indicates Alexa Fluor® 568-stained SNARE, and blue signal indicates cell nuclei stained with Hoechst 33342. Scale bar = 10 µm.

4.4.5. Analysis of p62 Protein Levels in ARCI patients

p62 is a cargo protein that assists the delivery of ubiquitinated substrates to the lysosomes for their breakdown in selective autophagy. In this mechanism, p62 noncovalently interacts with the ubiquitinated substrate via its C-terminal ubiquitin-associated domain, while it binds to the lipidated form of LC3 (ATG8) protein in the phagophore via its LIR region. Subsequently, p62 is degraded together with the targeted substrate via autophagic machinery (Bjørkøy et al., 2009; Johansen, 2019; Lamark, Svenning, & Johansen, 2017). Therefore, it can be used as a biomarker for analyzing the autophagic flux of the cells and

p62 protein levels can be associated with the autophagic activity. Accordingly, when the levels increase, this might indicate an inhibition or a deficiency of autophagy (Bjørkøy et al., 2009; W. J. Liu et al., 2016).

Previous studies showed the importance of p62 proteins for the lipophagic degradation of LDs. In the hepatic cells, colocalization of LC3 and p62 proteins with LDs was observed with ethanol treatment. p62 knockdown blocked the LC3 colocalization with LDs while increasing the triglyceride and cholesterol content of the cells. Additionally, colocalization of p62 and perilipin1 was revealed in the same study (L. Wang et al., 2017). The association of p62 and perilipin1 was further confirmed in another study conducted with rat L6 myocytes. It was suggested that when the lipophagy was activated, p62 and LDs were colocalized and perilipin1 proteins were co-immunoprecipitated with p62 proteins (Lam et al., 2016). In the light of these findings, we further investigated the lipophagic degradation of LDs by analyzing the p62 colocalization with LDs.

Under basal conditions p62 and LDs colocalization was partially observed in both patient and control cells, indicating the basal autophagy in patient and control cells. Even though the oleic acid induction caused an increment in the number of p62 proteins in both patient and control cells, colocalization was observed neither in control nor in patient cells. Oleic acid induction may lead to a deficiency in lipophagic pathway. Moreover, when autophagy is induced by Torin treatment, LDs and p62 proteins were partially colocalized in control and patient cells. Additionally, Torin treatment decreased the number of p62 proteins in all cells compared with the basal conditions. As expected, when lipophagy was induced by Torin treatment, the number of p62 proteins was decreased, because these proteins need to be degraded during the turnover of the targeted substrate. Under oleic acid-induced conditions, when cells were treated with Torin, colocalization was not observed in control and patient cells, and the number of p62 proteins was decreased compared to cells with oleic acid induction and without Torin treatment. The reduction of p62 proteins in the control and the patient cells treated with Torin under oleic acid-induced conditions may indicate the induction of lipophagy. However, although Torin treatment induces the lipophagy mechanism, it was not sufficient for the breakdown of accumulated lipid droplets in these cells. (**Fig.4-23**). This may be because the cells are

not capable enough for adapting to oleic acid induction or this induction causes a disruption in the lipophagy pathway.

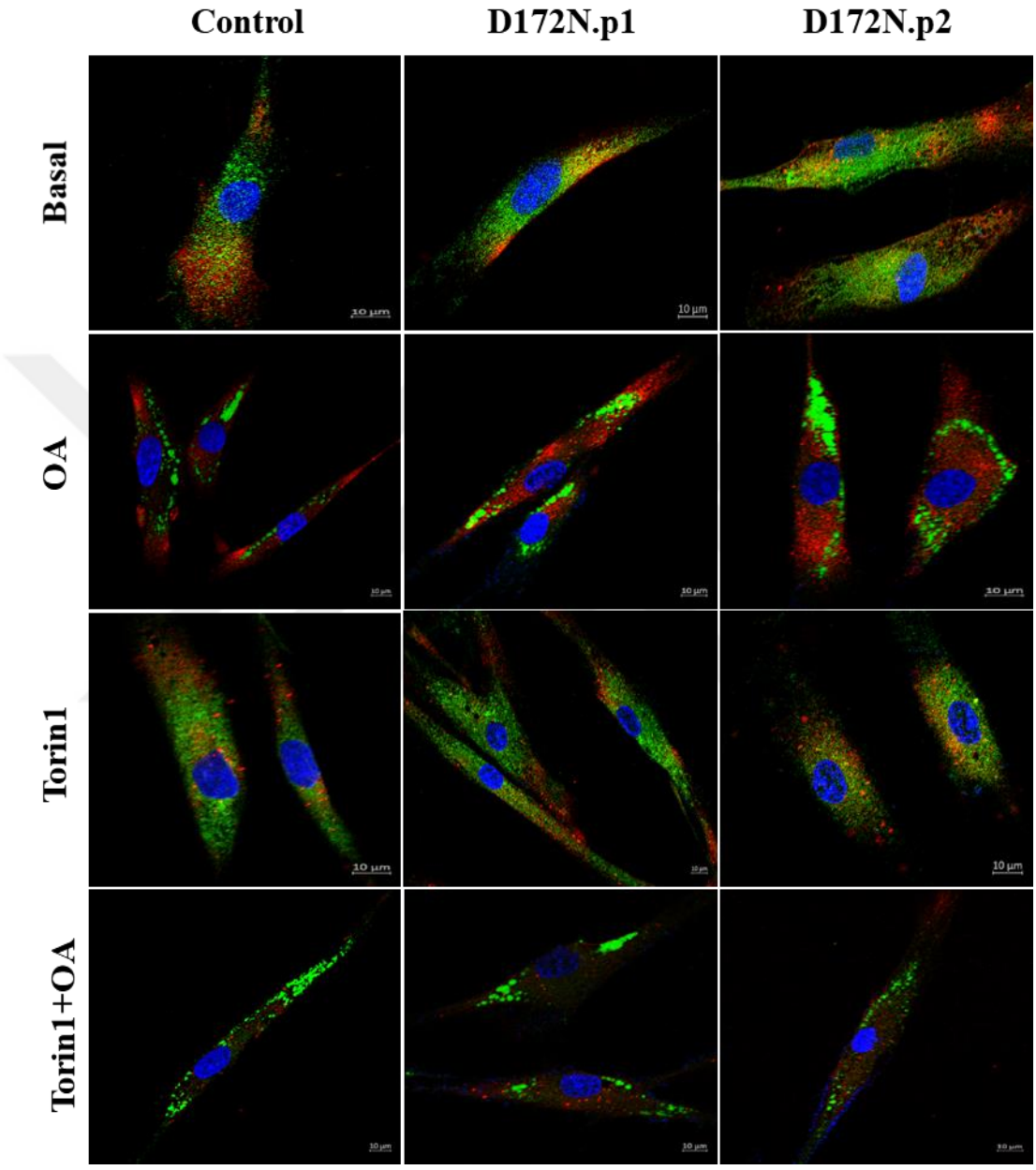

Figure 4-23: Colocalization analyzes of lipid droplets and p62 proteins in control and ARCI patient cells. For oleic acid induction, cells were treated with fatty acid supplemented media for 12hrs, and for autophagy induction, cells were treated with Torin for 4 hrs. Green signal indicates LDs stained with BODIPY®493/503, red signal indicates Alexa Fluor® 568-stained p62 and blue signal indicates cell nuclei stained with Hoechst 33342. Scale bar = 10 µm.

4.5. The Interaction Between Lipolysis, CMA, and Lipophagy

4.5.1. Colocalization of Lipid Droplets with PNPLA2

Recent studies revealed a novel mechanism involving the breakdown of intracellular LDs. It has been demonstrated that CMA is required for LD degradation and it is the upstream mediator of lipophagy and lipolysis in the LD catabolism. The study conducted with mouse fibroblasts showed that CMA inhibition blocks the recruitment of ATGL and lipophagic proteins to the LDs, increasing the LD accumulation. When the KFERQ motif of PLIN2 was mutated, this protein was accumulated on LD surfaces and reduced the ATGL and LD interaction (Kaushik & Cuervo, 2015; Kaushik & Cuervo, 2016). Therefore, the importance of CMA on lipolysis mechanism and LD turnover in the ARCI patient cells was investigated via colocalization analysis of PNPLA2 (ATGL) with LDs under basal and CMA-induced conditions. For CMA induction, retinoic acid was used as an antagonist of retinoic acid receptor α (RARα), since RARα signaling blocks CMA activity (Anguiano et al., 2013; Reynolds & Macian, 2018).

Our result suggested that PNPLA2 (ATGL) proteins were partially colocalized with LDs in both patient and control cells and retinoic acid treatment slightly increased the colocalization in these cells. Therefore, our findings were consistent with the previous studies demonstrating the interaction between CMA and lipolysis. However, there was no significant change was observed between the control and ARCI patient cells (**Fig.4-24**).

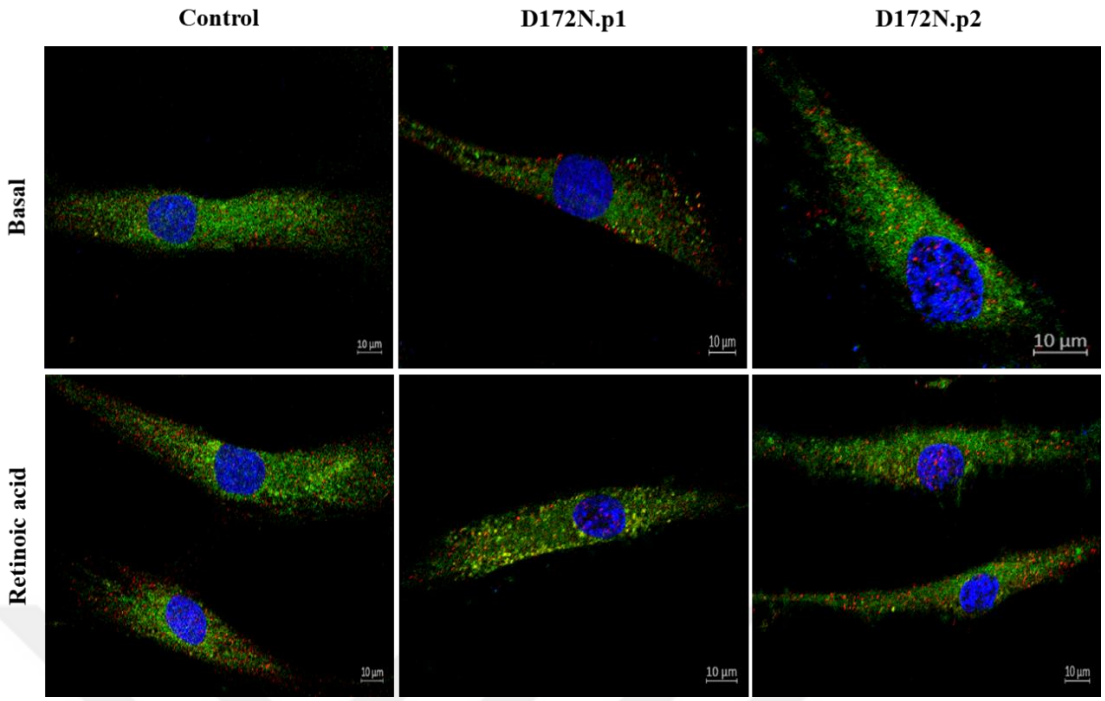

Figure 4-24: Colocalization analyzes of lipid droplets and PNPLA2 proteins in control and ARCI patient cells. For CMA induction, cells were treated with retinoic acid for 12 hrs. Green signal indicates LDs stained with BODIPY®493/503, red signal indicates Alexa Fluor® 568-stained PNPLA2, and blue signal indicates cell nuclei stained with Hoechst 33342. Scale bar = 10 µm.

5. CONCLUSION

LDs are crucial organelles that store neutral lipids such as triglycerides and sterol esters to protect cells from lipotoxicity. Except being a depot for excessive lipids, they are also involved in the regulation of lipid metabolism, cell signaling, and membrane trafficking through the proteins located on the LD surfaces. Additionally, in case of starvation, lipid droplets can provide the required energy to cells through their breakdown into free fatty acids. Subsequently, these fatty acids undergo a beta-oxidation process in mitochondria for ATP production. Three critical mechanisms mediate the LD catabolism, which are lipolysis, lipophagy, and chaperone-mediated autophagy (Barneda & Christian, 2017; Cohen, 2018; Onal et al., 2017).

In the preliminary studies, the lipolysis mechanism of patient cells was investigated by comparing them with healthy control cells. Thus, intracellular TG levels, beta-oxidation, oxygen consumption, mitochondrial disorder, and intracellular lipid mobilization of these cells were analyzed. The results indicated that even though TG levels of patient cells are higher than the control cells, oleic acid treatment did not show any significant increase in the patient cells. Additionally, beta-oxidation and oxygen consumption assays showed that patient cells consume oxygen via beta-oxidation process; however, the ratio was not as high as the control cells. Mitochondrial disorder and mitophagy analyses were indicated that morphological change in the mitochondrial network, as well as mitophagy, were increased in patient cells demonstrating a dysfunctionality in mitochondria. Additionally, LD size and number analysis revealed aberrant LD accumulation and sizes in ARCI patient cells compared to healthy control cells. These findings indicate defective lipolysis in the ARCI patient cells.

To analyze the possible reasons for aberrant LD number and size in ARCI patient cells, CMA mechanism was also investigated. These analyses revealed that LAMP2 and LDs were colocalized under basal conditions, however, colocalization was less than the control cells. Furthermore, inhibition of CMA did not show any effect on LD number and sizes in both control and patient cells. Lastly, the interaction between CMA and lipolysis was evaluated. The results indicated that CMA induction did not show any effect on the lipolysis mechanism. With these findings, it was found that PNPLA1 mutation did not show any significant effect on the CMA mechanism in ARCI patient fibroblast cells.

Another mechanism involved in LD breakdown, lipophagy, was investigated. According to the results, Bif-1 colocalization with LDs indicates autophagosome formation in both patient and control cells. Rab7 and SNARE proteins that mediate autophagosome and lysosome fusion showed separate colocalization with the LDs, indicating the possible impairment in the transport of autophagosomes to the lysosomes or impairment in the autophagosome-lysosome fusion. RFP-GFP-LC3 dot assay revealed decreased autolysosome formation in ARCI patient cells compared with the healthy control cells, supporting the findings in LD colocalization with Rab7 and SNARE. Additionally, P62 protein levels were decreased in both control and patient cells with the autophagy induction, however, this change was lower in the patient cells. Consequently, even though the autophagosomes were formed, defective lipolysis was observed in ARCI patient cells due to a possible defect in the formation of autolysosomes or a defect in the transport of autophagosomes to lysosomes.

As a summary, it was found that PNPLA1 gene mutations, which are p.Y245del and p.D172N, in ARCI patient cells show abnormal LD accumulation and sizes due to defective lipolysis and lipophagy mechanism, indicating the crucial role of PNPLA1 protein in the regulation of LD catabolism.

APPENDIX

Research Ethics Committee Approvals

Orhanlı
81474 Tuzla / İstanbul – Turkey
Telefon / Phone: +90 (0216) 483 9000
Faks / Facsimile: +90 (0216) 483 9005

İletişim Merkezi/ Communication Center:
Bankalar Caddesi 2
80820 Karaköy / İstanbul – Turkey
Telefon / Phone: +90 (0212) 292 4939
Faks / Facsimile: +90 (0212) 252 3293

www.sabanciuniv.edu

Sabancı Üniversitesi

TARİH : 04/01/2017

YER : Sabancı Üniversitesi, Orta Mah. Üniversite Cad. No:27, Tuzla 34956 İstanbul

KATILIMCILAR : Cengiz Kaya, Etik Kurul Başkanı
Ahmet Faik Kurtulmuş, Etik Kurul Üyesi
Çağla Aydın, Etik Kurul Üyesi
Müjdat Çetin, Etik Kurul Üyesi
Şerif Aziz Şimşir, Etik Kurul Üyesi
Zehra Sayers, Etik Kurul Üyesi

SABANCI ÜNİVERSİTESİ ARAŞTIRMA ETİK KURULU (AEK) ONAY FORMU	
PROJENİN ADI	"İktiyoz hastalığında yağ damlacıkları yıkım mekanizmalarının birbirleri ile etkileşimlerinin moleküler düzeyde araştırılması"
PROJENİN YÜRÜTÜCÜSÜ, İLETİŞİM BİLGİLERİ VE EKİBİ	**Proje Yürütücüsü:** YRD. DOÇ. DR ÖZLEM KUTLU- Sabancı Üniversitesi, Nanoteknoloji Araştırma ve Uygulama Merkezi (SUNUM), Tuzla / İstanbul- ozlemkutlu@sabanciuniv.edu 0-532-483 93 97 **Araştırmacı:** PROF. DR. SERAP DÖKMECİ Hacettepe Üniversitesi Tıp Fakültesi, Tıbbi Biyoloji Anabilim Dalı, 4.Kat, Sıhhıye, Ankara semre@hacettepe.edu.tr 0-312-305 25 41 **Araştırmacı:** PROF. DR. AYŞEN KARADUMAN Hacettepe Üniversitesi Tıp Fakültesi, Dermatoloji Anabilim Dalı, Sıhhıye, Ankara akaradum@hacettepe.edu.tr 0-312-305 17 04
PROJENİN AEK'YA BAŞVURMA NEDENİ	Hacettepe Üniversitesinden gelecek olan biyolojik örneğin SUNUM'da kullanılacak olması (Fibroblast primer hücre örneği)
PROJE BİR KURULUŞ TARAFINDAN DESTEKLENİYOR MU?	❑ **EVET** ■ **HAYIR ;** **EVET İSE, KURULUŞUN ADI:** TÜBİTAK-1001 kapsamında yeni proje başvurusu yapılacaktır.
PROJENİN BAŞLANGIÇ TARİHİ	Araştırmanın tahmini başlangıç tarihi Eylül 2017 olarak ön görülmektedir

PROJENİN AMACI	Projede, iktiyoz hastalığı patolojisine neden olan gen mutasyonlarının yağ damlacıkları yıkım mekanizmaları üzerindeki etkisinin moleküler düzeyde araştırılması amaçlanmaktadır.
PROJENİN ETİK İLE İLGİLİ GEREKÇESİ	Hacettepe Üniversitesi Tıbbi Biyoloji Anabilim Dalı'nda üretilen ve büyütülen fibroblast primer hücre örneklerinin SUNUM laboratuarına getirilmesi
PROJENİN YÖNTEMİ	**Hacettepe Üniversitesi Tıp Fakültesi** Bu çalışma kapsamında, hastaların dermatolojik muayeneleri, klinik değerlendirmeleri ve biyopsi örneklerinin alınması Hacettepe Üniversitesi Tıp Fakültesi Deri ve Zührevi Hastalıklar Anabilim Dalı'nda yapılacaktır. Bu aşamada, hastalardan çalışmaya özel ayrıca bir örnek alınmayacaktır. İktiyoz hastalarından, tanı koyabilmek için alınan cilt "punch" biyopsi örneklerinden bir miktar ayrılarak, uygun koşullar altında Tıbbi Biyoloji Anabilim Dalı'na getirilecektir. Tıbbi Biyoloji Anabilim Dalı'nda mutasyonları tanımlanan örneklerden fibroblast primer hücre kültürleri kurulacak ve bu örneklerden RNA ve protein izolasyonu yapılacaktır. Elde edilen RNA'lardan gerçek-zamanlı polimeraz zincir reaksiyonu (Real-time PCR) analizleri, proteinlerden ise immünblotlama (western blot) testleri yapılacaktır. Ticari olarak satın alınacak insan fibroblast hücre hattı kontrol olarak kullanılacaktır. (Hacettepe Üniversitesi Girişimsel Olmayan Klinik Araştırmalar Etik Kurulu onayı alınmış, ekte iletilmektedir). **Sabancı Üniversitesi Nanoteknoloji Araştırma ve Uygulama Merkezi (SUNUM):** İktiyoz hastalığının lipoliz ve lipofaji/CMA mekanizmalarına fonksiyonel etkileri SUNUM'da yapılacaktır. Bu amaçla, lipoliz mekanizmasının fonksiyonel olarak etki ettiği bilinen mitokondriyal analizler biyokimyasal yöntemler ile incelenecektir. Lipofaji/CMA mekanizmalarının fonksiyonel analizleri için ise sadece bu mekanizmaların aktive olduğu durumlarda görev alan ve yaygın olarak kullanılan protein belirteçlerindeki değişimler immünblotlama ve mikroskobik yöntemler ile incelenecektir. SUNUM'da yapılacak olan analizler için, Hacettepe Üniversitesi Tıbbi Biyoloji Anabilim Dalı'ndan getirilecek olan fibroblast primer hücre örnekleri kullanılacaktır.
~~**ETİK İLE İLGİLİ**~~ **KULLANILACAK BİYOLOJİK, PSİKOLOJİK VE TEKNİK VB TÜM YÖNTEMLER**	~~**Hacettepe Üniversitesi Tıp Fakültesi**~~ • İktiyoz hastalarının iç yüzündeki ciltten tek bir kez tanı amaçlı "punch" biyopsi örnekleri alınacaktır. 'Punch' biyopsi, deriden tam kat silindir şeklinde doku örneği alınması işlemidir. Biyopsi alınacak bölgeye local

	anestezi uygulanır ve ilgili bölge antiseptik solüsyon ile silinir, daha sonra anestezinin etkisinin de başlaması ile uygun bölgeden 2- 4 mm'lik, tek kullanımlık kalem şeklindeki steril 'punch' aletiyle küçük bir parça alınır. Basit ve kısa süreli bir işlemdir. İşlem sonrası dikiş atılması gerekmez, pansuman yapılıp biyopsi yeri steril spanç ile kapatılır. • Örneklerin bir kısmı, bu çalışma için Hacettepe Üniversitesi Tıbbi Biyoloji Anabilim Dalı'na getirilecek ve burada fibroblast primer hücre kültürleri kurulacaktır. Mutasyonları tanımlanan örneklerden RNA ve protein izolasyonu yapılacaktır. Elde edilen RNA'lardan gerçek-zamanlı polimeraz zincir reaksiyonu (Real-time PCR) analizleri, proteinlerden ise immünblotlama (western blot) testleri yapılacaktır. (Hacettepe Üniversitesi Girişimsel Olmayan Klinik Araştırmalar Etik Kurulu onayı alınmış, ekte iletilmektedir). **Sabancı Üniversitesi Nanoteknoloji Araştırma ve Uygulama Merkezi (SUNUM):** • Hacettepe Üniversitesi Tıbbi Biyoloji Anabilim Dalı'nda elde edilen fibroblast primer hücreler SUNUM'a getirilecektir. Burada lipoliz mekanizmasının fonksiyonel olarak etki ettiği bilinen mitokondriyal analizler biyokimyasal yöntemler ile incelenecektir. Lipofaji/CMA mekanizmalarının fonksiyonel analizleri için ise sadece bu mekanizmaların aktive olduğu durumlarda görev alan ve yaygın olarak kullanılan protein belirteçlerindeki değişimler immünblotlama ve mikroskobik yöntemler ile incelenecektir.
ETİK İLE İLGİLİ KULLANILACAK PROSEDÜR VE İLGİLİ RİSKLER YA DA TEHDİTLER	**Hacettepe Üniversitesi Tıp Fakültesi** 'Punch' biyopsi, deriden tam kat silindir şeklinde doku örneği alınması işlemidir. Biyopsi alınacak bölgeye local anestezi uygulanır ve ilgili bölge antiseptik solüsyon ile silinir, daha sonra anestezinin etkisinin de başlaması ile uygun bölgeden 2- 4 mm'lik, tek kullanımlık kalem şeklindeki steril 'punch' aletiyle küçük bir parça alınır. Basit ve kısa süreli bir işlemdir. İşlem sonrası dikiş atılması gerekmez, pansuman yapılıp biyopsi yeri steril spanç ile kapatılır. *'Punch' biyopsi sırasında oluşabilecek riskler:* Biyopsi alınan bölgede kanama olması Az bir ihtimalle işlem sonrası biyopsi alınan bölgede enfeksiyon gelişmesi Çok düşük bir ihtimalle biyopsi alınan bölgede hipertrofik skar gelişimi veya renk değişikliği ortaya çıkabilir. *Doku alınması sırasında oluşabilecek riskler:* Kesici alete bağlı az miktarda bir acı hissedebilirsiniz.

	Az bir miktarda da olsa iğne batması sonrasında kanamanın uzaması ve enfeksiyon riski bulunmaktadır. Örneklerin bir kısmı, bu çalışma için Hacettepe Üniversitesi Tıbbi Biyoloji Anabilim Dalı'na getirilecek ve burada fibroblast primer hücre kültürleri kurulacaktır. Hücre kültürü kurulması sırasında az da olsa kontaminasyon riski ile karşılaşılabilir. (Hacettepe Üniversitesi Girişimsel Olmayan Klinik Araştırmalar Etik Kurulu onayı alınmış, ekte iletilmektedir). **Sabancı Üniversitesi Nanoteknoloji Araştırma ve Uygulama Merkezi (SUNUM)** Hacettepe Üniversitesi Tıbbi Biyoloji Anabilim Dalı'nda mutasyon tanımlamaları yapılmış örneklerden elde edilecek olan fibroblast primer hücreler SUNUM BSL-2 seviyesindeki laboratuara getirilecek ve araştırmanın fonksiyonel analizleri burada yapılacaktır. Hacettepe Üniversitesi Tıp Fakültesi Hastanesi'nde patolojik analizleri yapılmış, herhangi bir bulaşıcı hastalık taşımayan hücre örnekleri getirileceğinden ve SUNUM BSL-2 seviyesindeki laboratuarlarda insan primer hücreleri için güvenlik kuralları oluşturularak hazırlanan özel çalışma alanları bulunduğundan ciddi bir tehdit oluşturmamaktadır. Örneklerin imha edilmesi, SUNUM biyolojik atık kurallarına uygun olarak yapılacaktır.
RİSKLER YA DA TEHDİTLERİ ENGELLEYECEK ÖNLEMLER NELERDİR?	**Hacettepe Üniversitesi Tıp Fakültesi** Biyopsi sırasında bir sağlık sorunu ile karşılaşıldığında, Prof. Dr. Ayşen Karaduman günün herhangi bir saatinde müdahale edebilecektir. Primer hücre kültürü sırasında karşılaşılacak herhangi bir sorunda Prof. Dr. Serap Dökmeci müdahale edecektir. **Sabancı Üniversitesi Nanoteknoloji Araştırma ve Uygulama Merkezi (SUNUM)** Hacettepe Üniversitesi Tıp Fakültesi Hastanesi laboratuarlarında test edilen ve hastalık taşımayan fibroblast primer hücre örnekleri, soğuk ortamda ve kapalı özel kutularla SUNUM laboratuarlarına getirilecektir. Analizler, bu tip örnekler için özel olarak ayrılmış alanlarda, BSL-2 güvenlik kuralları dahilinde yapılacaktır.
PROJENİN İÇERİĞİNDE HERHANGİ BİR ÖDÜL YA DA ÜCRET UYGULAMASI OLUP OLMADIĞINI AÇIKLAYINIZ	Örnek alınacak hastalar, bu araştırma için yapılacak harcamalarla ilgili herhangi bir parasal sorumluluk altına girmeyecektir. Hastaya bir ödeme yapılmayacak ve hastadan herhangi bir ücret talep edilmeyecektir.
VERİ SAĞLANACAK KİŞİLERDEN/EVEBEYNLERDEN BU ÇALIŞMA İÇİN İZİN FORMU ALINDI MI?	"Hacettepe Üniversitesi Girişimsel Olmayan Klinik Araştırmalar Etik Kurulu" yönetmelikleri dahilinde, bu çalışma ile ilgili hastaların bilgilendirilmesini sağlayan hekim açıklaması ve hastaların çalışmaya gönüllü olarak katıldığına dair beyanının bulunduğu "Araştırma amaçlı

	çalışma için aydınlatılmış onam formu" hazırlanmıştır. Örnekler, hekim ve hastaların bu formu imzalamasının ardından alınabilecektir.
BU ÇALIŞMANIN YAPILACAĞI BAŞKA KURUM VARSA O KURUMDAN ONAY ALINDI MI?	(Hacettepe Üniversitesi Girişimsel Olmayan Klinik Araştırmalar Etik Kurulu onayı alınmış, ekte iletilmektedir).

Sabancı Üniversitesi Nanoteknoloji Araştırma ve Uygulama Merkezi araştırmacılarımızdan Sayın Özlem Kutlu'nun "İktiyoz hastalığında yağ damlacıkları yıkım mekanizmalarının birbirleri ile etkileşimlerinin moleküller düzeyde araştırılması" adlı projesi/araştırması AEK tarafından değerlendirilmiştir.

Proje etik açısından uygun bulunmuştur. ■

Projenin etik açısından geliştirilmesi gerekmektedir. ❑

Proje etik açısından uygun bulunmamıştır. ❑

İmzalar:

T.C.
HACETTEPE ÜNİVERSİTESİ
Girişimsel Olmayan Klinik Araştırmalar Etik Kurulu

Sayı : 16969557 – 44

Konu : *ARAŞTIRMA PROJESİ DEĞERLENDİRME RAPORU*

REFERENCES

Adeva-Andany, M. M., Carneiro-Freire, N., Seco-Filgueira, M., Fernández-Fernández, C., & Mouriño-Bayolo, D. (2019). Mitochondrial β-oxidation of saturated fatty acids in humans. *Mitochondrion, 46*, 73-90. doi:https://doi.org/10.1016/j.mito.2018.02.009

Akiyama, M. (2010). ABCA12 mutations and autosomal recessive congenital ichthyosis: a review of genotype/phenotype correlations and of pathogenetic concepts. *Hum Mutat, 31*(10), 1090-1096. doi:10.1002/humu.21326

Akiyama, M. (2017). Corneocyte lipid envelope (CLE), the key structure for skin barrier function and ichthyosis pathogenesis. *J Dermatol Sci, 88*(1), 3-9. doi:10.1016/j.jdermsci.2017.06.002

Almeida, L., Dhillon-LaBrooy, A., Carriche, G., Berod, L., & Sparwasser, T. (2021). CD4+ T-cell differentiation and function: Unifying glycolysis, fatty acid oxidation, polyamines NAD mitochondria. *Journal of Allergy and Clinical Immunology, 148*(1), 16-32. doi:https://doi.org/10.1016/j.jaci.2021.03.033

Anguiano, J., Garner, T. P., Mahalingam, M., Das, B. C., Gavathiotis, E., & Cuervo, A. M. (2013). Chemical modulation of chaperone-mediated autophagy by retinoic acid derivatives. *Nature Chemical Biology, 9*(6), 374-382. doi:10.1038/nchembio.1230

Araujo, T. F., Cordeiro, A. V., Vasconcelos, D. A. A., Vitzel, K. F., & Silva, V. R. R. (2018). The role of cathepsin B in autophagy during obesity: A systematic review. *Life Sciences, 209*, 274-281. doi:https://doi.org/10.1016/j.lfs.2018.08.024

Barneda, D., & Christian, M. (2017). Lipid droplet growth: regulation of a dynamic organelle. *Current Opinion in Cell Biology, 47*, 9-15. doi:https://doi.org/10.1016/j.ceb.2017.02.002

Bjørkøy, G., Lamark, T., Pankiv, S., Øvervatn, A., Brech, A., & Johansen, T. (2009). Chapter 12 Monitoring Autophagic Degradation of p62/SQSTM1. In *Methods in Enzymology* (Vol. 452, pp. 181-197): Academic Press.

Catarino, S., Pereira, P., & Girão, H. (2017). Molecular control of chaperone-mediated autophagy. *Essays Biochem, 61*(6), 663-674. doi:10.1042/ebc20170057

Chang, P. A., Sun, Y. J., Huang, F. F., Qin, W. Z., Chen, Y. Y., Zeng, X., & Wu, Y. J. (2013). Identification of human patatin-like phospholipase domain-containing protein 1 and a mutant in human cervical cancer HeLa cells. *Mol Biol Rep, 40*(10), 5597-5605. doi:10.1007/s11033-013-2661-9

Cohen, S. (2018). Chapter Three - Lipid Droplets as Organelles. In L. Galluzzi (Ed.), *International Review of Cell and Molecular Biology* (Vol. 337, pp. 83-110): Academic Press.

Cuervo, A. M., & Wong, E. (2014). Chaperone-mediated autophagy: roles in disease and aging. *Cell Research, 24*(1), 92-104. doi:10.1038/cr.2013.153

Cui, W., Sathyanarayan, A., Lopresti, M., Aghajan, M., Chen, C., & Mashek, D. G. (2021). Lipophagy-derived fatty acids undergo extracellular efflux via lysosomal exocytosis. *Autophagy, 17*(3), 690-705. doi:10.1080/15548627.2020.1728097

Dalhaimer, P. (2019). Lipid Droplets in Disease. *Cells, 8*(9), 974. doi:10.3390/cells8090974

Deevska, G. M., & Nikolova-Karakashian, M. N. (2017). The expanding role of sphingolipids in lipid droplet biogenesis. *Biochimica et Biophysica Acta (BBA) - Molecular and Cell Biology of Lipids, 1862*(10, Part B), 1155-1165. doi:https://doi.org/10.1016/j.bbalip.2017.07.008

Dikic, I., & Elazar, Z. (2018). Mechanism and medical implications of mammalian autophagy. *Nature Reviews Molecular Cell Biology, 19*(6), 349-364. doi:10.1038/s41580-018-0003-4

Fachal, L., Rodríguez-Pazos, L., Ginarte, M., Carracedo, A., Toribio, J., & Vega, A. (2014). Identification of a novel PNPLA1 mutation in a Spanish family with autosomal recessive congenital ichthyosis. *Br J Dermatol, 170*(4), 980-982. doi:10.1111/bjd.12757

Feingold, K. R., & Jiang, Y. J. (2011). The mechanisms by which lipids coordinately regulate the formation of the protein and lipid domains of the stratum corneum. *Dermato-Endocrinology, 3*(2), 113-118. doi:10.4161/derm.3.2.14996

Freedman, J. C., Parry, T. J., Zhang, P., Majumdar, A., Krishnan, S., Regula, L. K., . . . Agarwal, P. (2021). Preclinical Evaluation of a Modified Herpes Simplex Virus Type 1 Vector Encoding Human TGM1 for the Treatment of Autosomal Recessive Congenital Ichthyosis. *J Invest Dermatol, 141*(4), 874-882.e876. doi:10.1016/j.jid.2020.07.035

Gao, M., Huang, X., Song, B. L., & Yang, H. (2019). The biogenesis of lipid droplets: Lipids take center stage. *Prog Lipid Res, 75*, 100989. doi:10.1016/j.plipres.2019.100989

Gondi, C. S., & Rao, J. S. (2013). Cathepsin B as a cancer target. *Expert Opin Ther Targets, 17*(3), 281-291. doi:10.1517/14728222.2013.740461

Gornicka, A., Fettig, J., Eguchi, A., Berk, M. P., Thapaliya, S., Dixon, L. J., & Feldstein, A. E. (2012). Adipocyte hypertrophy is associated with lysosomal permeability both in vivo and in vitro: role in adipose tissue inflammation. *Am J Physiol Endocrinol Metab, 303*(5), E597-606. doi:10.1152/ajpendo.00022.2012

Grall, A., Guaguère, E., Planchais, S., Grond, S., Bourrat, E., Hausser, I., . . . Fischer, J. (2012). PNPLA1 mutations cause autosomal recessive congenital ichthyosis in golden retriever dogs and humans. *Nat Genet, 44*(2), 140-147. doi:10.1038/ng.1056

Gross, D. A., Zhan, C., & Silver, D. L. (2011). Direct binding of triglyceride to fat storage-inducing transmembrane proteins 1 and 2 is important for lipid droplet formation. *Proc Natl Acad Sci U S A, 108*(49), 19581-19586. doi:10.1073/pnas.1110817108

Guerra, F., & Bucci, C. (2016). Multiple Roles of the Small GTPase Rab7. *Cells, 5*(3), 34. doi:10.3390/cells5030034

Hah, Y. S., Noh, H. S., Ha, J. H., Ahn, J. S., Hahm, J. R., Cho, H. Y., & Kim, D. R. (2012). Cathepsin D inhibits oxidative stress-induced cell death via activation of autophagy in cancer cells. *Cancer Lett, 323*(2), 208-214. doi:10.1016/j.canlet.2012.04.012

Hansen, M., Rubinsztein, D. C., & Walker, D. W. (2018). Autophagy as a promoter of longevity: insights from model organisms. *Nature Reviews Molecular Cell Biology, 19*(9), 579-593. doi:10.1038/s41580-018-0033-y

He, S., Ni, D., Ma, B., Lee, J.-H., Zhang, T., Ghozalli, I., . . . Li, B. (2013). PtdIns (3) P-bound UVRAG coordinates Golgi–ER retrograde and Atg9 transport by differential interactions with the ER tether and the beclin 1 complex. *Nature cell biology, 15*(10), 1206-1219.

Henne, W. M., Reese, M. L., & Goodman, J. M. (2019). The assembly of lipid droplets and their roles in challenged cells. *The EMBO Journal, 38*(9), e101816. doi:https://doi.org/10.15252/embj.2019101816

Hirabayashi, T., Murakami, M., & Kihara, A. (2019). The role of PNPLA1 in ω-O-acylceramide synthesis and skin barrier function. *Biochimica et Biophysica Acta (BBA) - Molecular and Cell Biology of Lipids, 1864*(6), 869-879. doi:https://doi.org/10.1016/j.bbalip.2018.09.010

Hugenroth, M., & Bohnert, M. (2020). Come a little bit closer! Lipid droplet-ER contact sites are getting crowded. *Biochimica et Biophysica Acta (BBA) - Molecular Cell Research, 1867*(2), 118603. doi:https://doi.org/10.1016/j.bbamcr.2019.118603

Itakura, E., Kishi-Itakura, C., & Mizushima, N. (2012). The hairpin-type tail-anchored SNARE syntaxin 17 targets to autophagosomes for fusion with endosomes/lysosomes. *Cell, 151*(6), 1256-1269. doi:10.1016/j.cell.2012.11.001

Itakura, E., & Mizushima, N. (2013). Syntaxin 17. *Autophagy, 9*(6), 917-919. doi:10.4161/auto.24109

Itakura, E., & Mizushima, N. (2013). Syntaxin 17: the autophagosomal SNARE. *Autophagy, 9*(6), 917-919. doi:10.4161/auto.24109

Jarc, E., & Petan, T. (2019). Lipid Droplets and the Management of Cellular Stress. *Yale J Biol Med, 92*(3), 435-452.

Johansen, T. (2019). Selective Autophagy: RNA Comes from the Vault to Regulate p62/SQSTM1. *Current Biology, 29*(8), R297-R299. doi:https://doi.org/10.1016/j.cub.2019.03.008

Jones, B. (2012). A histone anchor on lipid droplets. *Nature Reviews Molecular Cell Biology, 13*(12), 753-753. doi:10.1038/nrm3480

Juste, Y. R., & Cuervo, A. M. (2019). Analysis of Chaperone-Mediated Autophagy. *Methods in molecular biology (Clifton, N.J.), 1880*, 703-727. doi:10.1007/978-1-4939-8873-0_47

Kaizuka, T., Morishita, H., Hama, Y., Tsukamoto, S., Matsui, T., Toyota, Y., . . . Mizushima, N. (2016). An Autophagic Flux Probe that Releases an Internal Control. *Molecular Cell, 64*(4), 835-849. doi:https://doi.org/10.1016/j.molcel.2016.09.037

Katayama, H., Kogure, T., Mizushima, N., Yoshimori, T., & Miyawaki, A. (2011). A Sensitive and Quantitative Technique for Detecting Autophagic Events Based on Lysosomal Delivery. *Chemistry & Biology, 18*(8), 1042-1052. doi:https://doi.org/10.1016/j.chembiol.2011.05.013

Kaushik, S., & Cuervo, A. M. (2012). Chaperone-mediated autophagy: a unique way to enter the lysosome world. *Trends Cell Biol, 22*(8), 407-417. doi:10.1016/j.tcb.2012.05.006

Kaushik, S., & Cuervo, A. M. (2015). Degradation of lipid droplet-associated proteins by chaperone-mediated autophagy facilitates lipolysis. *Nat Cell Biol, 17*(6), 759-770. doi:10.1038/ncb3166

Kaushik, S., & Cuervo, A. M. (2016). AMPK-dependent phosphorylation of lipid droplet protein PLIN2 triggers its degradation by CMA. *Autophagy, 12*(2), 432-438. doi:10.1080/15548627.2015.1124226

Kaushik, S., & Cuervo, A. M. (2018). The coming of age of chaperone-mediated autophagy. *Nature Reviews Molecular Cell Biology, 19*(6), 365-381. doi:10.1038/s41580-018-0001-6

Khawar, M. B., Abbasi, M. H., Rafiq, M., Naz, N., Mehmood, R., & Sheikh, N. (2021). A Decade of Mighty Lipophagy: What We Know and What Facts We Need to Know? *Oxidative Medicine and Cellular Longevity, 2021*, 5539161. doi:10.1155/2021/5539161

Khawar, M. B., Gao, H., & Li, W. (2019). Autophagy and Lipid Metabolism. *Adv Exp Med Biol, 1206*, 359-374. doi:10.1007/978-981-15-0602-4_17

Kien, B., Grond, S., Haemmerle, G., Lass, A., Eichmann, T. O., & Radner, F. P. W. (2018). ABHD5 stimulates PNPLA1-mediated ω-O-acylceramide biosynthesis essential for a functional skin permeability barrier[S]. *Journal of Lipid Research, 59*(12), 2360-2367. doi:https://doi.org/10.1194/jlr.M089771

Kienesberger, P. C., Oberer, M., Lass, A., & Zechner, R. (2009). Mammalian patatin domain containing proteins: a family with diverse lipolytic activities involved in multiple biological functions. *J Lipid Res, 50 Suppl*(Suppl), S63-68. doi:10.1194/jlr.R800082-JLR200

Kloska, A., Węsierska, M., Malinowska, M., Gabig-Cimińska, M., & Jakóbkiewicz-Banecka, J. (2020). Lipophagy and Lipolysis Status in Lipid Storage and Lipid Metabolism Diseases. *International Journal of Molecular Sciences, 21*(17), 6113. Retrieved from https://www.mdpi.com/1422-0067/21/17/6113

Kocaturk, N. M., Akkoc, Y., Kig, C., Bayraktar, O., Gozuacik, D., & Kutlu, O. (2019). Autophagy as a molecular target for cancer treatment. *European Journal of Pharmaceutical Sciences, 134*, 116-137. doi:https://doi.org/10.1016/j.ejps.2019.04.011

Koncha, R. R., Ramachandran, G., Sepuri, N. B. V., & Ramaiah, K. V. A. (2021). CCCP-induced mitochondrial dysfunction - characterization and analysis of integrated stress response to cellular signaling and homeostasis. *Febs j, 288*(19), 5737-5754. doi:10.1111/febs.15868

Kong, J., Ji, Y., Jeon, Y. G., Han, J. S., Han, K. H., Lee, J. H., . . . Kim, J. B. (2020). Spatiotemporal contact between peroxisomes and lipid droplets regulates fasting-induced lipolysis via PEX5. *Nature Communications, 11*(1), 578. doi:10.1038/s41467-019-14176-0

Kounakis, K., Chaniotakis, M., Markaki, M., & Tavernarakis, N. (2019). Emerging Roles of Lipophagy in Health and Disease. *Frontiers in cell and developmental biology, 7*, 185-185. doi:10.3389/fcell.2019.00185

Kumar, S., Gu, Y., Abudu, Y. P., Bruun, J. A., Jain, A., Farzam, F., . . . Deretic, V. (2019). Phosphorylation of Syntaxin 17 by TBK1 Controls Autophagy Initiation. *Dev Cell, 49*(1), 130-144.e136. doi:10.1016/j.devcel.2019.01.027

Lam, T., Harmancey, R., Vasquez, H., Gilbert, B., Patel, N., Hariharan, V., . . . Taegtmeyer, H. (2016). Reversal of intramyocellular lipid accumulation by lipophagy and a p62-mediated pathway. *Cell Death Discov, 2*, 16061. doi:10.1038/cddiscovery.2016.61

Lamark, T., Svenning, S., & Johansen, T. (2017). Regulation of selective autophagy: the p62/SQSTM1 paradigm. *Essays in Biochemistry, 61*(6), 609-624. doi:10.1042/ebc20170035

Lescat, L., Véron, V., Mourot, B., Péron, S., Chenais, N., Dias, K., . . . Seiliez, I. (2020). Chaperone-Mediated Autophagy in the Light of Evolution: Insight from Fish. *Molecular Biology and Evolution, 37*(10), 2887-2899. doi:10.1093/molbev/msaa127

Li, W., Nie, T., Xu, H., Yang, J., Yang, Q., & Mao, Z. (2019). Chaperone-mediated autophagy: Advances from bench to bedside. *Neurobiol Dis, 122*, 41-48. doi:10.1016/j.nbd.2018.05.010

Li, W., Oberlin, K. E., Wilson, T. E., & Haggstrom, A. N. (2020). Bathing suit ichthyosis: Two Burmese siblings and a review of the literature. *Pediatric Dermatology, 37*(1), 165-170. doi:https://doi.org/10.1111/pde.14030

Liu, W. J., Ye, L., Huang, W. F., Guo, L. J., Xu, Z. G., Wu, H. L., . . . Liu, H. F. (2016). p62 links the autophagy pathway and the ubiqutin–proteasome system upon ubiquitinated protein degradation. *Cellular & Molecular Biology Letters, 21*(1), 29. doi:10.1186/s11658-016-0031-z

Liu, Y., Takahashi, Y., Desai, N., Zhang, J., Serfass, J. M., Shi, Y. G., . . . Wang, H. G. (2016). Bif-1 deficiency impairs lipid homeostasis and causes obesity accompanied by insulin resistance. *Scientific Reports, 6*. doi:10.1038/srep20453

Lizaso, A., Tan, K.-T., & Lee, Y.-H. (2013). β-adrenergic receptor-stimulated lipolysis requires the RAB7-mediated autolysosomal lipid degradation. *Autophagy, 9*(8), 1228-1243. doi:10.4161/auto.24893

Lopez, A., Fleming, A., & Rubinsztein, D. (2018). Seeing is believing: methods to monitor vertebrate autophagy in vivo. *Open Biology, 8*, 180106. doi:10.1098/rsob.180106

Man, S. M., & Kanneganti, T.-D. (2016). Regulation of lysosomal dynamics and autophagy by CTSB/cathepsin B. *Autophagy, 12*(12), 2504-2505. doi:10.1080/15548627.2016.1239679

Martinez-Lopez, N., Garcia-Macia, M., Sahu, S., Athonvarangkul, D., Liebling, E., Merlo, P., . . . Singh, R. (2016). Autophagy in the CNS and Periphery Coordinate Lipophagy and Lipolysis in the Brown Adipose Tissue and Liver. *Cell Metabolism, 23*(1), 113-127. doi:https://doi.org/10.1016/j.cmet.2015.10.008

Martinez-Lopez, N., & Singh, R. (2015). Autophagy and Lipid Droplets in the Liver. *Annual Review of Nutrition, 35*(1), 215-237. doi:10.1146/annurev-nutr-071813-105336

Meyers, A., Weiskittel, T. M., & Dalhaimer, P. (2017). Lipid Droplets: Formation to Breakdown. *Lipids, 52*(6), 465-475. doi:10.1007/s11745-017-4263-0

Missaglia, S., Coleman, R. A., Mordente, A., & Tavian, D. (2019). Neutral Lipid Storage Diseases as Cellular Model to Study Lipid Droplet Function. *Cells, 8*(2). doi:10.3390/cells8020187

Mizunoe, Y., Kobayashi, M., Hoshino, S., Tagawa, R., Itagawa, R., Hoshino, A., . . . Higami, Y. (2020). Cathepsin B overexpression induces degradation of perilipin 1 to cause lipid metabolism dysfunction in adipocytes. *Scientific Reports, 10*(1), 634. doi:10.1038/s41598-020-57428-6

Mizunoe, Y., Sudo, Y., Okita, N., Hiraoka, H., Mikami, K., Narahara, T., . . . Higami, Y. (2017). Involvement of lysosomal dysfunction in autophagosome accumulation and early pathologies in adipose tissue of obese mice. *Autophagy, 13*(4), 642-653. doi:10.1080/15548627.2016.1274850

Murase, Y., Takeichi, T., Kawamoto, A., Tanahashi, K., Okuno, Y., Takama, H., . . . Akiyama, M. (2020). Reduced stratum corneum acylceramides in autosomal recessive congenital ichthyosis with a NIPAL4 mutation. *Journal of*

Dermatological Science, 97(1), 50-56. doi:https://doi.org/10.1016/j.jdermsci.2019.12.001

Nettebrock, N. T., & Bohnert, M. (2020). Born this way – Biogenesis of lipid droplets from specialized ER subdomains. *Biochimica et Biophysica Acta (BBA) - Molecular and Cell Biology of Lipids, 1865*(1), 158448. doi:https://doi.org/10.1016/j.bbalip.2019.04.008

O'Connor, R. S., Guo, L., Ghassemi, S., Snyder, N. W., Worth, A. J., Weng, L., . . . Milone, M. C. (2018). The CPT1a inhibitor, etomoxir induces severe oxidative stress at commonly used concentrations. *Scientific Reports, 8*(1), 6289. doi:10.1038/s41598-018-24676-6

Ohsaki, Y., Suzuki, M., & Fujimoto, T. (2014). Open questions in lipid droplet biology. *Chem Biol, 21*(1), 86-96. doi:10.1016/j.chembiol.2013.08.009

Olzmann, J. A., & Carvalho, P. (2019). Dynamics and functions of lipid droplets. *Nature Reviews Molecular Cell Biology, 20*(3), 137-155. doi:10.1038/s41580-018-0085-z

Onal, G., Kutlu, O., Gozuacik, D., & Dokmeci Emre, S. (2017). Lipid Droplets in Health and Disease. *Lipids in health and disease, 16*(1), 128-128. doi:10.1186/s12944-017-0521-7

Onal, G., Kutlu, O., Ozer, E., Gozuacik, D., Karaduman, A., & Dokmeci Emre, S. (2019). Impairment of lipophagy by PNPLA1 mutations causes lipid droplet accumulation in primary fibroblasts of Autosomal Recessive Congenital Ichthyosis patients. *J Dermatol Sci, 93*(1), 50-57. doi:10.1016/j.jdermsci.2018.11.013

Pinkova, B., Buckova, H., Borska, R., & Fajkusova, L. (2020). Types of congenital nonsyndromic ichthyoses. *Biomedical papers, 164*(4), 357-365. doi:10.5507/bp.2020.050

Renne, M. F., Klug, Y. A., & Carvalho, P. (2020). Lipid droplet biogenesis: A mystery "unmixing"? *Seminars in Cell & Developmental Biology, 108*, 14-23. doi:https://doi.org/10.1016/j.semcdb.2020.03.001

Reynolds, C. A., & Macian, F. (2018). Chaperone mediated autophagy and T cell function. *The Journal of Immunology, 200*(1 Supplement), 47.26. Retrieved from http://www.jimmunol.org/content/200/1_Supplement/47.26.abstract

Richard, G. (1993). Autosomal Recessive Congenital Ichthyosis. In M. P. Adam, H. H. Ardinger, R. A. Pagon, S. E. Wallace, L. J. H. Bean, G. Mirzaa, & A. Amemiya (Eds.), *GeneReviews(®)*. Seattle (WA): University of Washington, Seattle

Roberts, M. A., & Olzmann, J. A. (2020). Protein Quality Control and Lipid Droplet Metabolism. *Annu Rev Cell Dev Biol, 36*, 115-139. doi:10.1146/annurev-cellbio-031320-101827

Rodríguez-Pazos, L., Ginarte, M., Vega, A., & Toribio, J. (2013). Autosomal recessive congenital ichthyosis. *Actas Dermosifiliogr, 104*(4), 270-284. doi:10.1016/j.adengl.2011.11.021

Rui, Y.-N., Xu, Z., Patel, B., Chen, Z., Chen, D., Tito, A., . . . Zhang, S. (2015). Huntingtin functions as a scaffold for selective macroautophagy. *Nature cell biology, 17*(3), 262-275. doi:10.1038/ncb3101

Sarkar, C., Zhao, Z., Aungst, S., Sabirzhanov, B., Faden, A. I., & Lipinski, M. M. (2014). Impaired autophagy flux is associated with neuronal cell death after

traumatic brain injury. *Autophagy, 10*(12), 2208-2222. doi:10.4161/15548627.2014.981787
Sathyanarayan, A., Mashek, M. T., & Mashek, D. G. (2017). ATGL Promotes Autophagy/Lipophagy via SIRT1 to Control Hepatic Lipid Droplet Catabolism. *Cell Reports, 19*(1), 1-9. doi:https://doi.org/10.1016/j.celrep.2017.03.026
Schmuth, M., Martinz, V., Janecke, A. R., Fauth, C., Schossig, A., Zschocke, J., & Gruber, R. (2013). Inherited ichthyoses/generalized Mendelian disorders of cornification. *European journal of human genetics : EJHG, 21*(2), 123-133. doi:10.1038/ejhg.2012.121
Schott, M. B., Weller, S. G., Schulze, R. J., Krueger, E. W., Drizyte-Miller, K., Casey, C. A., & McNiven, M. A. (2019). Lipid droplet size directs lipolysis and lipophagy catabolism in hepatocytes. *Journal of Cell Biology, 218*(10), 3320-3335. doi:10.1083/jcb.201803153
Schroeder, B., Schulze, R. J., Weller, S. G., Sletten, A. C., Casey, C. A., & McNiven, M. A. (2015). The small GTPase Rab7 as a central regulator of hepatocellular lipophagy. *Hepatology, 61*(6), 1896-1907. doi:10.1002/hep.27667
Schuldiner, M., & Bohnert, M. (2017). A different kind of love - lipid droplet contact sites. *Biochim Biophys Acta Mol Cell Biol Lipids, 1862*(10 Pt B), 1188-1196. doi:10.1016/j.bbalip.2017.06.005
Schulze, R. J., Sathyanarayan, A., & Mashek, D. G. (2017). Breaking fat: The regulation and mechanisms of lipophagy. *Biochimica et Biophysica Acta (BBA) - Molecular and Cell Biology of Lipids, 1862*(10, Part B), 1178-1187. doi:https://doi.org/10.1016/j.bbalip.2017.06.008
Schweiger, M., Lass, A., Zimmermann, R., Eichmann, T. O., & Zechner, R. (2009). Neutral lipid storage disease: genetic disorders caused by mutations in adipose triglyceride lipase/PNPLA2 or CGI-58/ABHD5. *Am J Physiol Endocrinol Metab, 297*(2), E289-296. doi:10.1152/ajpendo.00099.2009
Schweiger, M., & Zechner, R. (2015). Breaking the Barrier—Chaperone-Mediated Autophagy of Perilipins Regulates the Lipolytic Degradation of Fat. *Cell Metabolism, 22*(1), 60-61. doi:https://doi.org/10.1016/j.cmet.2015.06.017
Singh, R., Kaushik, S., Wang, Y., Xiang, Y., Novak, I., Komatsu, M., . . . Czaja, M. J. (2009). Autophagy regulates lipid metabolism. *Nature, 458*(7242), 1131-1135. doi:10.1038/nature07976
Spandl, J., Lohmann, D., Kuerschner, L., Moessinger, C., & Thiele, C. (2011). Ancient Ubiquitous Protein 1 (AUP1) Localizes to Lipid Droplets and Binds the E2 Ubiquitin Conjugase G2 (Ube2g2) via Its G2 Binding Region*, ♦. *Journal of Biological Chemistry, 286*(7), 5599-5606. doi:https://doi.org/10.1074/jbc.M110.190785
Steinfeld, R., Reinhardt, K., Schreiber, K., Hillebrand, M., Kraetzner, R., Brück, W., . . . Gärtner, J. (2006). Cathepsin D Deficiency Is Associated with a Human Neurodegenerative Disorder. *The American Journal of Human Genetics, 78*(6), 988-998. doi:https://doi.org/10.1086/504159
Sugiura, K., & Akiyama, M. (2015). Update on autosomal recessive congenital ichthyosis: mRNA analysis using hair samples is a powerful tool for genetic diagnosis. *Journal of Dermatological Science, 79*(1), 4-9. doi:https://doi.org/10.1016/j.jdermsci.2015.04.009
Sztalryd, C., & Brasaemle, D. L. (2017). The perilipin family of lipid droplet proteins: Gatekeepers of intracellular lipolysis. *Biochimica et Biophysica Acta (BBA) - Molecular and Cell Biology of Lipids, 1862*(10, Part B), 1221-1232. doi:https://doi.org/10.1016/j.bbalip.2017.07.009

Takahashi, Y., Coppola, D., Matsushita, N., Cualing, H. D., Sun, M., Sato, Y., . . . Mul, J. J. (2007). Bif-1 interacts with Beclin 1 through UVRAG and regulates autophagy and tumorigenesis. *Nature cell biology, 9*(10), 1142-1151.
Takahashi, Y., Meyerkord, C. L., Hori, T., Runkle, K., Fox, T. E., Kester, M., . . . Wang, H.-G. (2011). Bif-1 regulates Atg9 trafficking by mediating the fission of Golgi membranes during autophagy. *Autophagy, 7*(1), 61-73.
Takeichi, T., & Akiyama, M. (2016). Inherited ichthyosis: Non-syndromic forms. *J Dermatol, 43*(3), 242-251. doi:10.1111/1346-8138.13243
Tasset, I., & Cuervo, A. M. (2016). Role of chaperone-mediated autophagy in metabolism. *Febs j, 283*(13), 2403-2413. doi:10.1111/febs.13677
Tekirdag, K., & Cuervo, A. M. (2018). Chaperone-mediated autophagy and endosomal microautophagy: Joint by a chaperone. *J Biol Chem, 293*(15), 5414-5424. doi:10.1074/jbc.R117.818237
Thiam, A. R., Farese Jr, R. V., & Walther, T. C. (2013). The biophysics and cell biology of lipid droplets. *Nature Reviews Molecular Cell Biology, 14*(12), 775-786. doi:10.1038/nrm3699
Traupe, H., Fischer, J., & Oji, V. (2014). Nonsyndromic types of ichthyoses - an update. *J Dtsch Dermatol Ges, 12*(2), 109-121. doi:10.1111/ddg.12229
Turk, V., Stoka, V., Vasiljeva, O., Renko, M., Sun, T., Turk, B., & Turk, D. (2012). Cysteine cathepsins: From structure, function and regulation to new frontiers. *Biochimica et Biophysica Acta (BBA) - Proteins and Proteomics, 1824*(1), 68-88. doi:https://doi.org/10.1016/j.bbapap.2011.10.002
Uitto, J., Youssefian, L., Saeidian, A. H., & Vahidnezhad, H. (2020). Molecular Genetics of Keratinization Disorders - What's New About Ichthyosis. *Acta Derm Venereol, 100*(7), adv00095. doi:10.2340/00015555-3431
Vahlquist, A., Fischer, J., & Törmä, H. (2018). Inherited Nonsyndromic Ichthyoses: An Update on Pathophysiology, Diagnosis and Treatment. *American Journal of Clinical Dermatology, 19*(1), 51-66. doi:10.1007/s40257-017-0313-x
Walther, T. C., Chung, J., & Farese, R. V., Jr. (2017). Lipid Droplet Biogenesis. *Annu Rev Cell Dev Biol, 33*, 491-510. doi:10.1146/annurev-cellbio-100616-060608
Walther, T. C., & Farese, R. V., Jr. (2012). Lipid droplets and cellular lipid metabolism. *Annu Rev Biochem, 81*, 687-714. doi:10.1146/annurev-biochem-061009-102430
Wang, C.-W. (2016). Lipid droplets, lipophagy, and beyond. *Biochimica et Biophysica Acta (BBA) - Molecular and Cell Biology of Lipids, 1861*(8, Part B), 793-805. doi:https://doi.org/10.1016/j.bbalip.2015.12.010
Wang, L., Zhou, J., Yan, S., Lei, G., Lee, C.-H., & Yin, X.-M. (2017). Ethanol-triggered Lipophagy Requires SQSTM1 in AML12 Hepatic Cells. *Scientific Reports, 7*(1), 12307. doi:10.1038/s41598-017-12485-2
Wang, T., Wei, Q., Liang, L., Tang, X., Yao, J., Lu, Y., . . . Cao, X. (2020). OSBPL2 Is Required for the Binding of COPB1 to ATGL and the Regulation of Lipid Droplet Lipolysis. *iScience, 23*(7), 101252. doi:https://doi.org/10.1016/j.isci.2020.101252
Ward, C., Martinez-Lopez, N., Otten, E. G., Carroll, B., Maetzel, D., Singh, R., . . . Korolchuk, V. I. (2016). Autophagy, lipophagy and lysosomal lipid storage disorders. *Biochimica et Biophysica Acta (BBA) - Molecular and Cell Biology of Lipids, 1861*(4), 269-284. doi:https://doi.org/10.1016/j.bbalip.2016.01.006
Welte, M. A. (2015). Expanding roles for lipid droplets. *Current biology : CB, 25*(11), R470-R481. doi:10.1016/j.cub.2015.04.004
Wilfling, F., Haas, J. T., Walther, T. C., & Farese, R. V., Jr. (2014). Lipid droplet biogenesis. *Curr Opin Cell Biol, 29*, 39-45. doi:10.1016/j.ceb.2014.03.008

Xu, S., Zhang, X., & Liu, P. (2018). Lipid droplet proteins and metabolic diseases. *Biochim Biophys Acta Mol Basis Dis, 1864*(5 Pt B), 1968-1983. doi:10.1016/j.bbadis.2017.07.019

Yang, Q., Wang, R., & Zhu, L. (2019). Chaperone-Mediated Autophagy. In Z.-H. Qin (Ed.), *Autophagy: Biology and Diseases: Basic Science* (pp. 435-452). Singapore: Springer Singapore.

Yang, Y., & Klionsky, D. J. (2020). Autophagy and disease: unanswered questions. *Cell Death & Differentiation, 27*(3), 858-871. doi:10.1038/s41418-019-0480-9

Youssefian, L., Vahidnezhad, H., Saeidian, A. H., Sotoudeh, S., Mahmoudi, H., Daneshpazhooh, M., . . . Uitto, J. (2017). Autosomal recessive congenital ichthyosis: CERS3 mutations identified by a next generation sequencing panel targeting ichthyosis genes. *European journal of human genetics : EJHG, 25*(11), 1282-1285. doi:10.1038/ejhg.2017.137

Youssefian, L., Vahidnezhad, H., Saeidian, A. H., Touati, A., Sotoudeh, S., Mahmoudi, H., . . . Uitto, J. (2019). Autosomal recessive congenital ichthyosis: Genomic landscape and phenotypic spectrum in a cohort of 125 consanguineous families. *Hum Mutat, 40*(3), 288-298. doi:10.1002/humu.23695

Yu, J., & Li, P. (2017). The size matters: regulation of lipid storage by lipid droplet dynamics. *Science China Life Sciences, 60*(1), 46-56. doi:10.1007/s11427-016-0322-x

Zechner, R., Madeo, F., & Kratky, D. (2017). Cytosolic lipolysis and lipophagy: two sides of the same coin. *Nature Reviews Molecular Cell Biology, 18*(11), 671-684. doi:10.1038/nrm.2017.76

Zechner, R., Zimmermann, R., Eichmann, T. O., Kohlwein, S. D., Haemmerle, G., Lass, A., & Madeo, F. (2012). FAT SIGNALS--lipases and lipolysis in lipid metabolism and signaling. *Cell Metab, 15*(3), 279-291. doi:10.1016/j.cmet.2011.12.018

Zehmer, J. K., Huang, Y., Peng, G., Pu, J., Anderson, R. G., & Liu, P. (2009). A role for lipid droplets in inter-membrane lipid traffic. *Proteomics, 9*(4), 914-921. doi:10.1002/pmic.200800584

Zembroski, A. S., & Buhman, K. K. (2020). Chapter 8 - Regulation of intracellular lipid storage and utilization. In J. M. Ntambi (Ed.), *Lipid Signaling and Metabolism* (pp. 131-156): Academic Press.

Zheng, W., Chen, Q., Wang, C., Yao, D., Zhu, L., Pan, Y., . . . Shao, C. (2020). Inhibition of Cathepsin D (CTSD) enhances radiosensitivity of glioblastoma cells by attenuating autophagy. *Molecular Carcinogenesis, 59*(6), 651-660. doi:https://doi.org/10.1002/mc.23194

Zhou, J., Tan, S.-H., Nicolas, V., Bauvy, C., Yang, N.-D., Zhang, J., . . . Shen, H.-M. (2013). Activation of lysosomal function in the course of autophagy via mTORC1 suppression and autophagosome-lysosome fusion. *Cell Research, 23*(4), 508-523. doi:10.1038/cr.2013.11